Julius-Maximilians-Universität Würzburg

Studies on the Contact-Kinin System and Macrophage Activation in Experimental Focal Cerebral Ischemia

* * *

Untersuchungen zum Kontakt-Kinin-System und zur Makrophagen-Aktivierung beim Experimentellen Schlaganfall

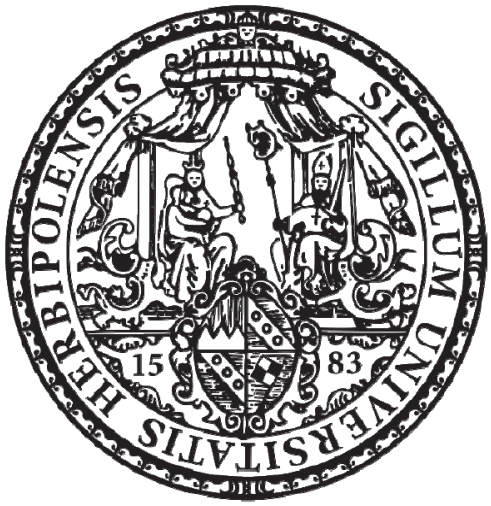

Doctoral Thesis for a Doctoral Degree

at the Graduate School of Life Sciences,

Section Biomedicine

submitted by

Nadine Heydenreich

from Freiberg

Würzburg, 2013

Submitted on:

Members of the *Promotionskomitee*:

Chairperson:	**Prof Dr Manfred Gessler**
Primary Supervisor:	**Prof Dr Guido Stoll**
Supervisor (Second):	**Prof Dr Thomas Dandekar**
Supervisor (Third):	**Prof Dr Bernhard Nieswandt**

Date of Public Defense:

Date of Receipt of Certificate:

SUMMARY

Traditionally, ischemic stroke has been regarded as the mere consequence of cessation of cerebral blood flow, e.g. due to the thromboembolic occlusion of a major brain supplying vessel. However, the simple restoration of blood flow via thrombolysis and/or mechanical recanalization alone often does not guarantee a good functional outcome. It appears that secondary detrimental processes are triggered by hypoxia and reoxygenation, which are referred to as ischemia/reperfusion (I/R) injury. During recent years it became evident that, beside thrombosis inflammation and edema formation are key players in the pathophysiology of cerebral ischemia. The contact-kinin system represents an interface between thrombotic, inflammatory and edematous circuits. It connects the intrinsic coagulation pathway with the plasma kallikrein-kinin system (KKS) via coagulation factor FXII.

The serine protease inhibitor C1-inhibitor (C1-INH) has a wide spectrum of inhibitory activities and counteracts activation of the contact-kinin system at multiple levels. The first part of the thesis aimed to multimodally interfere with infarct development by C1-INH and to analyze modes of actions of human plasma derived C1-INH Berinert® P in a murine model of focal cerebral ischemia. It was shown that C57BL/6 mice following early application of 15.0 units (U) C1-INH, but not 7.5 U developed reduced brain infarctions by ~60% and less neurological deficits in the model of transient occlusion of the middle cerebral artery (tMCAO). This protective effect was preserved at more advanced stages of infarction (day 7), without increasing the risk of intracerebral bleeding or affecting normal hemostasis. Less neurological deficits could also be observed with delayed C1-INH treatment, whereas no improvement was achieved in the model of permanent MCAO (pMCAO). Blood-brain-barrier (BBB) damage, inflammation and thrombosis were significantly improved following 15.0 U C1-INH application early after onset of ischemia. Based on its strong antiedematous, antiinflammatory and antithrombotic properties C1-INH constitutes a multifaceted therapeutic compound that protects from ischemic neurodegeneration in ‘clinically meaningful’ settings.

The second part of the thesis addresses the still elusive functional role of macrophages in the early phase of stroke, especially the role of the macrophage-specific adhesion molecule sialoadhesin (Sn). For the first time, sialoadhesin null ($Sn^{-/-}$) mice, homozygous deficient for Sn on macrophages were subjected to tMCAO

to assess the clinical outcome. Neurological and motor function was significantly improved in *Sn*$^{-/-}$ mice on day 1 after ischemic stroke compared with wildtype (*Sn*$^{+/+}$) animals. These clinical improvements were clearly detectable even on day 3 following tMCAO. Infarctions on day 1 were roughly the same size as in *Sn*$^{+/+}$ mice and did not grow until day 3. No intracerebral bleeding could be detected at any time point of data acquisition. Twenty four hours after ischemia a strong induction of Sn was detectable in *Sn*$^{+/+}$ mice, which was previously observed only on perivascular macrophages in the normal brain. Deletion of Sn on macrophages resulted in less disturbance of the BBB and a reduced number of CD11b^{+} (specific marker for macrophages/microglia) cells, which, however, was not associated with altered expression levels of inflammatory cytokines. To further analyze the function of macrophages following stroke this thesis took advantage of *LysM-Cre*$^{+/-}$*/IKK2*$^{-/-}$ mice bearing a nuclear factor (NF)-κB activation defect in the myeloid lineage, including macrophages. Consequently, macrophages were not able to synthesize inflammatory cytokines under the control of NF-κB. Surprisingly, infarct sizes and neurological deficits upon tMCAO were roughly the same in conditional knockout mice and respective wildtype littermates. These findings provide evidence that macrophages do not contribute to tissue damage and neurological deficits, at least, not by release of inflammatory cytokines in the early phase of cerebral ischemia. In contrast, Sn which is initially expressed on perivascular macrophages and upregulated on macrophages/microglia within the parenchyma following stroke, influenced functional outcome.

ZUSAMMENFASSUNG

Der ischämische Schlaganfall wird traditionell als unmittelbare und „einfache“ Folge der Unterbrechung des Blutflusses zum Gehirn z.B. durch thromboembolische Gefäßverschlüsse gesehen. Häufig führt die alleinige Wiederherstellung des Blutflusses durch Lysetherapie bzw. mechanische Rekanalisation jedoch nicht zu einer Funktionserholung. Dies rückt sekundäre pathophysiologische Prozesse in den Fokus, die durch die Hypoxie und anschließende Wiederversorgung mit Sauerstoff angestoßen werden und zu einem sogenannten Reperfusionsschaden führen. In den letzten Jahren wurde klar, dass neben der Thrombenbildung Entzündungsprozesse und Hirnschwellung zentrale Bestandteile der Pathophysiologie von ischämischen Schlaganfällen sind, die über ein komplexes Netzwerk von Signalwegen eng miteinander verknüpft sind. An dieser Schnittstelle setzt die vorliegende Dissertation an. Das Kontakt-Kinin-System verbindet das plasmatische Kallikrein-Kinin-System (KKS), welches entzündliche und ödematöse Prozesse anstößt, über den Blutgerinnungsfaktor FXII mit dem intrinsischen Blutgerinnungsweg, der letztlich für die Thrombenbildung verantwortlich ist.

Der endogene Serinprotease-Inhibitor C1-Inhibitor (C1-INH) besitzt ein breites Wirkungsspektrum und wirkt der Aktivierung des Kontakt-Kinin-Systems auf verschiedenen Ebenen entgegen. Ziel des ersten Teils der vorliegenden Dissertation war es, mittels C1-INH auf multimodale Weise ins Infarktgeschehen einzugreifen und die Wirkmechanismen des humanen C1-INH Berinert® P im Mausmodell nach fokaler zerebraler Ischämie zu untersuchen. Es konnte gezeigt werden, dass die frühe Behandlung von C57BL/6 Mäusen mit 15.0 Units (U) C1-INH im Modell der transienten Okklusion der Arteria cerebri media (tMCAO) eine drastische Reduzierung der Infarktvolumina um annähernd 60%, sowie deutlich weniger neurologische und funktionelle Defizite zur Folge hatte. Diese Schutzwirkung war auch im fortgeschrittenen Stadium (Tag 7) der Schlaganfallentwicklung zu beobachten, ohne das Risiko einer intrazerebralen Blutung zu erhöhen oder die normale Hämostase zu beeinflussen. Die Applikation von 7.5 U C1-INH hatte dagegen keinen Effekt. Ein wesentlich verbessertes neurologisches Verhalten konnte auch nach verzögerter Injektion von 15.0 U C1-INH erzielt werden. Im Gegensatz dazu bewirkte die Behandlung im Modell der permanenten MCAO (pMCAO) keine Verbesserung. Mechanistisch führte die Gabe von 15.0 U C1-INH zu einer deutlichen Stabilisierung der Bluthirnschranke und weniger Ödembildung. Darüber hinaus war

die lokale Entzündungsreaktion nach C1-INH-Applikation abgeschwächt und es bildeten sich weniger Thromben in der zerebralen Mikrozirkulation. Basierend auf seiner vielfältigen antithrombotischen, antientzündlichen und antiödematösen Potenz stellt C1-INH einen vielversprechenden Ansatz zum Schutz vor ischämischer Neurodegeneration nach Schlaganfall unter ‚klinisch relevanten' Bedingungen dar.

Der zweite Teil der Dissertation beschäftigt sich mit der bislang ungeklärten funktionellen Rolle von Makrophagen in der Frühphase nach Schlaganfall, speziell der Rolle des Makrophagen-spezifischen Signalmoleküls Sialoadhesin (Sn). Hierzu wurden erstmals Sialoadhesin-defiziente (*Sn*$^{-/-}$) Mäuse, deren Makrophagen kein Sn exprimieren, der tMCAO unterzogen und die klinischen Folgen bewertet. *Sn*$^{-/-}$ Tiere zeigten verglichen mit Wildtypen (*Sn*$^{+/+}$) verbesserte neurologische und motorische Funktionen an Tag 1 nach Schlaganfall. Diese Verbesserung war auch an Tag 3 nach Schlaganfall eindeutig nachweisbar. Die Infarkte an Tag 1 waren größenmäßig vergleichbar mit *Sn*$^{+/+}$ Mäusen und nahmen bis Tag 3 nicht an Größe zu. Zu keinem Zeitpunkt wurde eine intrazerebrale Blutung beobachtet. 24 Stunden nach Schlaganfall kam es bei *Sn*$^{+/+}$ Mäusen zu einer starken Induktion von Sn, welches im normalen Gehirn nur auf perivaskulären Makrophagen exprimiert wurde. Die Deletion von Sn auf Makrophagen wirkte einer Bluthirnschrankenstörung entgegen und hatte eine deutlich geringere Infiltration von CD11b^{+} (spezifischer Marker für Makrophagen/Mikroglia) Zellen ins ischämische Gewebe zur Folge. Dies war interessanterweise nicht mit einer Veränderung der Zytokinexpression verknüpft. Zur weiteren Untersuchung der Makrophagenrolle nach Schlaganfall wurde die Dissertation auf *LysM-Cre*$^{+/-}$*/IKK2*$^{-/-}$ Mäuse ausgedehnt. Diese wiesen einen Makrophagen-spezifischen Defekt in der Aktivierung des Transkriptionsfaktors Nuklearfaktor (NF)-κB auf, und konnten folglich inflammatorische Zytokine unter der Transkriptionskontrolle von NF-κB nicht synthetisieren. Die Infarktgrößen und neurologischen Defizite der transgenen Tiere waren überraschenderweise vergleichbar mit wildtypischen Wurfgeschwistern. Diese Ergebnisse deuten darauf hin, dass Makrophagen zumindest nicht durch die Synthese von inflammatorischen Zytokinen zum Gewebeschaden und zu neurologischen Defiziten in der Frühphase nach Schlaganfall beitragen, während Sn, das initial nur auf perivaskulären Makrophagen exprimiert und später im ischämischen Parenchym auf Makrophagen/Mikroglia hochreguliert wird, Einfluss auf das funktionelle Outcome hatte.

TABLE OF CONTENTS

1 INTRODUCTION

1.1 Human stroke – causes and limited treatment options

Stroke is the second leading cause of death and the most common cause of permanent disability worldwide (Murray & Lopez, 1997; WHO, 2008). The risk to experience a stroke is correlated with age (Roger et al., 2011), but due to increasing risk factors in our society young adults may also be affected. There are two different types of stroke, ischemic stroke resulting from the occlusion of a cerebral artery which accounts for approximately 87% of cases and which is the focus of this thesis, and intracerebral hemorrhage (Roger et al., 2011). Main sources of thrombo-embolism in the brain are either blood emboli emerging from the heart due to atrial fibrillation (irregular heart beat) or platelet-rich thrombi arising at instable atherosclerotic plaques of the carotid or vertebral arteries (Green et al., 2003; Stoll & Bendszus, 2006; Pham et al., 2012). The primary goal of acute stroke treatment is to achieve restoration of blood flow as soon as possible by recanalization. The only approved treatment for acute ischemic stroke is intravenous (i.v.) thrombolysis with the clot solving agent recombinant tissue plasminogen activator (rt-PA) (NINDS, 1995). Eligibility of acute stroke patients to rt-PA thrombolysis is low (< 10%) due to a narrow time window after onset of occlusion and many other contraindications (van den Berg & de Jong, 2009; Fulgham et al., 2004). The main exclusion criteria of patients from this therapy is their late arrival at the hospital (Tong et al., 2012), since the therapeutic time window for the effective and safe application of rt-PA is only 4.5 hours (Hacke et al., 2008) after first symptom onset. However, the treatment with rt-PA is associated with a risk of intracerebral hemorrhages which dramatically increases over time and beyond 4.5 hours neutralizes or exceeds the beneficial effect of recanalization (del Zoppo et al., 1992; Larrue et al., 1997). Given the situation that many patients are not amenable to this treatment and a significant number of patients with successful recanalization still develop significant neurological deficits (Chimowitz, 2013) additional therapeutic options are eagerly awaited in the clinic.

1.2 Pathomechanisms of ischemic stroke

1.2.1 The ischemic cascade and its effects on the penumbra

Acute cerebral ischemia as a result of cessation of cerebral blood flow (CBF) causes hypoxia and failure of the energy metabolism in the underlying brain parenchyma. Subsequently, a sequence of detrimental events referred to as ischemic cascade is initiated within minutes (Dirnagl et al., 1999). In brief, the ischemic cascade comprises the depolarization of neurons and glia cells due to energy failure and loss of membrane potential. The ionic gradient of Na^+, Cl^- and K^+ is shifted secondary to intracellular Ca^{2+} overload, release of the excitotoxic amino acid glutamate and generation of reactive oxygen species (ROS), which results in cell swelling and disruption of membrane structures. The brain is most sensitive to reductions in blood supply and only a short period of impaired CBF results in irreversible damage of brain tissue within the core of infarction due to acute necrotic and subacute apoptotic cell death. The brain tissue surrounding the ischemic core, known as penumbra, is still alive and supplied by a partially preserved energy metabolism due to a residual perfusion level from adjacent non-ischemic brain areas (Astrup et al., 1981; Marchal et al., 1996; Baron, 1999). Hence, the penumbra might be salvaged if CBF and energy metabolism are restored as early as possible, which might result in less postischemic neurological and motor-functional deficits and improved recovery of patients. However, the event of reperfusion - though it is indispensable to salvage the penumbra - paradoxically carries the risk of serious complications. On the other hand, if CBF is not reestablished, brain tissue of the penumbra will definitely undergo irreversible damage and become part of the ischemic core (Ginsberg, 2003).

1.2.2 Ischemia/reperfusion injury and experimental models of stroke

Despite successful recanalization a large number of patients develop severe infarctions and neurological deficits (Chimowitz, 2013). This phenomenon is referred to as ischemia/reperfusion (I/R) injury and characterized by tissue damage due to interrupted oxygen supply and a subsequent damage caused by reperfusion. I/R injury depends on duration and severity of ischemia and intensity of reperfusion. Hence, restoration of CBF as early as possible (Hacke et al., 2008) is of great importance.

Despite extensive research over the last decades the complex mechanisms underlying I/R injury are less understood, but there is an increasing number of evidence that inflammation is critically involved (Stoll et al., 1998; Wang et al., 2007; Zuidema & Zhang, 2010). The event of reperfusion of ischemic tissue initiates a cascade of deleterious processes leading to exacerbation of the injury. Most of them are triggered by extensive generation of ROS before but mainly during the process of reperfusion. Moreover, cytokines, chemokines and other inflammatory stimuli (del Zoppo et al., 2000) are released upon ischemic stroke from activated endothelial cells and immune cells and a pronounced sterile inflammation is initiated, characterized by massive recruitment of polymorphonuclear leukocytes. Neutrophils are the first immune cells recruited to sites of injury and are detectable in the ischemic vasculature within hours after onset of the insult (Garcia et al., 1994; Bednar et al., 1997; del Zoppo, 1997; Stoll et al., 1998; Gelderblom et al., 2009). Due to their huge number, platelet-leukocyte-interactions and fibrin accumulation neutrophils might obstruct microvasculature leading to a phenomenon referred to as no-reflow phenomenon (del Zoppo et al., 1991). Recruited immune cells cross the blood-brain-barrier (BBB) and migrate into the ischemic brain tissue leading to extensive collateral damage and development of infarction.

To understand the mechanisms of stroke pathophysiology several animal models of experimental stroke have been established. The most frequently used experimental model to induce focal cerebral ischemia in rodents is the occlusion of the middle cerebral artery (MCA) via an intraluminal thread (detailed information is provided in **2.2.1.1**) (Durukan & Tatlisumak, 2007; Carmichael, 2005). This technique, which was first described in 1986 in rats (Koizumi et al., 1986), and adjusted to mice (Clark et al., 1997), intends to imitate the human situation, since a large number of ischemic strokes involves the region of the MCA. The transient MCA occlusion (tMCAO), where the thread is withdrawn after a certain period, mimics recanalization and subsequent reperfusion after cessation of CBF as it is achieved in patients after successful thrombolysis or mechanical thrombectomy. In this model mainly the basal ganglia are affected, while the neocortex is involved to a variable amount depending on the duration of ischemia. Following removal of the thread the infarcts are surrounded by the penumbra, tissue that might be salvageable by reperfusion. In contrast, the model of permanent MCA occlusion (pMCAO), where the thread remains in the vessel, mimics the situation of permanent ischemia without

reperfusion. Here, tissue of the basal ganglia and neocortex die from ischemia, resulting in complete infarction of the whole MCA territory. Some experimental stroke studies have demonstrated that reperfusion after a certain period of brain vessel occlusion even resulted in larger infarctions compared with permanent ischemia (Aronowski et al., 1997; Yang & Betz, 1994).

Although a single model can cover only some aspects of a heterogeneous and complex disease such as ischemic stroke in humans, the model of MCAO turned out to be useful in elucidating basic pathomechanisms involved in stroke development. Moreover, the model of MCAO displays several advantages: it is less invasive, since it does not require craniectomy (removal of a part of the skull) (Hudgins & Garcia, 1970), the performance is simple, and it allows tissue reperfusion by withdrawing of the occluding filament (Braeuninger & Kleinschnitz, 2009).

1.2.3 Breakdown of the blood-brain-barrier and brain swelling

I/R injury following focal cerebral ischemia is accompanied by breakdown of the blood-brain-barrier (BBB) (Stoll & Jander, 1999). Products abundantly released and generated during the process of reperfusion degrade integral transmembrane proteins of the BBB, such as occludin, which is an important structural element between adjacent endothelial cells, the so called tight junctions. Consequently, major BBB properties, such as regulation of vascular barrier functions and vascular tone as well as control of hemostatic functions and immune cell trafficking are lost. Importantly, loss of the metabolic and physical barrier between circulation and brain tissue results in brain swelling, another pathophysiological component in stroke development. There are two major types of edema, (1) the intracellular cytotoxic edema and (2) the extracellular vasogenic edema (Ayata & Ropper, 2002). Formation of cytotoxic edema occurs within minutes after stroke onset in the ischemic core. This is primarily a consequence of water shift from the extracellular to the intracellular space. Since there is no change in the water content within the brain parenchyma, formation of cytotoxic edema does not induce brain swelling and occurs independently from BBB disruption. In contrast, vasogenic edema contributes significantly to formation of brain swelling and is caused by lost integrity of the BBB leading to leakage of fluids and proteins from intravascular to extravascular spaces (Rosenberg & Yang, 2007). Depending on the degree of water influx brain swelling

compresses midline structures and adjacent brain tissue (Aiyagari & Diringer, 2002) (**Fig. 1**), which results in secondary deterioration of patients. This is often the case in 'malignant' cerebral infarction, which completely involves the territory of the MCA (~10% of stroke cases). It represents a major life-threatening event with a mortality rate of approximately 80% (Hacke et al., 1996; Berrouschot et al., 1998) and usually becomes manifest within the first 72 hours after stroke onset (Shaw et al., 1959; Ng & Nimmannitya, 1970; Qureshi et al., 2003). Thus, in the subacute stage of infarct development, brain edema formation accounts for a significant number of additional stroke victims. Conventional antiedematous treatments such as corticosteroids are not effective in this situation since the glucocorticoid receptors are degraded (Kleinschnitz et al., 2011).

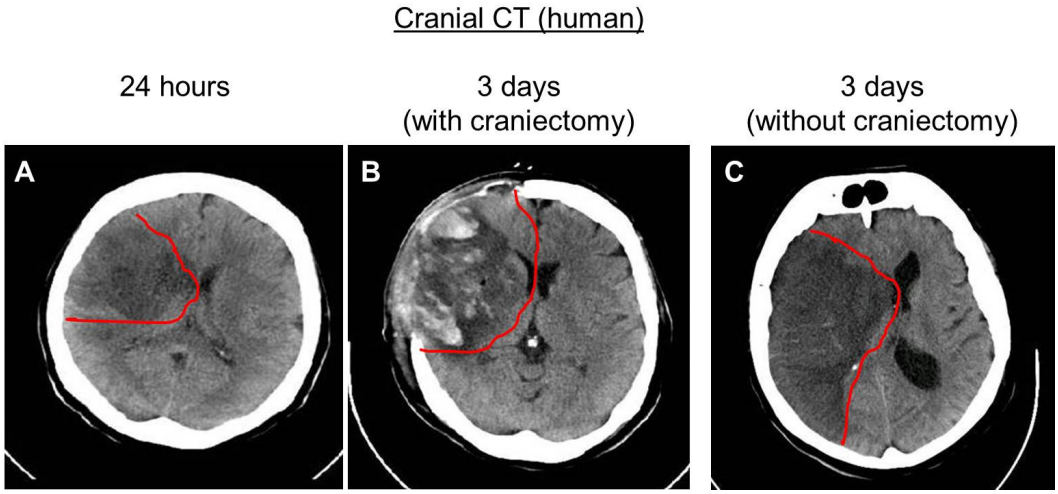

Figure 1: A) Cranial computed tomography (CT) scan of a patient 24 hours after a complete media infarct (red line). B) CT scan of the same patient 3 days post stroke, who underwent craniectomy within 48 hours to relieve the pressure of the developing infarct swelling (red line). C) CT scan of a patient 3 days after a complete media infarct without craniectomy due to relevant contraindications. The edema formation (red line) following stroke resulted in a midline shift with compression of the intact contralateral hemisphere.

1.3 The contact-kinin system

The contact-kinin system constitutes a framework of different plasma proteins, the coagulation factor FXII (Hageman factor), plasma prekallikrein (PK), coagulation factor FXI and high molecular weight kininogen (HMWK) (Cochrane & Griffin, 1982). In recent years it became evident that the contact-kinin system plays an important role in the pathophysiology of I/R injury after cerebral ischemia (Storini et al., 2005). Stroke outcome could be improved by deletion of the gene encoding bradykinin

receptor 1 (B1R) (Austinat et al., 2009) in transgenic mice or the serine protease kininogen (Langhauser et al., 2012). The protective effect was due to reduced edema formation and diminished inflammatory cell recruitment. Mice with a genetic disruption or pharmacological inhibition of FXII were similarly protected from ischemic stroke (Kleinschnitz et al., 2006; Hagedorn et al., 2010). FXII represents an interface between the plasma kallikrein-kinin system (KKS) and the intrinsic pathway of blood coagulation (*reviewed in* Schmaier, 2008) (**Fig. 2**).

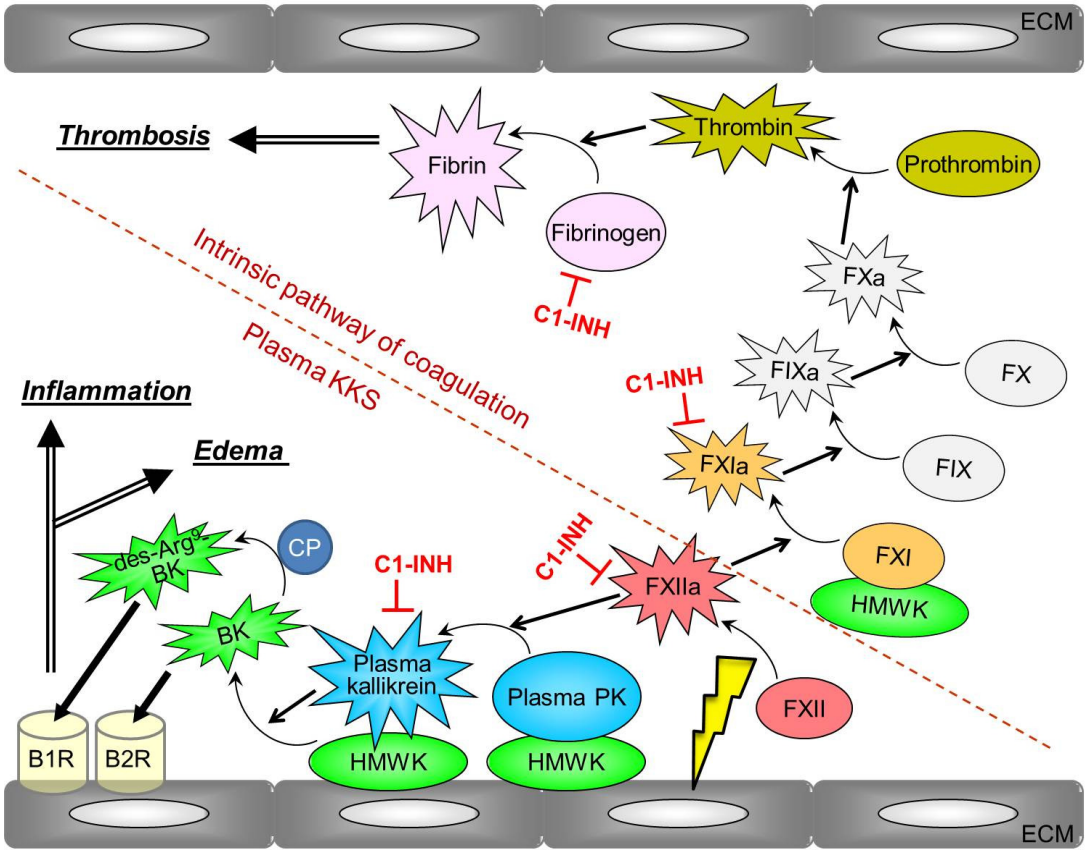

Figure 2: Scheme of the plasma kallikrein-kinin system (KKS) and intrinsic coagulation pathway initiated by FXIIa. Plasma KKS is initiated by FXIIa-mediated conversion of the inactive precursor plasma PK into its active form plasma kallikrein (Mandle & Kaplan, 1977; Revak et al., 1978). Plasma kallikrein in turn reciprocally activates additional FXII (Cochrane et al., 1973; Griffin, 1978) and liberates BK through cleavage of the precursor kininogen HMWK (Wiggins, 1983). BK preferentially binds to B2R, a G-protein coupled transmembrane receptor (GPCR). By actions of CP BK is converted into its active metabolite des-Arg^9-BK, the physiological agonist of GPCR B1R (Rodi et al., 2005). Binding of BK and des-Arg^9-BK to B1R and B2R on the ECM mediates signaling of inflammatory processes and edema formation by increased vascular permeability. FXII triggers the sequential activation of the zymogens FXI, FIX, FX and prothrombin. Cleavage of fibrinogen by thrombin leads to generation of the single molecule fibrin, which then accumulates with other fibrin molecules to form a fibrin clot. C1-INH counteracts activation of FXIIa, FXIa and plasma kallikrein. FXII/FXI/FIX/FX (coagulation factors XII/XI/IX/X, a: activated form), PK (prekallikrein), HMWK (high molecular weight kininogen), (des-Arg^9)-BK ((des-Arginin^9)-bradykinin), B1R/B2R (bradykinin receptor 1/2), CP (carboxypeptidase), C1-INH (C1-inhibitor), endothelial cell membrane (ECM).

Following ischemic stroke, FXII is activated (FXIIa) and triggers activation of plasma KKS leading to release of extremely short-living peptides bradykinin (BK) and des-Arginin^9-BK (Décarie et al., 1996). Upon their binding to B2R and B1R, respectively on the endothelial cell membrane (ECM) several intracellular signaling pathways are triggered. Some stimulate cellular release of nitric oxide (NO), prostacyclin, histamine and superoxide (Hong, 1980; Holland et al., 1990; Sarker et al., 2000; Ignjatovic et al., 2004), which also affect the vascular system and lead to enhanced vascular permeability and plasma extravasation but also mediation of typical inflammatory symptoms such as pain, redness and swelling.

Furthermore, FXIIa triggers activation of the intrinsic coagulation pathway, which culminates in generation of the single molecule fibrin by cleavage of fibrinogen. Single fibrin molecules then assemble with each other to form a fibrin clot (Furie & Furie, 1992) (**Fig. 2**).

The involvement of BK release in brain injury had been demonstrated in models of global and focal cerebral ischemia (Kamiya et al., 1993; Relton et al., 1997; Xia et al., 2004; Gröger et al., 2005) and all components of the KKS had been identified in the brain of laboratory animals. Moreover, KKS activation was described in human brain following ischemic stroke (Wagner et al., 2002).

1.4 C1-inhibitor and its spectrum of activities

C1-inhibitor (C1-INH) represents one of the main natural inhibitors of FXIIa and plasma kallikrein of the plasma KKS and controls activation of FXIa (Schapira et al., 1982; Pixley et al., 1985; Wuillemin et al., 1995) (**Fig. 2**). Hence, C1-INH regulates swelling via controlled liberation of BK, and the release of inflammatory mediators in healthy individuals.

C1-INH represents a single chain polypeptide of 478 amino acids and belongs to the superfamily of serine protease inhibitors (serpins) (Bock et al., 1986; Davis III, 1988). The main function of C1-INH is the regulation of serine protease activity, but it is also involved in several non-covalent interactions that are independent from protease inhibition. C1-INH consists of two distinct domains, a serpin-domain containing the reactive center loop responsible for its serine protease inhibitory function, and an amino-terminal heavily glycosylated domain.

Deficiency or dysfunction of C1-INH causes hereditary angioedema (HAE) type-1 or type-2 which is a relatively rare and partly life-threatening disease (Carugati et al., 2001). HAE is characterized by recurrent events of acute local swelling attacks due to a reversible increase of vascular permeability that may affect any area of the skin, abdomen or respiratory tract (Bork et al., 2003). Acute attacks of HAE can be treated by replacement therapy with C1-INH concentrate to restore normal functional levels of C1-INH (Waytes et al., 1996).

Over the past decades different C1-INH concentrates have been tested in humans (Cicardi et al., 2007). One of them is the pasteurized and purified preparation Berinert® P (CSL Behring, Marburg), which is derived from human plasma and approved by the Food and Drug Administration (FDA) for treatment of acute attacks of HAE since 2009 in Europe, Argentina, Australia and North America (Craig et al., 2009). Based on the properties of C1-INH Berinert® P in blocking components of the plasma KKS, this study addresses the question whether C1-INH application could ameliorate the clinical outcome of mice in the tMCAO stroke model.

1.5 Immune responses in cerebral ischemia

1.5.1 Cellular infiltration upon breakdown of the blood-brain-barrier

Breakdown of the BBB during cerebral ischemia allows access of blood components to the perivascular space and cellular infiltration into the brain parenchyma. The first hematogenous (blood-born) cells penetrating the brain in a time-coordinated fashion are neutrophils (Stoll et al., 1998; Bednar et al., 1997; del Zoppo, 1997; Garcia et al., 1994; Gelderblom et al., 2009) followed by monocytes/macrophages (Garcia et al., 1994; Schroeter et al., 1994; Jander et al., 1995; Schroeter et al., 1997; Schilling et al., 2003; Gelderblom et al., 2009; Gliem et al., 2012) and T lymphocytes (Schroeter et al. 1994; Jander et al., 1995).

The resident macrophages of the brain are microglia, a cell type that, if seen under steady state conditions (non-inflamed, non-activated), differs morphologically and phenotypic from the hematogenous macrophages (Perry & Gordon, 1991). Upon activation following cerebral ischemia microglia undergo morphological changes and migrate to sites of injury, where they become indistinguishable from infiltrating phagocytosing macrophages (Perry et al., 1993; Stoll et al., 1998). Once activated

immune cells have the potential to secrete a set of various pro- and antiinflammatory mediators.

The perivascular compartment contains a special subtype of macrophages, the 'perivascular' macrophages. Their functional role is largely unknown, but evidence in experimental autoimmune encephalomyelitis suggests that perivascular macrophages may present antigens to brain-infiltrating T cells. In the normal brain, perivascular macrophages express a unique adhesion molecule, sialoadhesin (Sn) (Hartnell et al., 2001).

1.5.2 The macrophage-restricted adhesion molecule sialoadhesin

Sn is a signaling molecule that, in contrast to many others, is restricted to macrophage-like cells (Crocker & Gordon, 1986, 1989; Hartnell et al., 2001) and hence, thought to be involved in macrophage-specific functions. Sn belongs to the superfamily of sialic acid immunoglobulin (Ig)-like lectins (siglec) and was discovered by Crocker and Gordon (1985, 1986). It specifically binds to sialic acids (negatively charged carbohydrate residues) on the cell surface of glycoproteins (sialoglycoproteins) (Crocker & Gordon, 1989). Sn (other names: siglec-1 or CD169) has a molecular weight of 185 kDa and consists of 17 extracellular Ig-like domains, a transmembrane domain and a relatively short cytosolic domain (Crocker et al., 1994). Sn is missing any inhibitory tyrosine-based motifs, unlike most other members of the siglec family (Crocker et al., 2007). The extracellular region can be further categorized into the N-terminal single V-set domain, containing the sialic acid-binding site (Vinson et al., 1996) and 16 C2-set domains (Crocker et al., 1994) (**Fig. 3**).

Besides its expression on specific subpopulations of macrophages at different levels in normal tissue (Crocker & Gordon, 1986, 1989; Hartnell et al., 2001), Sn expression has also been observed on inflammatory macrophages within injured tissue in different disorders (Pope et al., 1998; Gijbels et al., 1999; Jiang et al., 1999; Nath et al., 1999; Hartnell et al., 2001; Ip et al., 2007). In contrast, resident brain microglia cells under steady-state conditions do not express detectable Sn levels (Perry et al., 1992). The molecular architecture of Sn and its high conservation from mouse to human (Hartnell et al., 2001) suggest a role in mediating cell-cell interactions (Crocker et al., 1990, 1995; Hartnell et al., 2001), especially during inflammation.

To assess the role of Sn in stroke development this study took advantage of mice deficient for Sn.

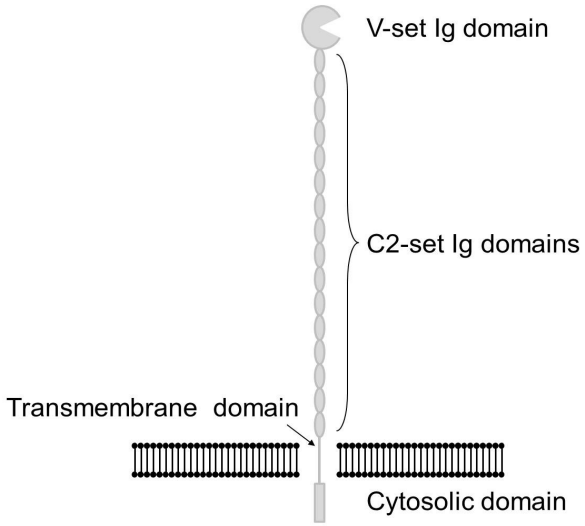

Figure 3: Structural features of sialoadhesin (Sn). The N-terminal single V-set Ig domain contains the sialic acid-binding site and is followed by 16 C2-set Ig domains, the transmembrane domain and a relatively short cytosolic domain.

1.6 Aim of the study

The contact-kinin system, as recently shown, is critically involved in the pathophysiology of I/R injury in the brain and represents an interface via FXIIa between the key processes brain swelling, inflammation, and thrombosis. In this context, blocking of distinct members of the contact-kinin system has the potential to become an effective strategy to combat neurological disorders like ischemic stroke.

Following breakdown of the BBB after focal cerebral ischemia a massive infiltration of macrophage-like cells and other immune cells into the brain is initiated. Until today, signaling molecules involved in macrophage activation and cell communication in brain stroke are elusive.

Therefore, this thesis addresses two key questions: (1) Is it possible to influence the outcome of cerebral ischemia by a multifaceted C1-inhibitor (C1-INH), already clinically approved for human use in a different indication (hereditary angioedema)? For this purpose, human plasma derived C1-INH Berinert® P was used at two doses of 7.5 U and 15.0 U, respectively. The efficacy of C1-INH was analyzed in a model of tMCAO in C57BL/6 mice with application of the inhibitor 1 hour and 6 hours, respectively after onset of ischemia as well as in a model of pMCAO with C1-INH application 1 hour post stroke. The neurological outcome of mice upon cerebral ischemia was evaluated by means of functional scoring and survival rate,

measurement of infarct volume and brain swelling, and analysis of BBB disruption, microvascular thrombosis and postischemic inflammation.

(2) What is the functional contribution of macrophage-restricted sialoadhesin (Sn) to ischemic brain injury in mice? To address the role of Sn in breakdown of the BBB and stroke development following tMCAO the study took advantage of Sn deficient mice. For further advancement of the analysis of macrophage-specific contribution to stroke development, conditional knock-out mice with a non-functional transcription factor nuclear factor (NF)-κB within the myeloid cell lineage were included in the tMCAO study. The neurological outcome of transgenic mice upon cerebral ischemia was evaluated by means of functional scoring, determination of infarct size and analysis of BBB disruption and postischemic inflammation.

2 MATERIALS AND METHODS

2.1 Materials

2.1.1 Biological reagents

C1-INH (Berinert® P) (CSL Behring GmbH, Marburg)
Goat serum (DakoCytomation)
POD biotinylated peroxidase (Vector Laboratories)
Proteinase inhibitor (Roche)

2.1.2 Buffers

All buffers were prepared and diluted in double distilled water (ddH_2O).

- **General buffers**

4% PFA (pH 7.4)

1.33 M PFA
1 drop NaOH

2% TTC

60 mM TTC

PBS (pH 7.4) (10x stock)

1.37 M NaCl
26.8 mM KCl
100 mM Na_2HPO_4
115 mM NaH_2PO_4 x H_2O

PBST (pH 7.4) (10x stock)

PBS (10x stock)
0.05% Tween® 20

- **Buffers for electrophoresis**

2x sample loading buffer (pH 6.8)

120 mM TRIS
10% SDS
20% Glycerine
20% β-Mercaptoethanol
Tip of a spatula of bromophenol blue

Running buffer (10x stock)

35 mM SDS
250 mM TRIS
1.92 M Glycine

TAE buffer (50x stock)

2 M TRIS
0.05 M EDTA
0.05% acetic acid

- **Buffers for protein isolation**

RIPA buffer (pH 7.4)

25 mM TRIS
150 mM NaCl
1% NP-40
0.1% SDS

- **Buffers for semi dry blotting and development of immunoblots**

Blocking buffer (10x stock)

PBST (10x stock)
5% milk powder

Blotting buffer (10x stock)

1.92 M Glycine
250 mM Tris
ad 1 l ddH_2O
16.66% MeOH

Stripping buffer

15% H_2O_2 in 1x PBST

Washing buffer (10x stock)

see PBST (10x stock)

2.1.3 Chemicals

Acetone (Sigma-Aldrich)
Acidic acid (Sigma-Aldrich)
Agarose (Sigma)
APS (Merck)
Aqua ad injectabilia (Braun)
Aquatex (Merck)
BCA (Sigma)
BSA (Sigma)
Bromophenol blue (Sigma)
Chloroform (Sigma-Aldrich)
Copper(II)sulfate solution (Sigma)
Tissue Tec® (Sakura Finetek)
DEPC-water (RNase-free) (Ambion)
DAB (Kem-En-Tec Diagnostics)
ECLplus (GE Healthcare)
EDTA (Sigma)
Eosin G. (Millipore)
EtOH (Sigma-Aldrich)

Ethidium bromide (Sigma-Aldrich)

Evans blue dye (Sigma-Aldrich)

Glycerine (Merck)

Glycine (Sigma)

Hematoxylin solution (Millipore)

Hydrogen peroxide 30% (Merck)

Isoflurane (Abbott or CP Pharma, respectively)

Isopropyl alcohol (Sigma-Aldrich)

KCl (Merck)

Ketamin 10% (Sigma-Aldrich)

β-Mercaptoethanol (Merck)

Methanol (Sigma-Aldrich)

Milk powder (Roth)

Mowiol 4-88 Reagent (Calbiochem)

NaCl (Sigma-Aldrich)

NaCl 0.9% in aqua ad injectabilia, isotonic (Diaco)

Na_2HPO_4 (Merck)

NaH_2PO_4 x H_2O (Merck)

NaOH (Merck)

Nonidet™P40 (NP-40) Substitute (for RIPA buffer) (Sigma)

PFA (Sigma)

Rotiphorese®Gel 30 (Roth)

Rompun 2% (Bayer Health Care)

SDS (Merck)

Sucrose (Merck)

TEMED (Sigma)

TRIS (Merck)

Triton-X-100 (Sigma-Aldrich)

TRIzol® Reagent (Invitrogen)

TTC (Sigma-Aldrich)

Tween®20 (Roth)

Vitro Clud® (R. Langenbrinck Labor- und Medizintechnik)

Xylene (Sigma-Aldrich)

2.1.4 Kits

- **DNA amplification**

PCR Mastermix (2x) Maxima^{TM} Hot Start Green (Fermentas)

The following compounds were already mixed in a ready to use - solution:
dATP, dGTP, dCTP, dTTP, $MgCl_2$, and Taq DNA-Polymerase

- **DNA purification**

DNeasy Blood & Tissue Kit 250 (Qiagen; 69506)

Contains ATL-buffer, Proteinase K, AL buffer, AW1 buffer, AW2 buffer, AE buffer and collection tubes

- **Immunoblot development**

ECLplus (GE Healthcare, RPN2132)

- **Immunoperoxidase staining**

Avidin/Biotin blocking solution (Avidin/Biotin Blocking Kit, Sp-2001, Vector Laboratories)

- **Reverse transcription (cDNA synthesis)**

TaqMan® Reverse Transcription Reagents (Applied Biosystems; N808-0234):
MuLV Reverse Transkriptase; N808-0018; 50 U/µl

RNAse Inhibitor; N808-0119; 20 U/µl

Random Hexamer; N808-0127; 50 µm

GeneAMP dNTP Blend 10 mM; N808-0260

GeneAMP 10x PCR buffer II (500 mM KCl, 100mM Tris/HCl pH 8.3) + $MgCl_2$ (25 mM); N808-0130

- **Semiquantitative RT-PCR**

TaqMan® 2x PCR Master Mix; Applied Biosystems; 4304437 (5 ml)

TaqMan® Predeveloped Assay Reagents (primer) for gene expression; Applied Biosystems

Table 1: Mouse primer used for semiquantitative RT-PCR

Primer	Part Number	Reporter	Quencer
GAPDH	4352339E	VIC	MGB
Edn-1	Mm00438656_m1	FAM	MGB
IL-1β	Mm00434228_m1	FAM	MGB
IL-10	Mm00439616_m1	FAM	MGB
TGFβ-1	Mm00441724_m1	FAM	MGB
TNF-α	Mm00443258_m1	FAM	MGB

2.1.5 Markers

Precision Plus Protein™ Dual Color Standards (Biorad)
DNA ladder 1 kb (peqlab)

2.1.6 Animals

Mice were housed in plastic cages with access to food and water ad libitum and kept under specific pathogen-free conditions at the Department of Neurology, University Clinic, Würzburg. All animal procedures were approved by the responsible animal care committee of the University of Würzburg and the appropriate authorities of the State of Bavaria (Regierung von Unterfranken).

C57BL/6 mice

C57BL/6 is the most widely used inbred strain and the first to have its genome sequenced (Mouse Genome Sequencing Consortium, 2002). C57BL/6 mice are commonly used in the production of transgenic (TG) mice. Overall, C57BL/6 mice breed well, are long-lived, and have a low susceptibility to tumors. Adult male C57BL/6N mice were purchased from Charles River (Sulzfeld, Germany).

Genetically modified mice

As TG mice only mice, which are homozygous deficient for the target gene were used in this study. All TG strains have been backcrossed onto a C57BL/6 background (C57BL/6N or C57BL/6J, respectively) for at least 8 generations. Wildtype (WT) littermates served as controls.

Sialoadhesin deficient (*Sn*$^{-/-}$) mice

Sn$^{-/-}$ mice possess a deletion in both alleles of the adhesion molecule sialoadhesin (Sn), which is restricted to macrophage-like cells.

Sn$^{-/-}$ mice, backcrossed onto a C57BL/6N background for at least eight generations, were obtained from Paul Crocker and generated as previously described (Oetke et al., 2006) by conventional gene-targeting in embryonic stem cells using homologous recombination. In brief, the Sn gene was disrupted via insertion of a neomycin resistance gene expression cassette. *Sn*$^{-/-}$ mice were genotyped for insertion of the neomycin cassette by conventional PCR, which resulted in a 1729 base pairs (bp) product for the mutated allele (**Fig. 4**) in *Sn*$^{-/-}$ mice. The WT allele (size 468 bp) was absent, indicating that *Sn*$^{-/-}$ mice used in this study were homozygous deficient for Sn.

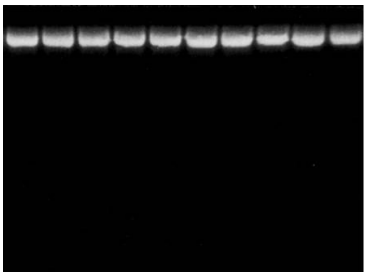

Figure 4: Representative agarose gel-electrophoresis of DNA from *Sn*$^{-/-}$ mice with insertion of the neomycin resistance gene expression cassette into the Sn gene. The mutated allele has a size of 1729 bp (TG-bond). The wildtype bond at 468 bp was absent.

Sn$^{-/-}$ have been first described in 2006 as a viable strain, exhibiting only a mild phenotype. *Sn*$^{-/-}$ mice displayed relatively increased numbers of CD8$^+$ T cells, accompanied by little decreased numbers of B220$^+$ B cells in spleen and lymph nodes. Levels of IgM were found to be reduced by about 50% compared with WT (*Sn*$^{+/+}$) mice (Oetke et al., 2006).

Nuclear factor-kappa B (NF-κB) defective (*LysM-Cre*$^{+/-}$*/IKK2*$^{fl/fl}$) mice

LysM-Cre$^{+/-}$*/IKK2*$^{fl/fl}$ mice bear a myeloid cell type-specific deletion of the inhibitor of NF-κB (IκB) kinase 2 (IKK2), the activator of NF-κB resulting in an activation defect of NF-κB in mature macrophages, microglia and granulocytes. *LysM-Cre*$^{+/-}$*/IKK2*$^{fl/fl}$ mice onto a C57BL/6J background were generated as previously described (Kanters et al., 2003) using the bacteriophage P1-derived Cre/lox P recombination system.

In brief, mice carrying two floxed (fl) IKK2 alleles (flanked by loxP sites; *IKK2$^{fl/fl}$*) (Pasparakis et al., 2002) have been crossed with *LysM-Cre$^{+/-}$* knock-in mice (Clausen et al., 1999), expressing Cre-recombinase under the control of an endogenous lysozyme M promotor in the myeloid cell lineage.

LysM-Cre$^{+/-}$/IKK2$^{fl/fl}$ mice, homozygous for the IKK2 deletion in cells of the myeloid lineage, are viable, fertile, standard in size and do not display any immoderate physical or behavioral abnormalities. As WT littermates served *LysM-Cre$^{-/-}$/IKK2$^{fl/fl}$* mice. *LysM-Cre$^{+/-}$/IKK2$^{fl/fl}$* mice and coeval WT littermates (*LysM-Cre$^{-/-}$/IKK2$^{fl/fl}$*) were obtained from Prof Dr Stefan Frantz, University Clinic, Würzburg and had been successfully tested for deletion of the IKK2 gene in his laboratory.

2.1.7 Anesthesia

Inhalation

2.5% isoflurane in a 70% N_2O/30% O_2 mixture

Intraperitoneal (i.p.) injection

10% Ketamine	500 µl (0.8%)	Inject 10 µl/g of mouse body weight
2% Rompun	250 µl (0.08%)	
NaCl (0.9%)	5500 µl (0.8%)	

2.1.8 Gels

Table 2: Composition of polyacrylamide gels

	Separating gel (12%)	**Stacking gel (5%)**
ddH_2O	1.65 ml	1.35 ml
Rotiphorese®Gel 30	2 ml	0.335 ml
1.5 M TRIS pH 8.8	1.25 ml	-
1 M TRIS pH 6.8	-	0.25 ml
10% SDS	0.05 ml	0.02 ml
10% APS	0.05 ml	0.02 ml
TEMED	0.004 ml	0.004 ml

Table 3: Composition of agarose gel (2%)

	medium (200 ml)	**large (300 ml)**
Agarose	4 g	6 g
1x TAE	200 ml	300 ml
EtBr	20 µl	30 µl

2.1.9 Antibodies and dyes

Table 4: Primary antibodies

	Antibody	**Company**	**Part number**	**Labeling**
Anti-Fibrinogen	pAb rabbit anti-mouse	Acris Antibodies	AP00766PU-N	-
Anti-Occludin	pAb rabbit anti-mouse	Abcam	ab31721	-
Anti-β-Actin	mAb mouse anti-mouse	Sigma-Aldrich	A5441	-
Anti-CD11b	mAb rat anti-mouse	AbD Serotec	MCA711	-
Anti-Ly-6B.2 alloantigen	mAb rat anti-mouse	AbD Serotec	MCA771GA	-
Anti-CD169	mAb rat anti-mouse	Serotec	MCA884	-
Anti-CD11b	mAb rat anti-mouse	Serotec	MCA74B	Biotin

Table 5: Secondary antibodies

	Antibody	**Company**	**Part number**	**Labeling**
Anti-IgG	pAb rabbit anti-mouse	Vector Laboratories	BA-4001	Biotin
Anti-IgG	pAb goat anti-rabbit	Dianova/Jackson	111-165-144	Cy3
Anti-IgG	pAb goat anti-rabbit	Abcam	ab96883	DyLight® 488
Anti-IgG	pAb donkey anti-rabbit	Dianova/Jackson	711-035-152	HRP
Anti-IgG	pAb donkey anti-mouse	Dianova/Jackson	715-035-150	HRP
Anti-IgG	pAb goat anti-rat	Abcam	Ab98386	DyLight® 488

Fluorescent dyes

Cy3-labeled streptavidin (Biozol, CLCSA1010)

Hoechst dye (Sigma-Aldrich, 33342)

2.2 Methods

2.2.1 *In vivo* experiments

2.2.1.1 Induction of focal cerebral ischemia in mice

All experiments were conducted according to the recommendations for research in mechanism-driven basic stroke studies (Dirnagl, 2006).
Male C57BL/6N mice (6-8 weeks), *Sn*$^{-/-}$ mice (8-12 weeks) or *LysM-Cre*$^{+/-}$/*IKK2*$^{fl/fl}$ mice (8-12 weeks), respectively and coeval WT littermates underwent transient middle cerebral artery occlusion (tMCAO) to induce focal cerebral ischemia (Clark et al., 1997; Kleinschnitz et al., 2010a). Additionally, C57BL/6N mice were subjected to permanent middle cerebral artery occlusion (pMCAO) (Pham et al., 2010).
For performance of MCAO mice were anesthetized through a silicon tube with an isoflurane/oxygen mixture (Anesthesia Unit, Abbott, Vapor 19.1) and placed under the operating microscope (OPMI 6-CFC; Carl Zeiss AG) in supine position on a feedback controlled heating device (TSE Systems TempControl II) to maintain the animals' body temperature at 37 °C throughout surgery. After a midline skin incision in the neck and stepwise shifting of adjacent connective tissue, the right common carotid artery (CCA) was exposed. The proximal external (ECA) and internal carotid arteries (ICA) were dissected from surrounding tissue (**Fig. 5A**). Then, the proximal CCA and the ECA were ligated and a non-permanent ligature was loosely tied around the distal CCA (**Fig. 5B**) using appropriate sterile silk suture material (3-0, 4-0, and 7-0). Finally a vessel clip (Fine Science Tools Inc., Foster City, CA, USA) was applied to the proximal ICA (**Fig. 5B**) to isolate a stretch of the artery from blood circulation between the proximal CCA ligature and the vessel clip. Following incision in this part of the blood vessel, a standardized silicon rubber-coated 6.0 nylon monofilament (6021; Doccol Corporation, Redlands, USA) was inserted (**Fig. 5C**). Upon removal of the vessel clip, the monofilament was advanced via the right ICA to occlude the origin of the middle cerebral artery (MCA) and thereby interrupting

cerebral blood flow to the territory of the MCA. Immediately after positioning of the monofilament mice in the tMCAO model were allowed to wake up in an isolated cage under heating control (heating device, Nagel GmbH). After 60 min the animals were reanaesthetized and the occluding monofilament was withdrawn to allow reperfusion. Finally, wounds were properly sutured using appropriate silk suture material (4-0) (Braeuninger et al., 2012).

For pMCAO, the occluding monofilament was left *in situ* and wounds were properly sutured. The monofilament was removed immediately before sacrificing the animals, i.e. 24 hours after onset of MCAO. The average operation time for MCAO per animal was 8 min and never exceeded 13 min.

Animals whose proximal CCA and ECA were ligated without occlusion of the MCA served as sham-operated mice.

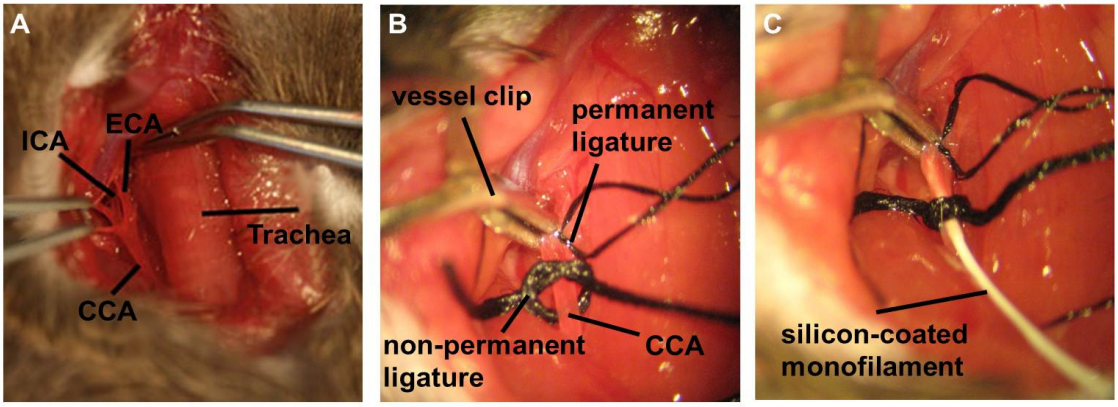

Figure 5: Representative images of the MCAO operating procedure. A) Exposed right common carotid artery (CCA), internal carotid artery (ICA) and external carotid artery (ECA) next to the trachea. Image modified from Braeuninger et al., 2012. B) Permanent ligature and non-permanent ligature applied to the ECA or CCA, respectively plus vessel clip applied to the ICA. C) Insertion of a silicon-coated monofilament in the CCA. Images (B, C) are kindly provided by Dr Friederike Langhauser.

2.2.1.2 Assessment of functional outcome in mice

Global neurological status of mice was determined according to Bederson *et al.* (1986a) (**Tab. 6**). Motor function and coordination of mice were graded using the grip test score (Moran et al., 1995) (**Tab. 6**). Therefore, mice were placed midway on a string of 50 cm length that stuck between two vertical supports, elevated 40 cm from the flat surface, and rated by a blinded investigator.

Table 6: Score system of the Bederson score and grip test score to evaluate neurological or motor function and coordination, respectively in mice.

Test	Score	Description
Bederson score	0	no deficit
	1	forelimb flexion
	2	forelimb flexion plus decreased resistance to lateral push
	3	unidirectional circling
	4	longitudinal spinning
	5	no movement
Grip test score	0	falls off the string
	1	hangs onto string by one or both fore paws
	2	hangs onto string by one or both fore paws and attempts to climb onto string
	3	hangs onto string by one or both fore paws plus one or both hind paws
	4	hangs onto string by fore and hind paws plus tail wrapped around string
	5	escape (to the supports)

2.2.1.3 Application of human plasma derived C1-inhibitor Berinert® P

One hour after induction of tMCAO or pMCAO or 6 hours after induction of tMCAO, C57BL/6N mice received a single intravenous (i.v.) injection of human plasma derived C1-inhibitor (C1-INH) Berinert® P at a dose of 7.5 units (U) or 15.0 U, respectively, diluted in 150 µl aqua ad injectabilia (carrier solution). The respective doses were chosen based on previously published work in rodent models of cerebral ischemia and 15.0 U corresponds to the amount of C1-INH required to obtain 90% to 95% inhibition of complement hemolytic activity in mice (De Simoni et al., 2003; Storini et al., 2005; Longhi et al., 2009).

2.2.1.4 Stroke assessment by magnetic resonance imaging

Serial magnetic resonance imaging (MRI) is a non-invasive method to determine infarct volumes and the dynamics of infarct development in living animals. Using a protocol for detection of bleeding, which included blood-sensitive T2*weighted (T2*w) gradient-echo images presenting ischemic lesions as hyperintense (bright) areas

(Kleinschnitz et al., 2006), secondary hemorrhagic transformation in living animals can be assessed.

MRI in mice was performed repeatedly after tMCAO on a 1.5-Tesla MR unit (Vision, Siemens). For this purpose anesthetized (isoflurane) mice were placed in supine position on a heating device (TSE Systems TempControl II) (Kleinschnitz et al., 2006, 2007). A custom-made dual channel surface coil (A063HACG, Rapid Biomedical, Würzburg) was placed on their head for further examination, while inhalation anesthesia was maintained throughout imaging. The image protocol included a coronal T2*w sequence (slice thickness 2 mm) and a blood-sensitive coronal 3D T2*w gradient-echo constructed interference in steady state (CISS; slice thickness 1 mm) sequence. MR images were transferred to an external workstation (Leonardo; Siemens) for data processing, and were assessed blinded to group assignment with respect to infarct morphology and the occurrence of intracerebral bleeding. Infarct volumes were calculated by planimetry of the hyperintense (bright) area on high-resolution CISS images. MRI was carried out in cooperation with Dr Csanad Varallay and Virgil Michels.

2.2.1.5 Tail bleeding assay

Anesthetized (ketamine/rompun) C57BL/6N mice were injected with 15.0 U C1-INH or vehicle, respectively. After 15 min, a distal 2 mm segment of the tail tip was amputated with a scalpel. Bleeding was recorded by gently absorbing blood drops every 20 sec with filter paper (Whatman^{TM}, GE Health Care), without touching the wound surface. Bleeding time was stopped immediately after cessation of bleeding (Renné et al., 2005).

2.2.2 Physiological parameters

C57BL/6N mice were controlled for several physiological parameters as blood pressure, heart rate, and arterial blood gases, which can critically affect stroke outcome.

2.2.2.1 Invasive hemodynamics

For assessment of blood pressure and heart rate, C1-INH (7.5 U or 15.0 U, respectively)-treated mice and vehicle-treated Ctrl mice were placed on a heating device (TSE Systems TempControl II) to maintain normothermia (37 °C) and anaesthetized by i.p. injection of ketamine/rompun. A high-fidelity 1.4 microtip catheter (Millar Instruments) was inserted into the right carotid artery and advanced into the left cardiac ventricle. Correct positioning of the catheter was assessed by continuous monitoring of the pressure waveform. Hemodynamic data were digitized at 4000 Hertz via a MacLab system (AD Instruments) connected to an Apple G4 PowerPC computer and analyzed (Engelhardt et al., 1999; Brede et al., 2011). This experiment was performed in cooperation with Dr Mark Brede.

2.2.2.2 Blood gas analysis

An arterial blood sample of 150 µl was drawn from the left cardiac ventricle of C1-INH (7.5 U or 15.0 U, respectively)-treated mice and vehicle-treated Ctrl mice following i.p. anesthesia with ketamine/rompun via a heparinized syringe. Arterial pH, $PaCO_2$ (mm Hg), and PaO_2 (mm Hg) were measured using an ABL 77 automated blood gas analyzer (Radiometer Medical) (Kleinschnitz et al., 2007). This experiment was performed in cooperation with Dr Mark Brede.

2.2.3 Transcardially perfusion of mice

To remove blood from vessels in order to avoid interference with histological stainings TG mice (*Sn*$^{-/-}$, *LysM-Cre*$^{+/-}$*/IKK2*$^{fl/fl}$) and WT littermates (*Sn*$^{+/+}$, *LysM-Cre*$^{-/-}$*/IKK2*$^{fl/fl}$) were deeply anesthetized with i.p. injection of ketamine/rompun and transcardially perfused immediately after animals had been tested negatively for reflexes.

Animals were placed in supine position and fixed spread-eagled on a styrofoam block in a plastic tray. A skin incision was made over the abdominal cavity and the diaphragm was cut open along, to allow access to the rib cage. Then the sternum was removed carefully to expose the heart without cutting major vessels. While holding the still beating heart with forceps the needle of a syringe filled with 20 ml of cold PBS was placed in the left ventricle in a longitudinal orientation.

Following incision in the right atrium of the heart, PBS was injected with a steady pressure within 1 min into the left ventricle while blood was running out from the right atrium. The body was 'cleared' from blood when the color of the liver turned from dark red to bright red.

2.2.4 *In vitro* experiments

2.2.4.1 Preparation of mouse brain slices

C57BL/6N mice, TG mice and WT littermates were sacrificed in deep inhalation anesthesia on day 1 or day 3 (only *LysM-Cre*$^{+/-}$*/IKK2*$^{fl/fl}$ and *LysM-Cre*$^{-/-}$*/IKK2*$^{fl/fl}$ mice) after MCAO. The skin was removed from the skull and the skull was then cut open in the middle. Following removal of the skullcap the brains were quickly taken out with a scoop and cut in three 2 mm thick coronal sections (**Fig. 6**) using a mouse brain slice matrix (Harvard Apparatus).

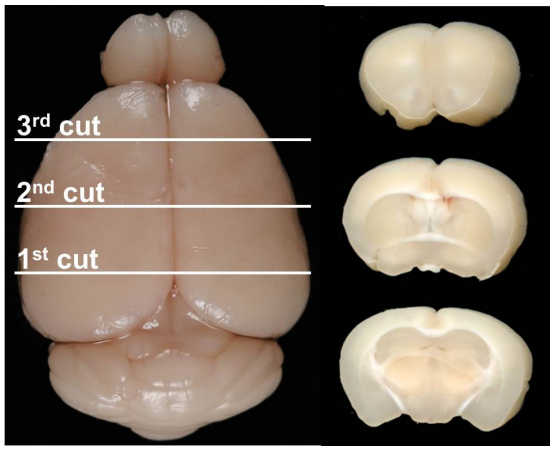

Figure 6: PFA-fixed mouse brain (left). Three coronal sections of a mouse brain (right).

2.2.4.2 Determination of infarct size

Immediately after dissection brain slices were stained with 2% 2,3,5-triphenyltetrazolium chloride (TTC) in polyphosphate buffered saline (PBS) for 10 min at room temperature to visualize the infarctions (Bederson et al., 1986b). In brief, the colorless redox-indicator TTC is enzymatically reduced to red formazan by dehydrogenases, which are abundantly arranged in the respiratory chain of the inner mitochondrial membrane. The staining intensity is well correlated with the amount of functional active mitochondria (Goldlust et al., 1996).

After scanning (Epson Perfection 3200 Photo) of the mouse brain slices, brain areas were traced and unstained areas were defined as ischemic lesions. Then the ipsilateral and contralateral hemispheric volumes of the three mouse brain slices were calculated by volumetry using the ImageJ software package (ImageJ software, National Institutes of Health, USA) as follows:

V_{direct} [mm^3] = (area TTC section 1 [mm^2] x 2.0 mm) + (area TTC section 2 [mm^2] x 2.0 mm) + (area TTC section 3 [mm^2] x 2.0 mm).

Afterwards infarctions were corrected for brain edema according to the following equation:

$V_{indirect}$ [mm^3] = $V_{infarct}$ x (1-(VI – VC)/VC),

whereas the term (VI – VC) represents the volume difference between the ischemic hemisphere and the control hemisphere and (VI – VC)/VC expresses this difference as a percentage of the control hemisphere (Ginsberg et al., 2003; Kleinschnitz et al., 2011).

2.2.4.3 Determination of blood-brain-barrier leakage with Evans blue

To determine the permeability of the BBB to macromolecules the vascular tracer Evans blue is frequently used. Evans blue displays high affinity for the blood plasma protein albumin and upon i.v. injection, immediately binds to serum albumin, using it as its transporter protein. Following disruption of the BBB albumin-bound Evans blue crosses the BBB and penetrates the brain parenchyma. Evans blue can easily be detected macroscopically within the tissue due to its intensive blue color (Hamer et al., 2002).

C57BL/6N mice treated with C1-INH (7.5 U or 15.0 U, respectively) or vehicle were i.v. injected with 100 µl of 2% Evans blue tracer diluted in 0.9% saline 1 hour after the induction of tMCAO (Belayev et al., 1996; Austinat et al., 2009). After 24 hours mice were sacrificed in deep anesthesia and brains were quickly removed and cut in 2 mm thick coronal sections as described above (**2.2.4.1**). Brain parenchyma stained by Evans blue was traced and volumetric measurements were performed using the ImageJ software package (ImageJ software, National Institutes of Health, USA) to estimate BBB damage.

2.2.4.4 Determination of brain edema formation

To assess the extent of brain edema, C1-INH (7.5 U or 15 U, respectively)-treated mice or vehicle-treated Ctrl mice were sacrificed in deep anesthesia 24 hours after tMCAO. Brains were removed, hemispheres separated, and individually weighed to assess the wet weight (WW). Thereafter, the hemispheres were dried for 72 hours at 60 °C (Incubator, Heraeus Function Line) and the dry weight (DW) was ascertained. Hemispheric water content (%) was calculated using the following formula:

((WW-DW)/WW) x 100 (Austinat et al., 2009).

2.2.4.5 Histology

Preparation of cryo-sections from mouse brain slices

TTC-stained native brain slices (**2.2.4.2)** or unstained PBS perfused brain slices (**2.2.3**) from C57BL/6N mice or $Sn^{-/-}$ and $Sn^{+/+}$ mice were embedded planar in a Cryomould (disposable vinyl specimen molds, 4566, Sakuro) with Tissue Tec® and immediately frozen in liquid nitrogen (-196 °C). Then cryo-embedded brain slices were cut into 10 µm thick coronal sections using a microtome (Leika CM 1950) and fit to a glass slide.

Hematoxylin/eosin (H&E) staining

Brain cryo-sections were stained for 8 min with hematoxylin, followed by a 10 min washing step using running tap water and 20 sec staining with 0.05% eosin. Then dehydration of the sections was carried out using the following EtOH concentrations: 3x 70%, 2x 96%, 2x 100%. Finally, sections were incubated twice in xylene for 3 min each and mounted onto an object plate with Vitro Cloud.

2.2.4.6 Immunohistochemistry

2.2.4.6.1 Immunoperoxidase staining

Staining for neutrophils

Brain sections were fixed in ice-cold acetone for 15 min at -20 °C.

Thereafter, epitopes were blocked by pretreatment with 10% of bovine serum albumin (BSA) in PBS for 45 min to prevent unspecific binding. For staining of invading neutrophils rat anti-mouse Ly-6B.2 alloantigen at a dilution of 1:1000 in PBS containing 1% BSA was added overnight at 4 °C. Afterwards, sections were incubated with a biotinylated rabbit anti-rat secondary antibody diluted 1:100 in PBS containing 1% BSA for 45 min at room temperature. Following 30 min treatment with Avidin/Biotin blocking solution to inhibit endogenous peroxidase activity, the secondary antibody was linked via streptavidin to a biotinylated peroxidase (POD) according to the manufacturer's instructions for 35 min at room temperature. Antigens were visualized via POD using the chromogen 3,3`-diaminobenzidin (DAB). The reaction was stopped with ddH_2O either when staining was observed or after 10 min. After each step, slices were washed gently. Finally, sections were mounted onto an object plate with Aquatex (Austinat et al., 2009). Negative controls for all immunohistochemical experiments included omission of primary antibody which produced no signals (not shown). Tissue sections from murine spleens served as positive controls (not shown).

Staining for macrophages/microglia

Brain sections were fixed in 4% paraformaldehyde (PFA) in PBS at 4 °C for staining of macrophages/microglia. Epitope blocking was achieved with 5% BSA in PBS containing 0.2% Triton-X-100. Staining of infiltrating macrophages and activated microglia was performed overnight using rat anti-mouse CD11b at a dilution of 1:100 in PBS containing 1% BSA as first antibody. The subsequent procedure was the same as for staining of neutrophils (Austinat et al., 2009).

2.2.4.6.2 Immunofluorescence staining

Staining for occludin

Following 10 min fixation of the brain sections in 4% PFA in PBS for immunofluorescence staining against occluding, epitope blocking was achieved by incubation with a solution containing 1% BSA, 10% goat serum, 1% Tween®20 and 0.3 M Glycine in PBS for 30 min. Thereafter, rabbit anti-mouse occludin antibody was applied overnight (4 °C) at a dilution of 1:100 in PBS containing 1% BSA.

Proteins were detected with Cy3-labeled goat anti-rabbit secondary antibodies and incubated at a dilution of 1:300 in 1% BSA in PBS at room temperature for 30 min. A fluorescent Hoechst dye was added for 15 min at a concentration of 0.4 mg/ml to stain the DNA. After each step, slices were washed gently. Finally, sections were mounted onto an object plate with Mowiol. Analysis of the sections was performed using a fluorescence microscope (Axiophot2; Carl Zeiss AG).

Staining for fibrin(ogen)

The staining procedure for fibrinogen was the same as for occludin except the blocking solution and the antibodies. Epitopes were blocked with 1% BSA in PBS containing 0.05% Triton-X-100 for 30 min at room temperature. The first antibody rabbit anti-mouse fibrinogen was applied at a dilution of 1:50 in 1% BSA in PBS overnight at 4 °C followed by incubation with the secondary antibody DyLight® 488 goat anti-rabbit at a dilution of 1:300 in PBS containing 1% BSA for 30 min at room temperature.

Double staining for sialoadhesin and macrophages/microglia

For immunofluorescence double staining cryo-embedded brain sections were fixed in 4% PFA in PBS for 10 min, followed by a 30 min epitope blocking step with PBS containing 5% BSA and 0.3% Triton-X-100. Detection of Sn was achieved with a rat anti-mouse CD169 antibody at a dilution of 1:300 in 1% BSA in PBS for 60 min at room temperature. Thereafter, brain slices were incubated with a goat anti-rat DyLight® 488 secondary antibody diluted 1:300 in PBS containing 1% BSA for 60 min at room temperature. Following treatment with Avidin/Biotin blocking solution a biotinylated primary antibody (rat anti-mouse CD11b) at a dilution of 1:100 in 1% BSA in PBS was applied for 60 min at room temperature to retrieve macrophages or activated microglia, respectively. Then sections were incubated with the fluorescent dye Cy3-labeled streptavidin at a dilution of 1:300 in PBS containing 1% BSA for 45 min at room temperature. Stained brain sections were analysed using a fluorescence microscope (Axiophot2; Carl Zeiss AG).

2.2.4.7 Quantification of immune cell infiltrates

Quantification of POD-detected immune cells was performed by selecting identical brain sections (thickness 10 µm) of ischemic hemispheres from C1-INH (7.5 U or 15.0 U, respectively)-treated mice and vehicle-treated Ctrl mice. Cells were counted at a 40-fold magnification from 5 subsequent slices (distance 100 µm) from 4 different animals under a Nikon microscope Eclipse 50i (Nikon GmbH) (Austinat.et al., 2009).

2.2.4.8 Quantification of thrombotic brain vessels

The whole brain was sliced 24 hours after tMCAO and H&E staining was performed as described above (**2.2.4.5**). Staining was examined in a blinded fashion under a microscope (Axiophot2; Carl Zeiss AG) equipped with a CCD camera (Visitron Systems). For calculation of the thrombosis index, the number of occluded blood vessels within the ischemic basal ganglia was counted in every 10^{th} slice for vehicle-treated Ctrl mice, or mice treated with 7.5 U or 15.0 U C1-INH, respectively, using a 40-fold magnification. The quantification of occluded brain vessels was performed by Dr Kerstin Göbel from the laboratory of Prof Dr Wiendl, University Clinic, Münster.

2.2.4.9 Polymerase chain reaction studies

Polymerase chain reaction (PCR) studies were used to finally quantify the relative amount of mRNA transcripts present in brain tissue of mice at 24 hours after tMCAO.

Processing for RNA isolation

Brain slices from C57BL/6N mice (treated with vehicle or 7.5 U or 15.0 U C1-INH, respectively), *Sn*$^{-/-}$ mice and WT littermates, were divided into contralateral and ipsilateral hemispheres, and then into cortex and basal ganglia. Thereafter, brain samples were covered with TRIzol® Reagent and shock-frozen in liquid nitrogen (-196 °C).

RNA isolation

Brain tissue samples were homogenized in 1 ml of TRIzol® Reagent according to the manufacturer`s instructions using a Polytron®PT MR 2100 (Kinematica AG)

homogenizer at 30.000 rpm. Following incubation for 5 min at room temperature, the homogenized samples were mixed with 0.2 ml of chloroform and shook vigorously by hand for 15 sec and incubated for another 5 min. Then, samples were centrifuged (Eppendorf Centrifuge 54152) at 12.000 rpm for 15 min at 4 °C and the upper aqueous phase, containing the RNA was transferred to a fresh tube. Thereafter, RNA solution was mixed with 0.5 ml isopropyl alcohol and incubated at room temperature for 10 min. Following centrifugation at 12.000 rpm for 10 min at 4 °C, the supernatant was removed and the RNA precipitate was washed twice with 1 ml of 75% EtOH by vortexing. After a further centrifugation step at 7.500 rpm for 5 min at 4 °C the RNA pellet was air-dried for at least 15 min. Finally, total RNA was dissolved in 10-20 µl RNase-free DEPC water by passing the solution a few times through a pipette tip, and incubating it for 10 min at 56 °C. Total RNA concentration was measured spectrophotometrically (Eppendorf BioPhotometer) and quantified using the A260/A280 absorption. Samples of total RNA were stored at -80 °C (Austinat et al., 2009).

Reverse transcription (cDNA synthesis) of total RNA

1 µg of total RNA was reverse transcribed to generate cDNA using the TaqMan® Reverse Transcription Reagents according to the manufacturer´s protocol. Thus, a mastermix was prepared (**Tab. 7**). Subsequently, the reaction tubes were each filled with 37.4 µl of mastermix, 1 µg of total RNA was pipetted and the tubes were refilled with DEPC water to the total volume of 60 µl per assay. Random Primer Hexamers were chosen for priming throughout the length of the RNA. All steps were performed wearing nitrile cloves, quickly and on ice to avoid RNase contamination. The reverse transcription was performed in a Labcycler (SensoQuest GmbH) according to the following incubation program: 10 min at 25 °C, 60 min at 42 °C and 5 min at 95 °C.

Table 7: Pipette schema for preparation of the reverse transcription mastermix

6 µl	10x RT-Buffer
13.2 µl	$MgCl_2$ (25 mM)
12 µl	dNTP-Mix
3 µl	Random-Hexamers
1.2 µl	RNase-Inhibitor
2 µl	Reverse Transcriptase

Semiquantitative real time (RT-) PCR

Semiquantitative RT-PCR was performed as previously described (Kleinschnitz et al., 2004) with a total amount of 75 ng cDNA (as total input RNA) per assay to quantify relative gene expression levels of endothelin (Edn)-1, transforming growth factor (TGF)β-1, tumor necrosis factor (TNF)-α, interleukin (IL)-1β and IL-10 with the fluorescent TaqMan® technology according to the manufacturer´s guidelines. Therefore, a mastermix was prepared (**Tab. 8**).
For relative quantification of mRNA transcripts the PCR was normalized for the amount of RNA (applied to the reverse transcription) via an endogenous control, i.e. the constitutively expressed housekeeping gene glyceraldehyde 3-phosphate dehydrogenase (GAPDH). For calibration cDNA samples received from sham-operated mice were applied and additionally, water controls were included to assure specificity and to exclude contamination. The real time PCR reactions with a total volume of 12.5 µl were run for 40 cycles using the following cycling conditions:

50 ˚C for 2 min, 95 ˚C for 10 min, (95 ˚C for 15 sec, 60 ℃ for 1 min) x 40 cycles

Table 8: Pipette scheme for mastermix for RT-PCR

6.25 µl	TaqMan® Universal 2x PCR Master Mix
0.625 µl	TaqMan® Predeveloped Assay Reagents for gene expression
0.5 µl	DEPC water
4.5 µl	cDNA sample

Each sample was measured in triplicate using a Fast 96-Well Reaction Plate (MicroAmp; Applied Biosystems) and data sets were examined for integrity by analysis of the amplification plot. The comparative Ct method was used for the relative quantification of gene expression (Winer et al., 1999; Livak & Schmittgen, 2001). Thereby $2^{-\Delta\Delta Ct}$ gives the amount of target (Edn-1, TGFβ-1, TNF-α, IL-1β and IL-10), normalized to the endogenous control (GAPDH) and relative to a calibrator (cDNA from basal ganglia or cortices, respectively of sham-operated mice). Ct indicates the number of the cycle at which the fluorescence signal of the PCR product (the fluorescence signal is increased proportional to the amount of PCR product) exceeds a certain threshold, which was arbitrarily set within the exponential phase of the PCR. ΔΔCt was calculated by the following equation:

$\Delta\Delta Ct = [(Ct_{target\ (unknown\ sample)} - Ct_{endogen\ control\ (unknown\ sample)})] - [(Ct_{target\ (calibrator\ sample)} - Ct_{endogen\ control\ (calibrator\ sample)})]$

2.2.4.10 Genotyping of mice

Genomic DNA isolation from mouse tail

Genomic DNA from *Sn*$^{-/-}$ mouse tails was purified using the DNeasy Blood & Tissue Kit 250 according to the guidelines of the manufacturer.
Therefore, tail tips were cut and dissolved in 175 µL ATL-buffer (EDTA (ethylenediaminetetraacetic acid)-SDS (sodium dodecyl sulfate)-based lysis buffer) containing 20 µl Proteinase K by overnight incubation at 56 °C using a heating device (Eppendorf Thermomixer comfort) whilst shaking (1.000 rpm). Thereafter, an additional 200 µl AL-buffer (guanidine-based lysis buffer) was pipetted to each sample and mixed gently. After addition of 200 µl EtOH and mixed by inverting for a number of times, all of the sample was applied to a mini spin column and centrifuged at 8.000 rpm for 1 min. Mini spin columns were placed in a new collection tube, 500 µl AW2 buffer (TRIS (tris(hydroxymethyl)-aminomethan)-based washing solution with EtOH) was added and mini spin columns were centrifuged for 3 min at 13.000 rpm. Then, collection tubes were replaced by fresh 2 ml reaction tubes. After adding 200 µl AE buffer (TRIS-EDTA-based elution buffer), incubation for 1 min and a further centrifugation step for 1 min at 8.000 rpm AE buffer was collected containing the DNA and stored at 4 °C.

Genotyping by PCR

Genotypes of *Sn*$^{-/-}$ mice were determined by conventional PCR analysis in a total volume of 50 µl per assay using the following primer pairs: forward 5' - CAC CAC GGT CAC TGT GAC AA - 3' and reverse 5' - GGC CAT ATG TAG GGT CGT CT - 3'. Therefore a mastermix was prepared (**Tab. 9**). Finally 1 µl of isolated genomic DNA of each mouse was added and PCR reaction was run using a special cycler program (**Tab. 10**). Afterwards amplificates were analyzed in an ethidium bromide (EtBr)-stained 2% agarose gel in 1x TAE (TRIS base-acetic acid-EDTA) buffer, which resulted in the respected amplification size of 1729 bp for the TG Sn allele.

Table 9: Pipette scheme for Sn genotyping mastermix

25.0 µl	PCR Mastermix (2x) Maxima^{TM} Hot Start Green
0.25 µl	forward primer (stock 100 µM)
0.25 µl	reverse primer (stock 100 µM)
2.5 µl	DMSO
21.0 µl	DEPC-H_2O

Table 10: Cycler program for genotyping of *Sn*$^{-/-}$ mice

5 min	94 °C	Hot start (initial denaturation)	
1 min	94 °C	Denaturation	40 cycles
1 min	61 °C	Annealing	
2 min	72 °C	Elongation	
5 min	72 °C	Final extension	
Hold	10 °C		

2.2.4.11 Western blot analysis

Western blot analysis was performed on protein lysates from ipsilateral and contralateral native basal ganglia and cortices from single mice to quantify the amount of fibrin(ogen) or occludin, respectively.
Therefore, brain slices from vehicle-treated and C1-INH (7.5 U or 15.0 U, respectively)-treated C57BL/6N mice were dissected into ipsilateral and contralateral cortices and basal ganglia and brain tissue was immediately frozen in liquid nitrogen (-196 °C) and stored at -20 °C.

Sample preparation and bicinchoninic acid (BCA) assay

Native brain samples mixed with 120 µl RIPA buffer containing 0.1% sodium dodecyl sulfate (SDS) and 4% proteinase inhibitor in a 1.5 ml reaction tube were crumbled using a teflon pestle (Bel-Art products). Samples were sonified (Bandelin Sonopuls HD60) for 15 sec to further homogenize and centrifuged for 30 min at 13.200 rpm at 4 °C. Afterwards, clear supernatants were quickly transferred to fresh reaction tubes and protein concentrations were measured using the BCA method. Different concentrations of BSA (0.05 mg/ml, 1.00 mg/ml, 2.50 mg/ml and 5.00 mg/ml) were used as standard. A mastermix composed of 1 ml BCA solution A + 20 µl Copper(II)

sulphate solution B per assay was prepared. To 1 ml mastermix 2.5 µl protein sample or 5 µl BSA or 5 µl DEPC water as blank, respectively was added. Following 30 min incubation at 37 °C protein concentrations were measured spectrophotometrically (Eppendorf BioPhotometer).

SDS-polyacrylamide gel electrophoresis (PAGE)

Equal amounts of protein (20 µg) were taken for Western blot analyses. Samples were mixed with 2x sample loading buffer containing 20% β-mercaptoethanol and denaturated for 10 min at 95 °C. Protein separation was performed on a 12% SDS polyacrylamide gel according to Laemmli (1970) with a Bio-Rad Mini-Protean® TetraCell module (Bio-Rad Laboratories) and a power supplier (Power Pac Basic, Bio-Rad Laboratories). After SDS-PAGE proteins were transferred to an activated (with MeOH) polyvinylidene fluoride (PVDF, 0.45 µm, GE Health Care) using a blotting chamber from PeqLab biotechnologies and a power supplier (Power Pac HC, Bio-Rad Laboratories GmbH) at 100 mA per gel for 1.5 hours.

Immunoblotting

After blocking for 30 min with a blocking buffer at room temperature to prevent unspecific antibody binding, membranes were incubated with the primary antibody on a shaking platform (Heidolph Duomax 1030) at 4 °C overnight with the following dilutions in blocking buffer: anti-fibrinogen pAb 1:500 or anti-occludin pAb 1:1000. After a washing step with TBST, membranes were incubated for 60 min with Horseradish peroxidase (HRP)-conjugated donkey anti-rabbit IgG with gentle shaking at a dilution of 1:5000 at room temperature and were finally developed using ECLplus according to the manufacturer´s guidelines. Chemiluminescence was detected on medical X-Ray films (Fujifilm Super RX; Hartenstein) for several time points.
Thereafter, membranes were incompletely stripped with 15% H_2O_2 in PBST for 30 min at room temperature and blocked again. To detect the loading control anti-actin mAb diluted 1:75.000 in blocking buffer was used as primary antibody and retrieved with donkey anti-mouse IgG. Visualization was performed with ECLplus and X-Ray films (Kraft et al, 2010a).

2.2.5 Statistical analysis

Mean values were reported as ± standard deviation (SD) and declared in the text, except for functional outcome scores, which were illustrated as scatter plots. The median with the 25% and 75% percentile was given in the text. Statistical analyses were performed using GraphPad Prism 5 (GraphPad software package). Data were tested for Gaussian distribution with the Kolmogorov-Smirnov test (with Dallal-Wilkinson-Lillie for P value) and the D´Agostino and Pearson omnibus normality test. $P < 0.05$ was considered statistically significant.

3 RESULTS

3.1 Assessment of the therapeutic effects of C1-inhibition in acute stroke in mice

3.1.1 Infarct size and outcome after tMCAO following immediate application of C1-inhibitor

Based on the fact that the contact-kinin system is activated during reperfusion the therapeutic potential of the human plasma derived C1-inhibitor (C1-INH) Berinert® P was tested under conditions of ischemia and reperfusion. Therefore, young adult male C57BL/6N mice were subjected to 1 hour of tMCAO and C1-INH was injected at a low dose of 7.5 units (U) and a high dose of 15.0 U per mouse 1 hour after onset of ischemia. Control (Ctrl) mice received equal amounts of vehicle (150 µl aqua ad injectabilia) instead of C1-INH. The therapeutic doses of C1-INH were chosen based on results of previous dose-finding studies (De Simoni et al., 2003, 2004). Twenty-four hours after tMCAO infarct volumes were assessed by staining of the brain slices with 2% 2,3,5-triphenyltetrazolium chloride (TTC), a technique which is frequently used to distinguish macroscopically between ischemic and healthy (viable) tissue (Chiamulera et al., 1993; Hatfield et al., 1991).

Mice treated with 15.0 U C1-INH displayed significantly reduced infarct sizes by approximately 60% compared with Ctrl mice, whereas the low dose of 7.5 U C1-INH did not change infarct volumes (mean 103.7 ± 27.2 mm^3 [Ctrl] versus (vs.) 81.3 ± 33.4 mm^3 [7.5 U] or 40.4 ± 27.9 mm^3 [15.0 U], respectively; $P > 0.05$ [Ctrl vs. 7.5 U] or $P < 0.0001$ [Ctrl vs. 15.0 U]) (**Fig. 7**).

To investigate whether C1-INH treatment is also of functional relevance the global neurological function was assessed by the Bederson score (Bederson et al., 1986a) and the motor function and coordination by the grip test score (Moran et al., 1995). Mice treated with 15.0 U C1-INH displayed significantly better overall neurological function as well as improved motor function and coordination compared with Ctrl mice. The low dose of 7.5 U C1-INH failed to significantly ameliorate functional outcome (**Fig. 7**) indicating a dose-dependent effect of C1-INH in focal cerebral ischemia (Bederson score: median 3.0 [3.0, 3.75] [Ctrl] vs. 3.0 [2.5, 3.0] [7.5 U] vs. 1.0 [0.75, 3.0] [15.0 U], respectively; $P > 0.05$ [Ctrl vs. 7.5 U] or $P < 0.001$ [Ctrl vs. 15.0 U]) (Grip test score: median 3.0 [0.5, 3.75] [Ctrl] vs. 3.0 [3.0, 3.25] [7.5 U] vs. 4.0

[4.0, 5.0] [15.0 U], respectively; P > 0.05 [Ctrl vs. 7.5 U] or P < 0.001 [Ctrl vs. 15.0 U]).

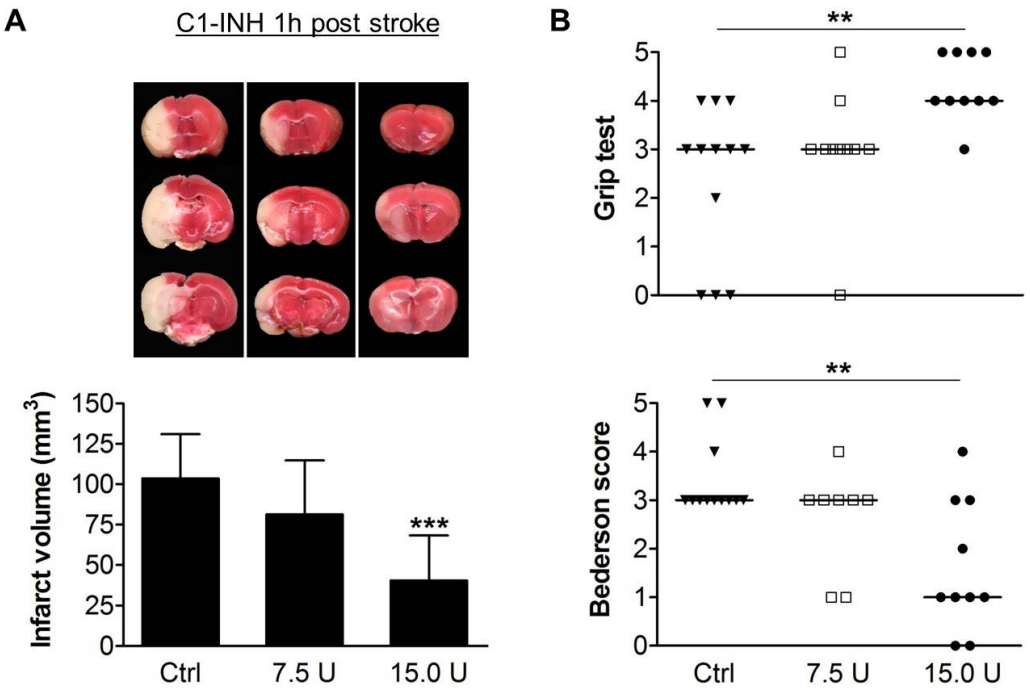

Figure 7: A) Representative 2,3,5-triphenyltetrazolium chloride (TTC) staining of three corresponding coronal brain sections (upper panel) and infarct volumetry from the coronal brain sections of control mice (Ctrl) and mice treated with 7.5 U or 15.0 U C1-INH 1 hour post stroke on day 1 after tMCAO (lower panel) (n = 10-12/group). ***P < 0.0001, 1-way analysis of variance (ANOVA), Bonferroni post hoc test, 15.0 U group compared with Ctrl group. B) Neurological Bederson score (lower panel) and grip test score (upper panel) on day 1 after tMCAO of the groups indicated (n = 10-12/group). **P < 0.001, Kruskal-Wallis test followed by Dunn multiple comparison test, 15.0 U group compared with Ctrl group.

3.1.2 Long-term outcome after immediate C1-inhibitor treatment

First, the functional outcome and mortality over a period of one week after ischemic stroke was determined between C1-INH-treated and sham-operated animals. Until day 7 after tMCAO, 9 out of 10 Ctrl mice (90%) had died, which confirmed previous studies of our group (Austinat et al., 2009; Kleinschnitz et al., 2010b). In contrast, only one out of 10 mice (10%) following treatment with 15.0 U C1-INH had dies until day 7 after cerebral ischemia (P < 0.001). The effect of 7.5 U C1-INH was less pronounces in reducing mortality, but low dose treatment was still effective since only three out of 10 mice had died (P < 0.05) (**Fig. 8**).

In line with these findings, mice received 15.0 U C1-INH 1 hour after onset of ischemic stroke performed significantly better in the Bederson score and grip test score between day 1 and day 7 post tMCAO compared with Ctrl mice or mice treated with 7.5 U C1-INH (Bederson score: day 3: median 3.0 [3.0, 3.0] [Ctrl] vs. 1.0 [1.0, 1.5] [7.5 U] or 1.0 [0.5, 1.0] [15.0 U], respectively; $P < 0.001$ [Ctrl vs. 7.5 U] and $P < 0.0001$ [Ctrl vs. 15.0 U]; day 5: median 2.0 [2.0, 3.0] [Ctrl] vs. 1.0 [0.25, 1.0] [7.5 U] or 0.0 [0.0, 1.0] [15.0 U], respectively; $P < 0.001$ [Ctrl vs. 15.0 U]) (grip test score: day 3: median 3.0 [2.0, 3.0] [Ctrl] vs. 3.5 [3.0, 4.0] [7.5 U] or 4.0 [4.0, 5.0] [15.0 U], respectively; $P < 0.001$ [Ctrl vs. 15.0 U]; day 5: median 3.0 [2.0, 3.0] [Ctrl] vs. 5.0 [4.0, 5.0] [7.5 U] or 5.0 [4.0, 5.0] [15.0 U], respectively; $P < 0.05$ [Ctrl vs. 7.5 U] and $P < 0.05$ [Ctrl vs. 15.0 U]) (**Fig. 9**). These findings indicate a sustained neurological protection mediated by early applied high dose (15.0 U) of C1-INH, even at later stages of ischemia.

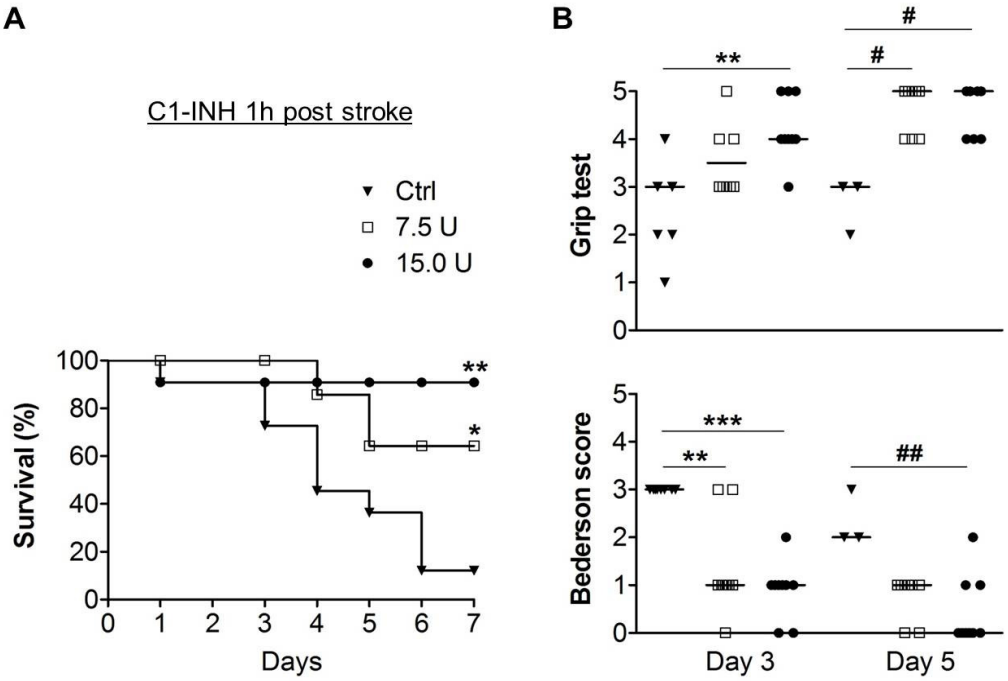

Figure 8: A) Survival of control mice (Ctrl) and mice treated with 7.5 U or 15.0 U C1-INH 1 hour post stroke until day 7 after tMCAO (n = 10/group). **P < 0.001, *P < 0.05, log rank test, 7.5 U or 15.0 U group, respectively compared with Ctrl group. B) Long-term neurological Bederson score (lower panel) and grip test score (upper panel). Figures show a selection of representative scores on day 3 and 5 after tMCAO of Ctrl mice and mice treated with 7.5 U or 15.0 U C1-INH 1 hour post stroke (n = 3-10/group). ***P < 0.0001, **P < 0.001, ##P < 0.001, #P < 0.05, Kruskal-Wallis test followed by Dunn multiple comparison test, 7.5 U or 15.0 U group, respectively compared with Ctrl group on day 3 (*) and day 5 (#), respectively.

Next, the safety profile of C1-INH treatment was tested by means of serial magnetic resonance imaging (MRI) on day 1 and 7 after ischemia to determine the dynamics of infarct development.

Twenty-four hours after tMCAO MRI reaffirmed smaller infarctions in animals received 15.0 U C1-INH (day 1: mean 84.4 ± 26.1 mm^3 [Ctrl] vs. 35.8 ± 19.2 mm^3 [15.0 U], respectively; $P < 0.001$; day 7: mean 42.5 ± 16.2 mm^3 [Ctrl] vs. 16.4 ± 12.8 mm^3 [15.0 U], respectively; $P < 0.05$), compared with TTC assessed infarct sizes of mice treated in the same way. Importantly, follow-up MRI on day 7 after onset of ischemia demonstrated that infarct sizes in mice after 15.0 U C1-INH application did not increase between day 1 and 7 ($P > 0.05$), indicating a long-term neuroprotective effect in cerebral ischemia by high dose (15.0 U) C1-INH treatment (**Fig. 9**).

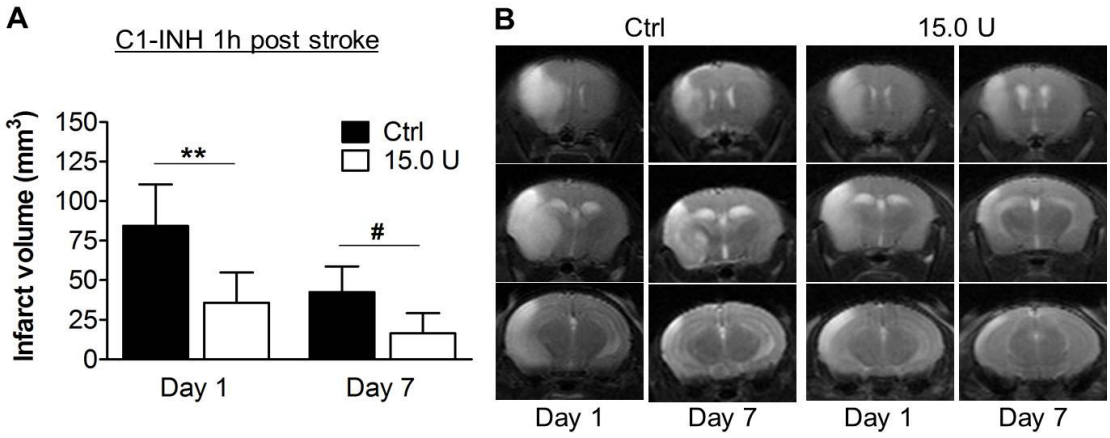

Figure 9: A) Magnetic resonance imaging (MRI)-based infarct volumetry of control mice (Ctrl) or mice treated with 15.0 U C1-INH 1 hour post stroke on day 1 and 7 after tMCAO (n = 5-7/group). **$P < 0.001$, $^{\#}P < 0.05$, unpaired, two-tailed Student´s *t*-test, 15.0 U group compared with Ctrl group on day 1 (*) and day 7 ($^{\#}$), respectively. B) Representative panel of MRI pictures from Ctrl mice and mice treated with 15.0 U C1-INH. Ischemic lesions on serial coronal T2*weighted gradient-echo MR sequences are depicted as hypointense (bright) areas.

The alleged reduction of infarct sizes on day 7 post stroke in treated and untreated animals (**Fig. 9**) was due to infarct maturation and subsequent fogging effects on MRI rather than true diminishment of infarction as described recently by Wagner *et al.* (2012). Importantly, infarcts always appeared hyperintense (bright) on T2*w MRI which represents a special sequence sensitive for intracerebral hemorrhage. Hypointense (dark) areas indicating intracerebral haemorrhage on T2*w MRI were always absent from C1-INH-treated mice as well as vehicle-treated Ctrl mice (**Fig. 9**).

This finding provides important safety data on C1-INH treatment early after infarction and at a more advanced stage of infarct development.

To determine the effect of C1-INH concentrate on normal haemostasis in mice, a tail-bleeding assay was performed with sham-operated mice. 15 min after injection of C1-INH (15.0 U) or vehicle, no differences in bleeding times could be detected between both groups (P > 0.05) (**Fig. 10**).

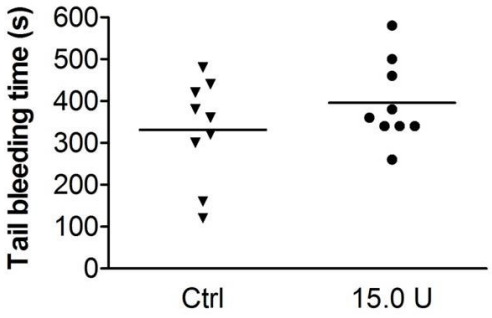

Figure 10:
Tail bleeding times of control mice (Ctrl) and 15.0 U C1-INH-treated mice 15 min after injection of vehicle or C1-INH, respectively (n = 9/group). Not significant, P > 0.05, unpaired, two-tailed Students *t*-test.

3.1.3 Consequences of delayed application of C1-inhibitor on stroke outcome

One critical issue in treatment of acute stroke patients is the narrow application window for thrombolysis with rt-PA, which is currently less than 4.5 hours after onset of stroke symptoms. Thus, treatments that can be given thereafter are eagerly awaited.

In an attempt to widen the critical therapeutic window of exogenously applied C1-INH, mice were subjected to 1 hour of tMCAO and injected with C1-INH 6 hours after stroke onset. Neither treatment with low dose of 7.5 U C1-INH nor high dose of 15.0 U C1-INH could reduce infarct sizes compared with vehicle-treated Ctrl mice (mean 102.5 ± 29.0 mm^3 [Ctrl] vs. 102.4 ± 29.6 mm^3 [7.5 U] or 94.7 ± 45.8 mm^3 [15.0 U], respectively; P > 0.05) (**Fig. 11**).

In contrast, global neurological and motor-functional deficits of mice following delayed treatment with 15.0 U C1-INH were strongly reduced compared with Ctrl mice or mice treated with 7.5 U C1-INH 6 hours after tMCAO (Bederson score: median 3.0 [3.0, 3.75] [Ctrl] vs. 3.0 [2.5, 3.0] [7.5 U] or 2.0 [1.0, 3.0] [15.0 U], respectively; P < 0.001 [Ctrl vs. 15.0 U]; grip test score: median 3.0 [0.75, 4.0] [Ctrl] vs. 4.0 [3.0, 4.0] [7.5 U] or 5.0 [3.75, 5.0] [15.0 U], respectively; P < 0.001 [Ctrl vs. 15.0 U]) (**Fig. 11**). This finding indicates that it is possible to improve outcome without affecting lesion size.

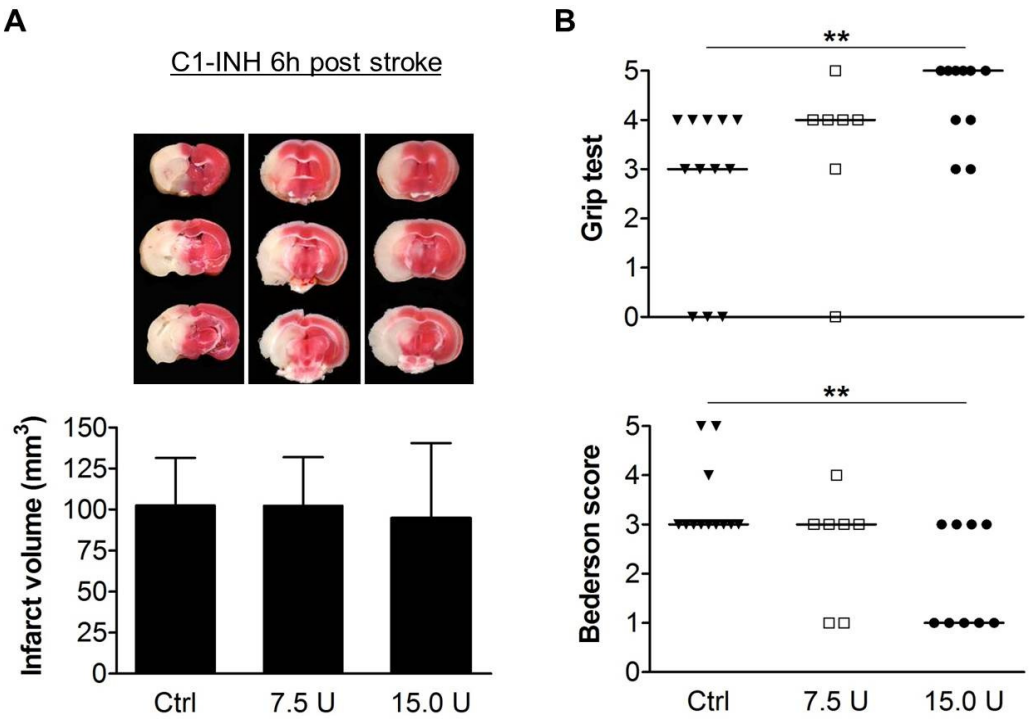

Figure 11: A) Representative 2,3,5-triphenyltetrazolium chloride (TTC) staining of three corresponding coronal brain sections (upper panel) and infarct volumetry from the coronal brain sections on day 1 after tMCAO of control mice (Ctrl) and mice treated with 7.5 U or 15.0 U C1-INH 6 hours post stroke (lower panel) (n = 9-12/group). P > 0.05, 1-way ANOVA, Bonferroni post hoc test, C1-INH (7.5 U and 15.0 U)-treated mice compared with Ctrl mice. B) Neurological Bederson score (lower panel) and grip test score (upper panel) of Ctrl mice and mice treated with 7.5 U or 15.0 U C1-INH 6 hours post stroke on day 1 after tMCAO (n = 9-12/group). **P < 0.001, Kruskal-Wallis test followed by Dunn multiple comparison test, 15.0 U group compared with Ctrl group.

In order to assure, that beneficial effects of C1-INH did not result from insufficient occlusion of the origin of the MCA the regional CBF (rCBF) was monitored before surgery, 10 min after occlusion and again 10 min after reperfusion applying Laser-Doppler flowmetry as described elsewhere (Dirnagl et al., 1989; Connolly et al., 1996; Brede et al., 2011). The rCBF analysis was performed in our group and showed full occlusion of the MCA origin by dramatically reduced blood flow in the territory of the MCA in vehicle- and C1-INH (7.5 U or 15.0 U, respectively)-treated mice. Upon removal of the monofilament rCBF was almost fully restored (**Fig. 12**).

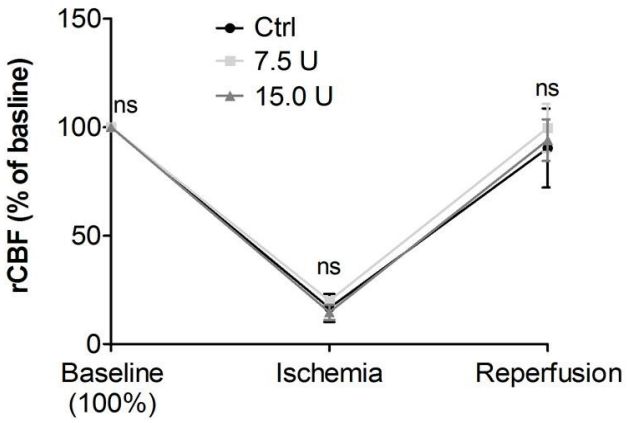

Figure 12: Regional cerebral blood flow (rCBF) in the territory of the right middle cerebral artery (MCA) as measured by Laser Doppler flowmetry in vehicle-treated control mice (Ctrl) and mice treated with 7.5 U or 15.0 U C1-INH (n = 3/group) at Baseline levels, after insertion of the filament (Ischemia) and again 10 min after removal of the filament (Reperfusion). No differences in rCBF were observed between the groups at any time point, 2-way ANOVA, Bonferroni post hoc test, ns: not significant.

3.1.4 Effects of C1-inhibitor after permanent cerebral ischemia

To investigate whether the therapeutic effects of C1-INH critically depend on reperfusion mice were challenged in the model of permanent occlusion of the MCA (pMCAO) and injected with C1-INH 1 hour after beginning of filament-induced occlusion.

In contrast to the striking results of tMCAO studies, C1-INH in neither dose (7.5 U and 15.0 U) was able to reduce infarct sizes (mean 137.2 ± 12.2 mm^3 [Ctrl] vs. 134.9 ± 44.2 mm^3 [7.5 U] or 138.1 ± 23.5 mm^3 [15.0 U], respectively; $P > 0.05$) (**Fig. 13**) or improve functional outcomes (Bederson score: median 3.0 [3.0, 4.0] [Ctrl] vs. 3.0 [3.0, 4.0] [7.5 U] or 3.0 [2.0, 3.0] [15.0 U], respectively; $P > 0.05$; grip test score: median 2.0 [0.0, 3.0] [Ctrl] vs. 2.0 [0.0, 3.0] [7.5 U] or 3.0 [3.0, 4.0] [15.0 U], respectively; $P > 0.05$) (**Fig. 13**) on day 1 after pMCAO compared with vehicle-treated Ctrl mice. This finding indicates a reperfusion-dependent effect of C1-INH in ischemic mice.

3.1.5 Assessment of physiological parameters of mice treated with C1-inhibitor

To exclude confounding effects on physiological parameters that by themselves may influence stroke development, additional studies to assess heart rate, blood pressure and blood gases in mice receiving vehicle or C1-INH immediately after injection were performed in cooperation with Dr Mark Brede, Department of Anaesthesiology, University of Würzburg. Effects of C1-INH in cardiovascular function were evaluated by invasive hemodynamic measurements (heart rate and blood pressure).

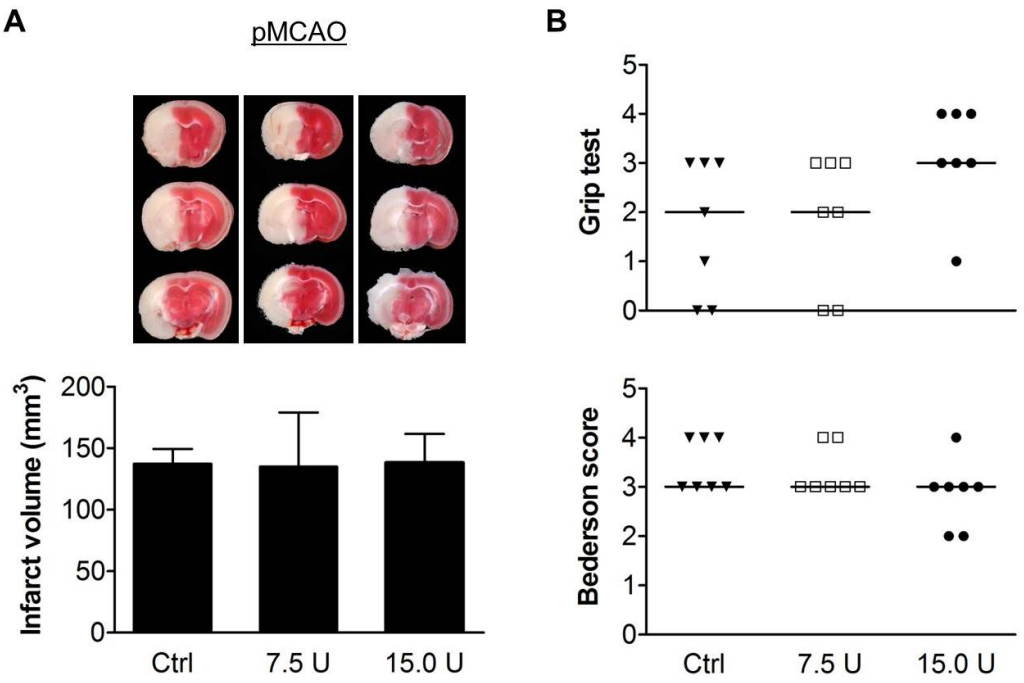

Figure 13: A) Representative 2,3,5-triphenyltetrazolium chloride (TTC) staining of three corresponding coronal brain sections (upper panel) and infarct volumetry from the coronal brain sections of control mice (Ctrl) and mice treated with 7.5 U or 15.0 U C1-INH 1 hour post stroke on day 1 after pMCAO (lower panel) (n = 7/group). P > 0.05, 1-way ANOVA, Bonferroni post hoc test, C1-INH (7.5 U and 15.0 U)-treated mice compared with Ctrl mice. B) Neurological Bederson score (lower panel) and grip test score (upper panel) on day 1 after pMCAO of the groups indicated (n = 7/group). P > 0.05, Kruskal-Wallis test followed by Dunn multiple comparison test, C1-INH (7.5 U and 15.0 U)-treated mice compared with Ctrl mice.

Following application of 15.0 U C1-INH or vehicle, respectively, neither heart rate nor mean arterial blood pressure (**Fig. 14**) showed a significant difference between the groups (heart rate: mean 475.3 ± 36.2 min^{-1} [Ctrl] vs. 462.7 ± 12.4 min^{-1} [15.0 U], P > 0.05; mean arterial blood pressure: 72.2 ± 6.5 mmHG [Ctrl] vs. 66.7 ± 5.6 mmHG [15.0 U], P > 0.05). These findings indicate that the clinically effective higher dose of 15.0 U C1-INH in ischemic stroke does not affect cardiovascular function. Blood analysis for PaO_2, $PaCO_2$ and pH was performed with an arterial blood sample from the left cardiac ventricle and likewise revealed no significant differences between mice following injection with 15.0 U C1-INH or vehicle (**Tab. 11**).

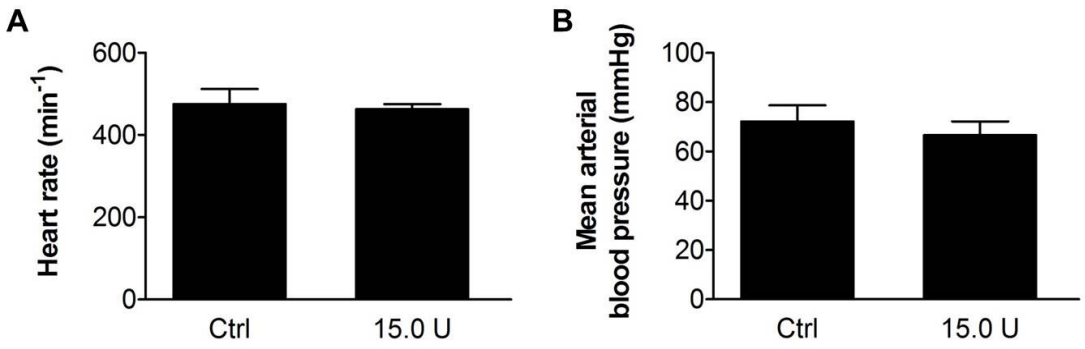

Figure 14: A) Measurement of heart rate and B) mean arterial blood pressure in control mice (Ctrl) or mice after treatment with 15.0 U C1-INH (n = 4/group). Not significant, P > 0.05, unpaired, two-tailed Student´s *t*-test.

Table 11: Results of blood gas analysis in vehicle-treated control mice (Ctrl) and mice that received 15.0 U C1-INH. ns, not significant, P > 0.05, unpaired, two-tailed Student´s *t*-test.

	Ctrl	**15.0 U**	**P**
N	3	3	
PaO_2 (mmHg)	67.1 ± 25.1	57.5 ± 6.2	ns
$PaCO_2$ (mmHg)	40.1 ± 18.9	42.5 ± 13.7	ns
pH	7.3 ± 0.05	7.3 ± 0.10	ns

3.2 Mechanisms of the therapeutic effects of C1-inhibitor on stroke outcome

3.2.1 The permeability of the blood-brain-barrier after C1-inhibitor treatment

Next, the effect of C1-INH on the patency of the blood-brain-barrier (BBB) after cerebral ischemia was examined. Therefore, the vascular tracer Evans blue was injected 1 hour after tMCAO, immediately after application of the C1-INH. The permeability of the BBB was assessed 24 hours after the procedure by means of volumetric measurements of the volume of Evans blue leakage into the brain parenchyma.

The Evans blue extravasation in mice treated with 15.0 U C1-INH 1 hour after MCA occlusion was found significantly less compared with Ctrl mice. The low dose of 7.5 U C1-INH showed only a small effect, but did not reach statistically significance (mean 51.6 ± 30.6 mm^3 [Ctrl] vs. 33.1 ± 25.0 mm^3 [7.5 U] or 13.9 ± 11.4 mm^3 [15.0 U], respectively; P < 0.001 [Ctrl vs. 15.0 U]) (**Fig. 15**). These findings indicate that 15.0 U C1-INH provides sealing of the BBB during cerebral ischemia.

Accordingly, brain edema formation was attenuated following therapeutical application of 15.0 U C1-INH compared with Ctrl mice. In contrast, the low dose of 7.5 U C1-INH failed to significantly reduce edema formation. Interestingly, there was no significant difference observable in brain edema between sham-operated mice and mice treated with 15.0 U C1-INH (mean 0.1 ± 1.3% [Sham] vs. 4.3 ± 1.1% [Ctrl] vs. 2.9 ± 1.0% [7.5 U] or 0.2 ± 1.0% [15.0 U], respectively; $P < 0.0001$ [Ctrl vs. 15.0 U]; $P < 0.0001$ [Sham vs. Ctrl]; $P < 0.001$ [Sham vs. 7.5 U]) (**Fig. 15**). This finding is remarkable because in the 1 hour tMCAO model small infarcts always occur in the basal ganglia despite successful antithrombotic treatments (*reviewed in* Stoll et al., 2008). To evaluate the degree of brain swelling, the difference of the brain water content in the ipsilateral (ischemic) and contralateral (healthy) hemisphere on day 1 after tMCAO was determined using the wet/dry weight method (Austinat et al., 2009).

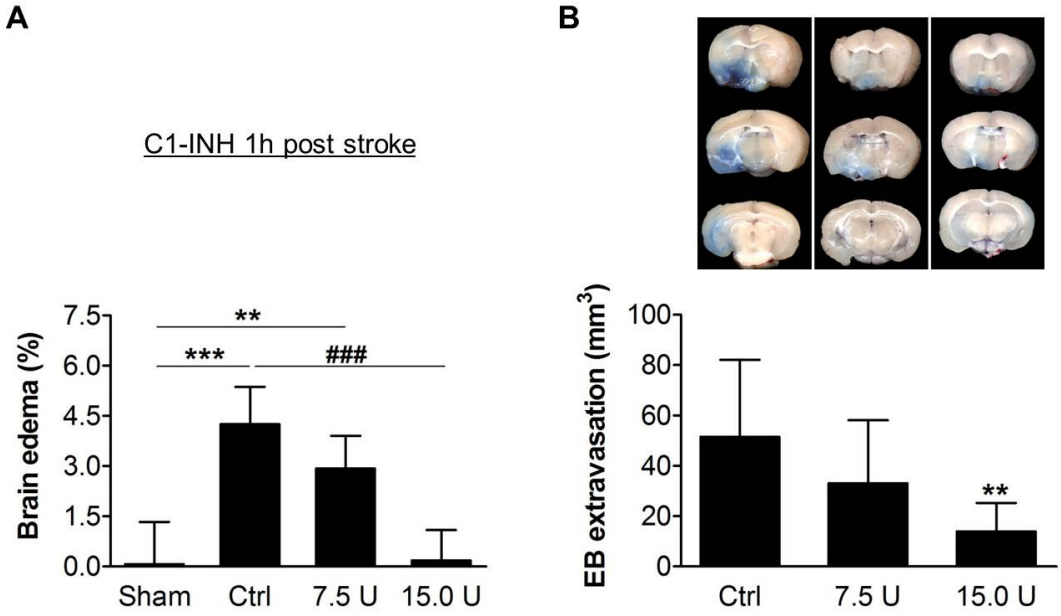

Figure 15: A) Brain edema formation as measured by the difference of brain water content in the ischemic and contralateral (healthy) hemisphere of sham-operated mice (Sham), control mice (Ctrl) and mice treated with 7.5 U or 15.0 U C1-INH, respectively, 1 hour post stroke on day 1 after tMCAO (n = 5/group). ***P < 0.0001 and **P < 0.001 or $^{\#\#\#}$P < 0.0001, respectively, 1-way ANOVA, Bonferroni post hoc test, (*) Sham group compared with Ctrl group and 7.5 U group or ($^{\#}$) Ctrl group compared with 15.0 U group, respectively. B) Representative corresponding coronal brain sections of Ctrl mice and mice treated with 7.5 U or 15.0 U C1-INH, respectively, 1 hour post stroke on day 1 after tMCAO after injection of the vascular tracer Evans blue (upper panel). Volume of Evans blue (EB) extravasation as determined by planimetry in the ischemic hemisphere of the indicated groups on day 1 after tMCAO (lower panel) (n = 7-10/group). **P < 0.001, Kruskal-Wallis test followed by Dunn multiple comparison test, 15.0 U group compared with Ctrl group.

To test whether C1-INH counteracts BBB disruption and thereby brain edema formation when applied at a delayed setting, mice were treated with C1-INH 6 hours after onset of ischemic stroke. However, the leakage of i.v. injected Evans blue at 1 hour after ischemia into the brain parenchyma did not significantly differ between C1-INH (7.5 U and 15.0 U)-treated mice and vehicle-treated Ctrl mice on day 1 after stroke (mean 44.6 ± 25.4 mm^3 [Ctrl] vs. 37.3 ± 26.8 mm^3 [7.5 U] or 14.9 ± 7.5 mm^3 [15.0 U], respectively; $P > 0.05$) (**Fig. 16**).

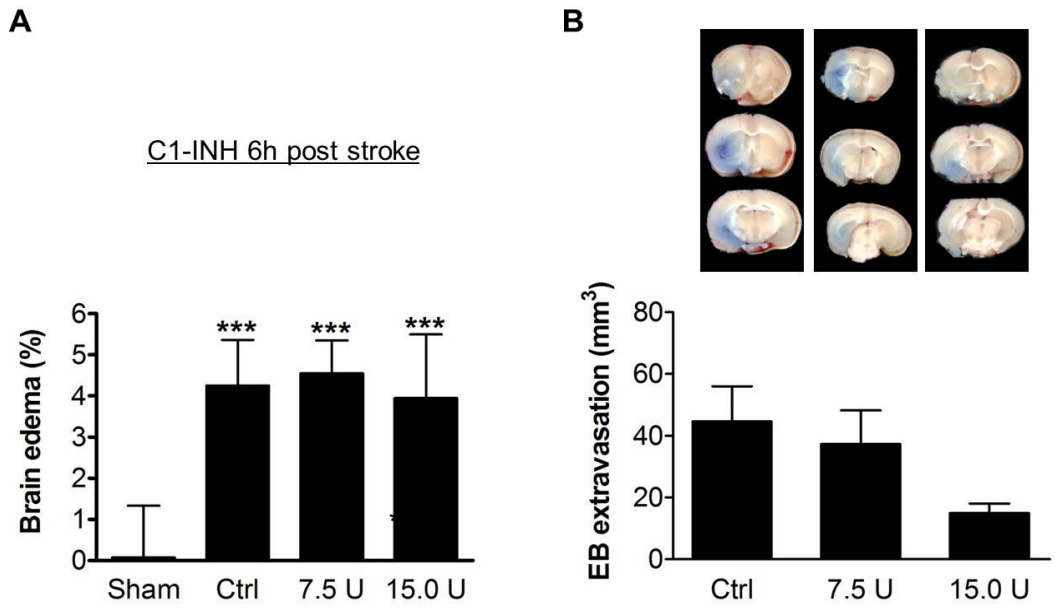

Figure 16: A) Brain edema formation as measured by the difference of brain water content in the ischemic and contralateral (healthy) hemisphere of sham-operated mice (Sham), control mice (Ctrl) and mice treated with 7.5 U or 15.0 U C1-INH, respectively, 6 hours post stroke on day 1 after tMCAO (n = 5/group). ***$P < 0.0001$, 1-way ANOVA, Bonferroni post hoc test, Sham group compared with Ctrl group, 7.5 U group and 15.0 U group, respectively. B) Representative corresponding coronal brain sections of Ctrl mice and mice treated with 7.5 U or 15.0 U C1-INH, respectively, 6 hours post stroke on day 1 after tMCAO upon injection of the vascular tracer Evans blue immediately after reperfusion (upper panel). Volume of Evans blue (EB) extravasation as determined by planimetry in the ischemic hemisphere of the indicated groups on day 1 after tMCAO (lower panel) (n = 5-6/group). $P > 0.05$, Kruskal-Wallis test followed by Dunn multiple comparison test, 15.0 U group compared with Ctrl group.

Accordingly, C1-INH of neither dose was effective in limiting edema formation when injected 6 hours after tMCAO compared with sham-operated animals (mean 0.1 ± 1.3% [Sham] vs. 4.3 ± 1.1% [Ctrl] or 4.6 ± 0.8% [7.5 U] or 3.9 ± 1.5% [15.0 U], respectively; $P < 0.0001$) (**Fig. 16**).

A similar result was obtained for edema formation in the pMCAO model. Brain edema fully evolved within 24 hours after stroke in mice treated with C1-INH (7.5 U and

15.0 U) or vehicle (Ctrl) compared with sham-operated mice (mean 0.1 ± 1.4% [Sham] vs. 4.9 ± 1.4% [Ctrl] or 4.4 ± 1.5% [7.5 U] or 4.6 ± 1.8% [15.0 U], respectively; P < 0.001) (**Fig. 17**).

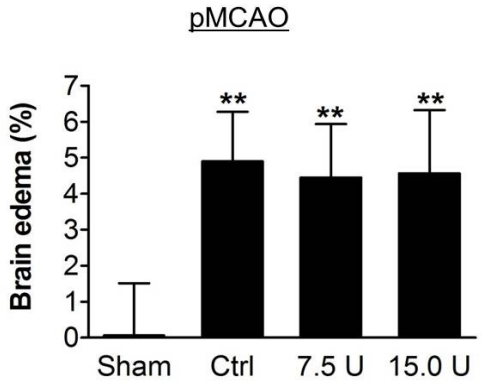

Figure 17: Brain edema formation as measured by the difference of brain water content in the ischemic and contralateral (healthy) hemisphere of sham-operated mice (Sham), control mice (Ctrl) and mice treated with 7.5 U or 15.0 U C1-INH, respectively, 1 hour after induction of stroke on day 1 after pMCAO (n = 5/group). **P < 0.001, 1-way ANOVA, Bonferroni post hoc test, Sham group compared with Ctrl group, 7.5 U group and 15.0 U group, respectively.

3.2.2 Mechanisms of C1-inhibitor action on the blood-brain-barrier

To assess the impact of C1-INH on the integrity of the BBB in mice on a molecular level the content of the tight junction protein occludin was quantified by Western blot analysis in ischemic brain lesions (**Fig. 18**). In ischemic basal ganglia of Ctrl mice the occludin expression was found strongly reduced, probably due to occludin degradation, whereas occludin expression was sustained in corresponding brain areas in mice treated with C1-INH (7.5 U and 15.0 U) (optical density: mean 0.08 ± 0.11 AU (arbitrary units) [Ctrl] vs. 0.57 ± 0.31 AU [7.5 U] or 0.54 ± 0.15 AU [15.0 U], respectively; P < 0.05 [Ctrl vs. 7.5 U] and P < 0.05 [Ctrl vs. 15.0 U]) (**Fig. 18**). This indicates a BBB stabilizing effect mediated by C1-INH.

Additionally, immunofluorescence staining was performed to further characterize the expression of occludin in ischemic brain capillaries. In accordance with the results obtained by Western blot analyses, occludin expression was preserved in vessels of C1-INH (15.0 U)-treated mice, but immunoreactivity was hardly detectable in vehicle-treated Ctrl mice or mice treated with 7.5 U C1-INH (**Fig. 19**).

Furthermore, the expression levels of endothelin (Edn)-1 in ischemic brains of Ctrl mice and mice treated with C1-INH was analyzed. Edn-1 is a vasoconstrictor peptide hormone that has been shown to be critically involved in the regulation of vascular integrity and edema formation under various pathophysiological conditions, including ischemic stroke (Matsuo et al., 2001; Lo et al., 2005).

On day 1 after tMCAO relative mRNA expression levels of Edn-1 were detected by semiquantitative real time (RT-) PCR and assessed using the Ct method (Winer et al., 1999; Livak & Schmittgen, 2001). mRNA transcripts of Edn-1 were significantly elevated in the cortices and basal ganglia of vehicle-treated mice and mice receiving 7.5 U C1-INH compared with sham-operated mice. In contrast, no significant induction of Edn-1 transcripts occurred in either brain region of mice after application of 15.0 U C1-INH (relative gene expression cortex: 1.0 ± 0.2 [Sham] vs. 16.0 ± 6.3 [Ctrl] or 16.6 ± 6.8 [7.5 U] or 3.2 ± 3.0 [15.0 U], respectively; $P < 0.0001$ [Sham vs. Ctrl]; $P < 0.0001$ [Sham vs. 7.5 U]; $P > 0.05$) (**Fig. 18**), although the basal ganglia showed ischemic lesions in all animals. Compared with Ctrl mice no upregulation of relative Edn-1 expression levels was seen in cortices of mice after 15.0 U C1-INH application ($P < 0.0001$).

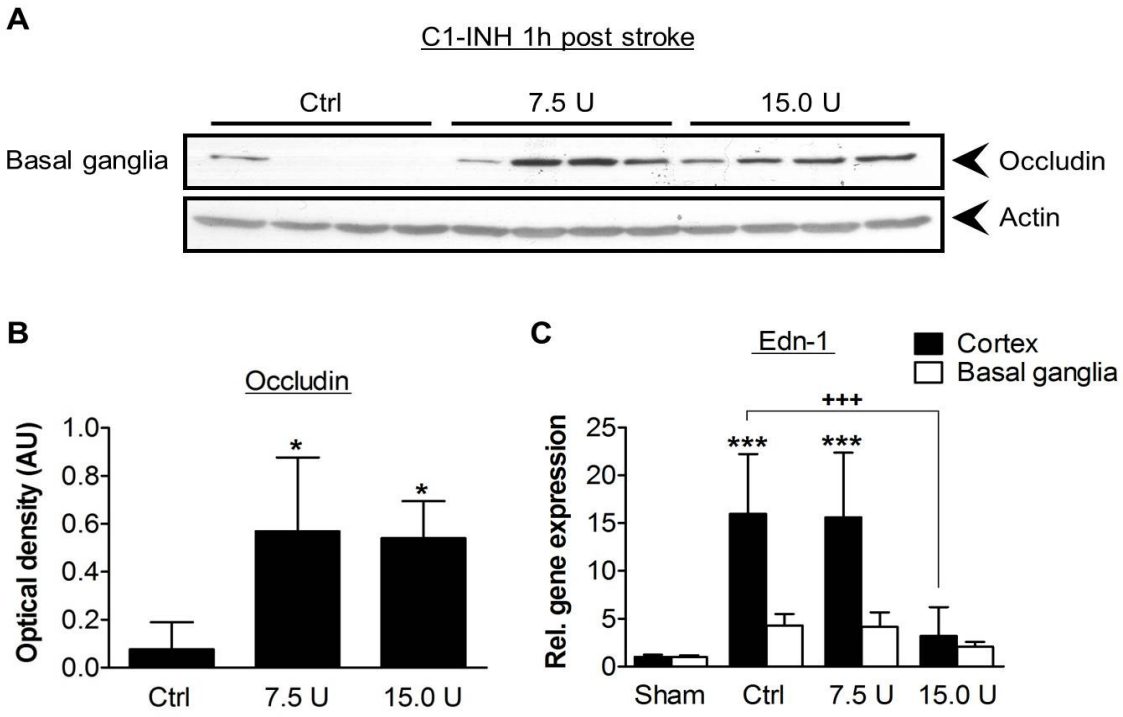

Figure 18: A) Occludin expression in the ischemic basal ganglia on day 1 after tMCAO in control mice (Ctrl) or mice receiving 7.5 U or 15.0 U C1-INH 1 hour post stroke as determined by immunoblotting. Immunoblots against occludin and actin (loading control) with 4 animals of each group are shown. B) Densitometric quantification of occludin immunoreactivity of the indicated groups (n = 4/group). *$P < 0.05$, 1-way ANOVA, Bonferroni post hoc test, 7.5 U or 15.0 U group, respectively compared with Ctrl group. C) Relative gene expression of endothelin-1 (Edn-1) in the cortices and basal ganglia of sham-operated mice (Sham), vehicle-treated controls (Ctrl), and mice treated with 7.5 U or 15.0 U C1-INH 1 hour post stroke on day 1 after tMCAO (n = 6-14/group). ***$P < 0.0001$, $^{+++}P < 0.0001$, 1-way ANOVA, Bonferroni post hoc test, 7.5 U group or 15.0 U group, respectively compared with Sham group (cortex (*)) or Ctrl group (cortex ($^{+}$)), respectively).

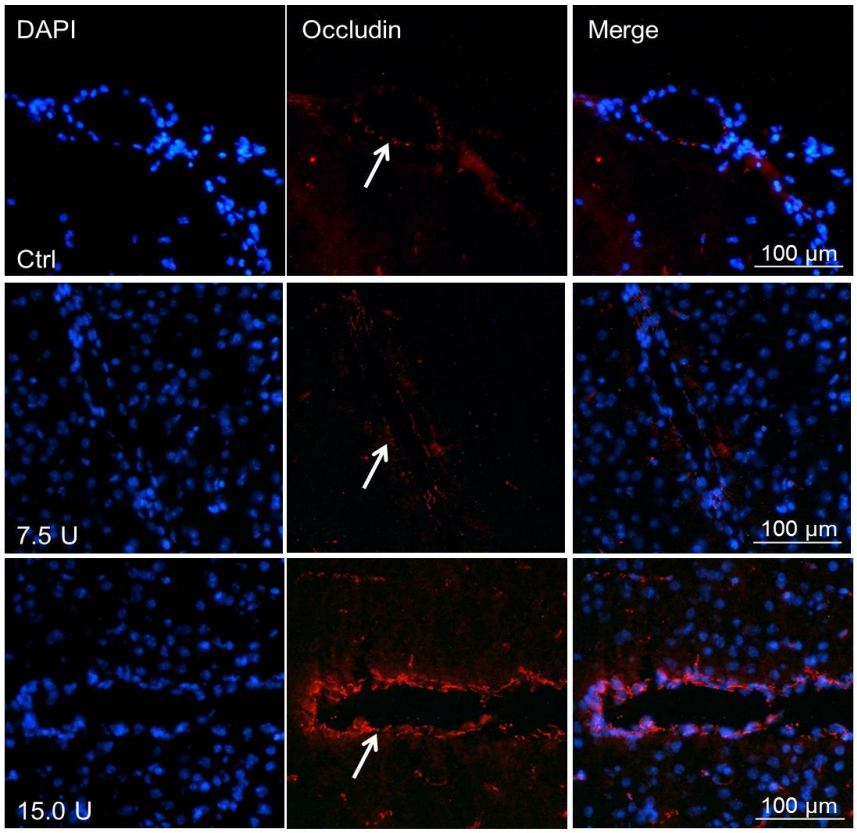

Figure 19: Immunofluorescent detection of occludin expression (white arrows) on day 1 after tMCAO in the infarcted basal ganglia of control mice (Ctrl) or mice receiving 7.5 U or 15.0 U C1-INH, respectively, 1 hour post stroke. DAPI staining depicts cell nuclei. One representative panel per group is shown.

3.2.3 Infiltration of immune cells from the circulation into the ischemic brain upon application of C1-inhibitor

Ischemic brain lesions induce a profound secondary inflammatory response (Stoll et al., 1998). Therefore, the infiltration of immune cells into the ischemic brain lesions after C1-INH treatment was assessed. Immunoperoxidase staining against neutrophilic granulocytes (neutrophils) and activated microglia/macrophages was performed on mouse brains slices (**Fig. 20**) followed by quantification of invading immune cells into ischemic hemispheres on day 1 after induction of tMCAO. The amount of neutrophils as well as activated microglia and macrophages that have entered the ischemic brains of mice treated with 15.0 C1-INH 1 hour post stroke was found strongly reduced compared with Ctrl mice or mice treated with 7.5 U C1-INH. Here, the quantity of inflammatory macrophages/microglia and neutrophils was in accordance with previously published data (Gelderblom et al., 2009) (neutrophils:

mean 299.1 ± 138.1 [Ctrl] vs. 242.9 ± 87.0 [7.5 U] or 107.2 ± 109.5 [15.0 U], respectively; $P < 0.05$ [Ctrl vs. 15.0 U]; activated microglia/macrophages: mean 676.3 ± 150.4 [Ctrl] vs. 532.9 ± 29.5 [7.5 U] or 117.1 ± 65.0 [15.0 U], respectively; $P < 0.0001$ [Ctrl vs. 15.0 U]) (**Fig. 20**). This finding indicates that application of 15.0 U C1-INH is accompanied with lower infiltration of leukocytes.

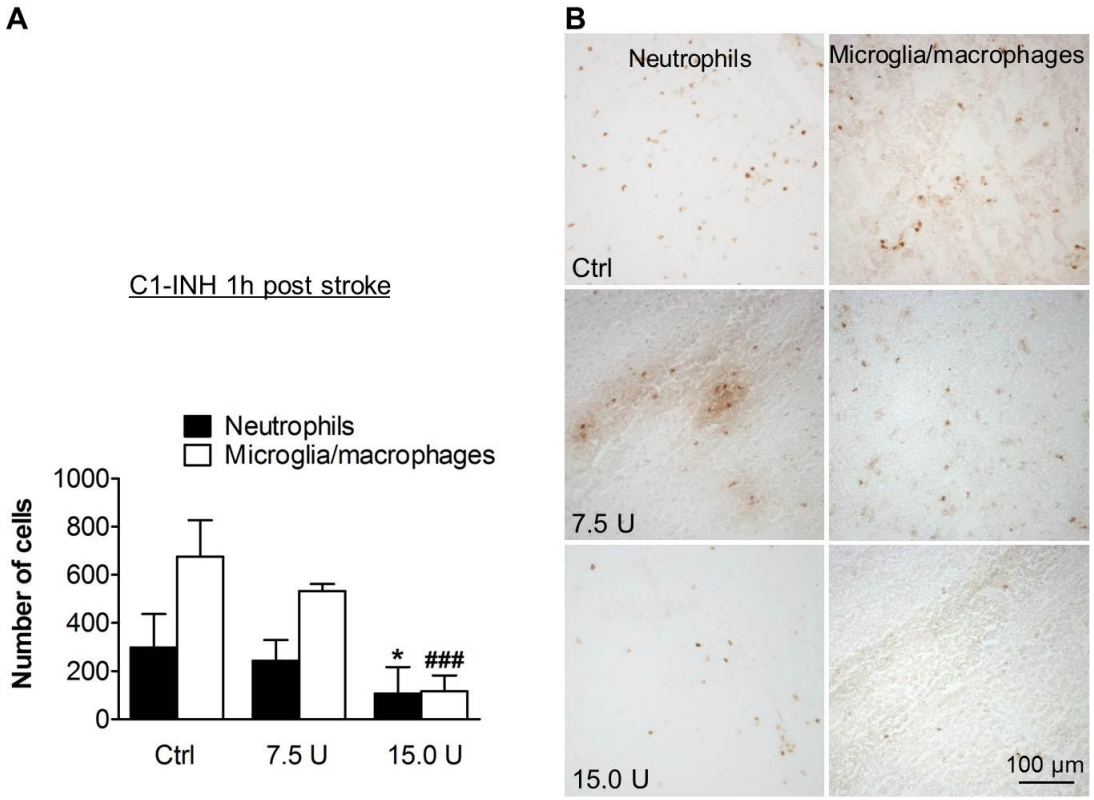

Figure 20: A) Cellular inflammatory response in the ischemic basal ganglia of control mice (Ctrl) and mice treated with 7.5 U or 15.0 U C1-INH, respectively, 1 hour post stroke on day 1 after tMCAO. Quantification of immune cell infiltration (neutrophils; macrophages/microglia) of the groups indicated (n = 3-7/group). *$P < 0.05$, $^{###}P < 0.0001$, 1-way ANOVA, Bonferroni post hoc test, 15.0 U group compared with Ctrl group (neutrophilic granulocytes (*) or microglia/macrophages ($^{\#}$), respectively). B) Representative immunohistochemistry for neutrophils (anti-Ly-6B.2) or activated microglia/macrophages (CD11b).

3.2.4 Expression levels of proinflammatory cytokines after C1-inhibitor treatment

Inflammatory mediators have shown to be upregulated secondary to ischemic stroke and may lead to exacerbation of the injury (*reviewed in* Allan & Rothwell, 2001). Hence, the mRNA expression level of a series of cytokine genes was quantified by RT-PCR and the possible impact of exogenous applied C1-INH on the expression

profile was investigated. In the ischemic basal ganglia no significant induction of gene expression on day 1 after tMCAO following vehicle or C1-INH (7.5 U and 15.0 U) treatment could be detected for the pro- and antiinflammatory cytokines interleukin (IL)-1β, tumor necrosis factor (TNF)-α, transforming growth factor (TGF)β-1 and IL-10 compared with sham-operated mice (**Tab. 12**).

Table 12: Results of relative gene expression levels of interleukin (IL)-1β, tumor necrosis factor (TNF)-α, transforming growth factor (TGF)β-1 and IL-10 in the cortices and basal ganglia of sham-operated mice (Sham), control mice (Ctrl) or mice treated with C1-INH (7.5 U or 15.0 U, respectively) obtained with RT-PCR; 1-way ANOVA following Bonferroni post hoc test, Ctrl mice or C1-INH-treated mice compared with Sham mice; ns: not significant ($P > 0.05$).

Cytokine	Ischemic area / Group	Cortex		Basal ganglia	
			P		P
IL-1β	Sham	1.1 ± 0.1		1.3 ± 0.3	
	Ctrl	77.7 ± 7.5	< 0.0001	24.4 ± 4.3	ns
	7.5 U	89.5 ± 11.7	< 0.0001	26.4 ± 4.1	ns
	15.0 U	32.1 ± 14.5	ns	22.9 ± 5.6	ns
TNF-α	Sham	1.1 ± 0.2		1.0 ± 0.3	
	Ctrl	122.2 ± 8.6	< 0.0001	23.4 ± 2.6	ns
	7.5 U	109.9 ± 8.8	< 0.0001	29.3 ± 4.4	ns
	15.0 U	56.0 ± 15.0	< 0.0001	27.2 ± 3.0	ns
TGFβ-1	Sham	1.1 ± 0.1		1.1 ± 0.1	
	Ctrl	6.6 ± 1.1	< 0.0001	1.9 ± 0.3	ns
	7.5 U	6.2 ± 0.7	< 0.0001	1.8 ± 0.4	ns
	15.0 U	3.8 ± 0.5	< 0.05	1.6 ± 0.2	ns
IL-10	Sham	1.3 ± 0.4		1.1 ± 0.2	
	Ctrl	26.8 ± 4.7	< 0.0001	6.5 ± 1.0	ns
	7.5 U	27.2 ± 3.3	< 0.0001	6.6 ± 1.2	ns
	15.0 U	12.8 ± 3.1	ns	5.3 ± 0.8	ns

In contrast, the expression levels of IL-1β transcripts (**Fig. 21**) in the infarcted cortices of vehicle-treated mice and mice receiving 7.5 U C1-INH 1 hour post stroke were found strongly elevated compared with the sham-operated group (**Tab. 12**) confirming previous investigations. Remarkably, no significant induction of IL-1β mRNA was found in cortices of mice following 15.0 U C1-INH application compared with the Sham group (**Tab. 12**). Hence, induction levels of IL-1β following treatment

with 15.0 U C1-INH were significantly reduced compared with IL-1β induction levels of the vehicle-treated group (P < 0.001).

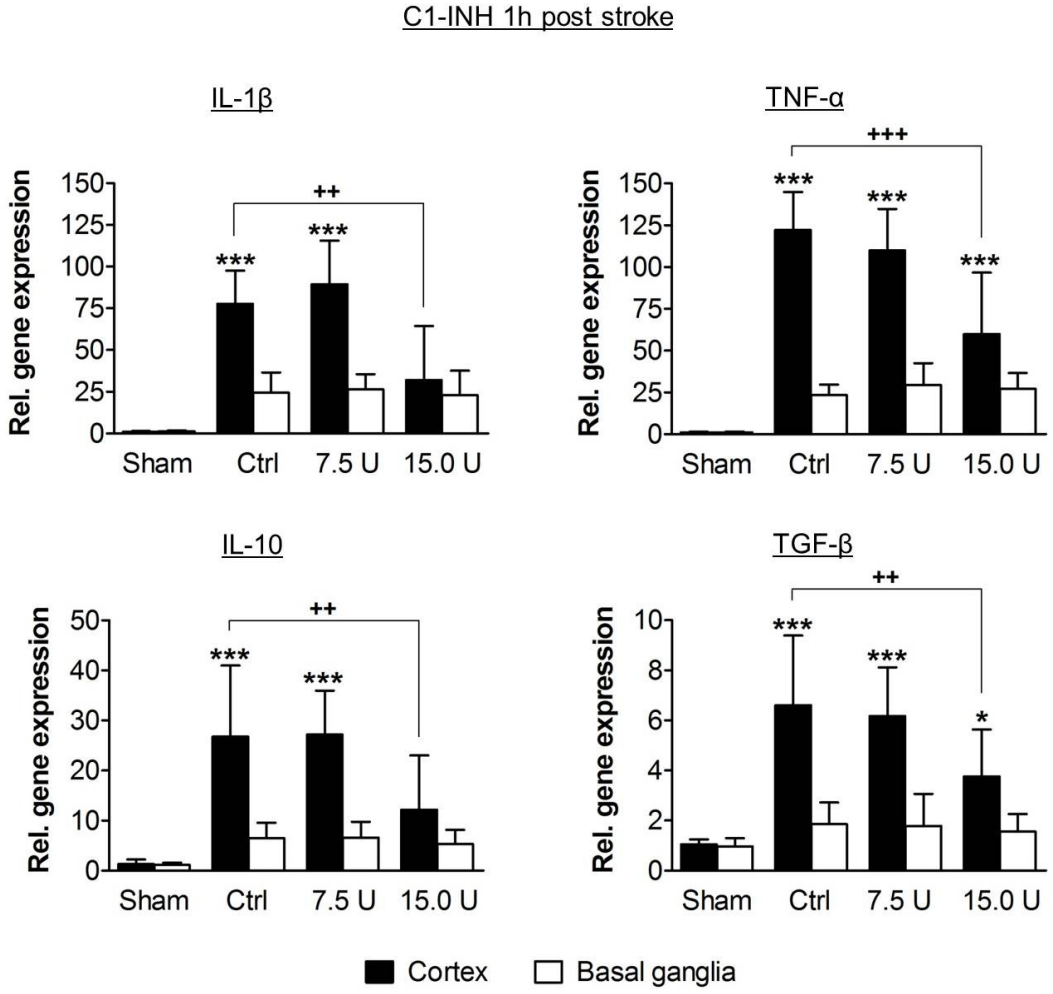

Figure 21: Relative gene expression of interleukin (IL)-1β, tumor necrosis factor (TNF)-α, transforming growth factor (TGF)β-1 and IL-10 on day 1 after tMCAO or sham-operation in the cortices and basal ganglia of sham-operated mice (Sham), control mice (Ctrl) and mice treated with 7.5 U or 15.0 U C1-INH, respectively, 1 hour post stroke (n = 5-14/group). *P < 0.001, ***P < 0.0001, $^{++}$P < 0.05, $^{+++}$P < 0.001, 1-way ANOVA, Bonferroni post hoc test, 7.5 U or 15.0 U group, respectively compared with Sham group (cortex (*)) or Ctrl group (cortex ($^{+}$)).

For TNF-α expression in the ischemic cortices (**Fig. 21**) a strong induction in all groups could be detected compared with sham-operated mice (**Tab. 12**). However, TNF-α induction in mice treated with 15.0 U was attenuated compared with untreated mice following tMCAO (P < 0.0001). Ischemic stroke also led to a significant induction of TGFβ-1 expression (**Fig. 21**) in ischemic cortices of vehicle-treated mice and mice treated with 7.5 U or 15.0 U C1-INH, respectively compared with sham-operated mice (**Tab. 12**). Again, expression of TGFβ-1 was significantly lower in mice

treated with 15.0 U C1-INH compared with Ctrl mice ($P < 0.001$). Significant upregulation of gene expression was also observed for IL-10 (**Fig. 21**) in mice treated with vehicle or 7.5 U C1-INH compared with sham-operated mice (**Tab. 12**). Induction of IL-10 was significantly reduced in mice following treatment with 15.0 U C1-INH ($P < 0.001$) compared with untreated Ctrl mice upon tMCAO. These findings suggest that efficacy of C1-INH secondary counteracts the synthesis of inflammatory cytokines probably due to smaller infarctions.

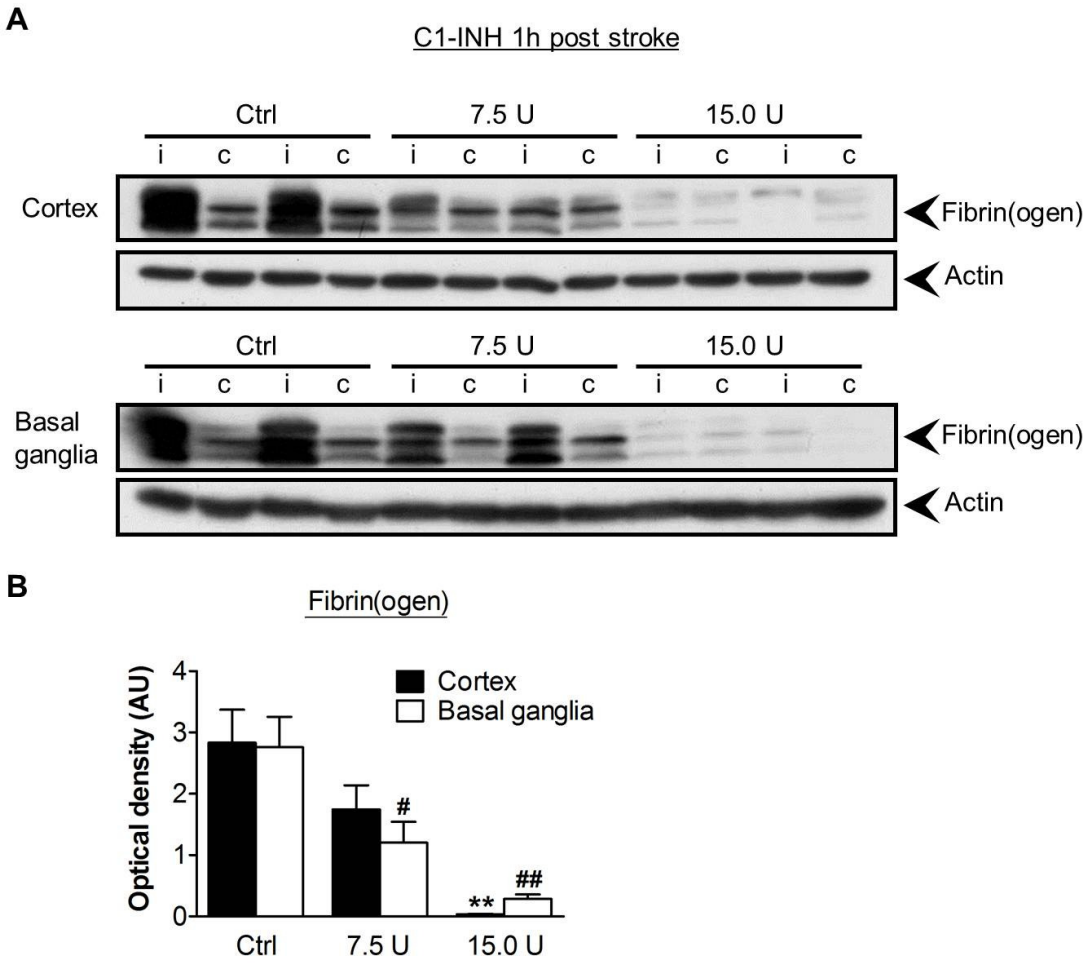

Figure 22: A) Accumulation of fibrin(ogen) in the infarcted (i) and contralateral (c) cortices (upper panel) and basal ganglia (lower panel) of control mice (Ctrl) and mice treated with 7.5 U or 15.0 U C1-INH, respectively, 1 hour post stroke as determined by immunoblotting on day 1 after tMCAO. Immunoblots against fibrin(ogen) and actin (loading control) with two animals of each group (ipsi- and contralateral hemisphere) are shown. B) Densitometric quantification of fibrin(ogen) formation in the mouse groups and infarcted brain regions indicated (n = 4/group). $^{**}P < 0.0001$, $^{\#}P < 0.05$, $^{\#\#}P < 0.001$, 1-way ANOVA, Bonferroni post hoc test, 7.5 U or 15.0 U group, respectively compared with Ctrl mice (cortex (*) or basal ganglia ($^{\#}$), respectively).

3.2.5 Microvascular thrombosis after treatment with C1-inhibitor

To test whether fibrin formation in ischemic microvessels is affected by injection of C1-INH, the amount of fibrin(ogen) within basal ganglia and cortices of mice on day 1 following ischemic stroke was quantified by Western blot analysis (**Fig. 22**).

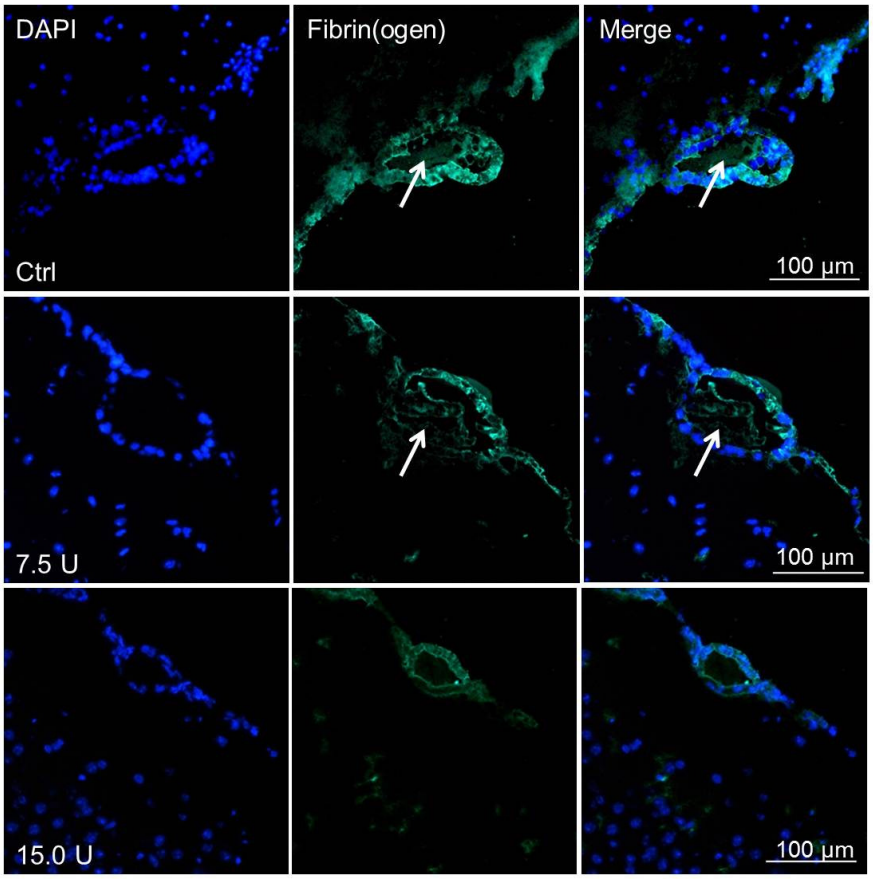

Figure 23: Immunofluorescent localization of fibrin(ogen) (white arrows) in the lumina of brain microvessels 1 day after tMCAO in the infarcted hemispheres of control mice (Ctrl) or mice treated with 7.5 U or 15.0 U C1-INH, respectively, 1 hour post stroke. DAPI staining depicts cell nuclei. One representative panel per group is shown.

The levels of fibrin(ogen) in ischemic brains of vehicle-treated mice and mice treated with 7.5 U C1-INH 1 hour post stroke were dramatically elevated in comparison with both ischemic basal ganglia and cortices following application of 15.0 C1-INH (optical density cortex: mean 2.83 ± 1.08 AU [Ctrl] vs. 1.74 ± 0.79 AU [7.5 U] or 0.03 ± 0.02 AU [15.0 U], respectively; $P < 0.001$ [Ctrl vs. 15.0 U]; optical density basal ganglia: mean 2.76 ± 1.00 AU [Ctrl] vs. 1.20 ± 0.68 AU [7.5 U] or 0.28 ± 0.15 AU [15.0 U], respectively; $P < 0.05$ [Ctrl vs. 7.5 U]; $P < 0.001$ [Ctrl vs. 15.0 U]) (**Fig. 22**). Compared with contralateral (c) hemispheres there was no clear difference of

fibrin(ogen) detectable in ipsilateral (i) sides in the 15.0 U C1-INH treatment group, whereas the fibrin(ogen) levels between ipsi- and contralateral sides in both other groups (Ctrl and 7.5 U C1-INH) highly differed.

The results obtained by immunoblot analysis could be validated by immunofluorescence staining (**Fig. 23**) demonstrating less fibrin(ogen) deposits in ischemic brain capillaries of mice treated with 15.0 C1-INH.

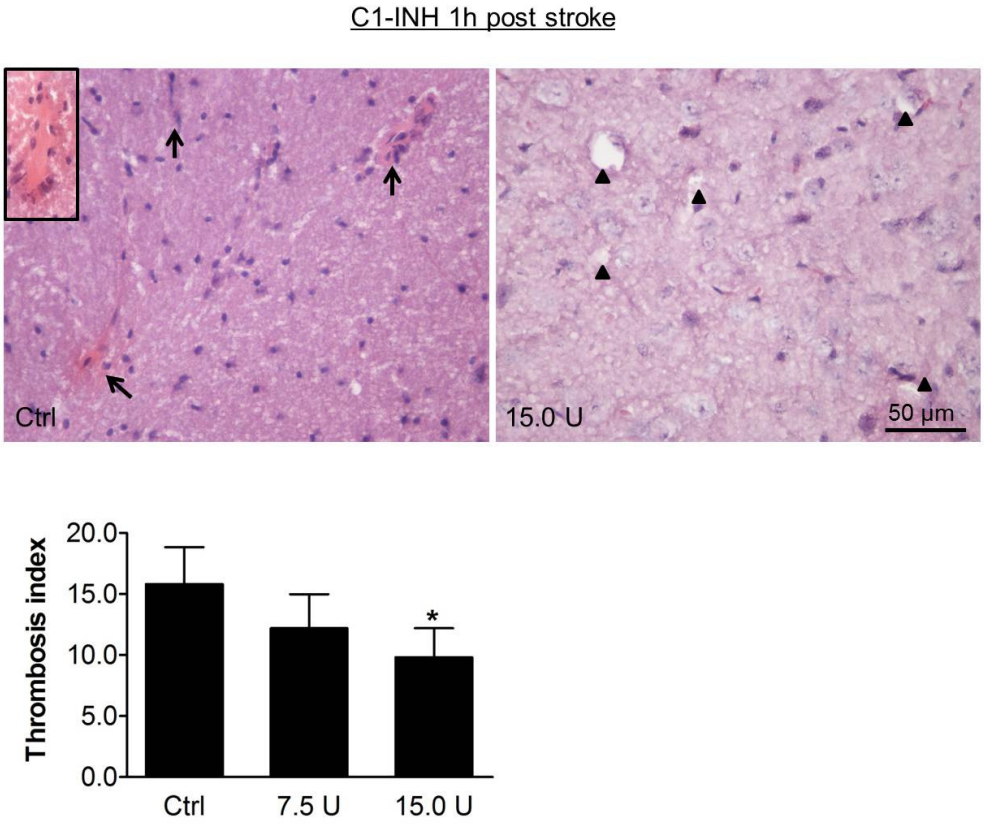

Figure 24: Representative hematoxylin/eosin (H&E) staining from the infarcted basal ganglia of control mice (Ctrl) and mice treated with 15.0 U C1-INH 1 hour after onset of ischemia on day 1 after tMCAO (upper panel). Thrombotic vessels are indicated by arrows and patent vessel by arrowheads. Amount of occluded vessels in the infarcted basal ganglia of control mice (Ctrl) and mice treated with 7.5 U or 15.0 U C1-INH, respectively, 1 hour post stroke on day 1 after tMCAO as assessed by the thrombosis index (lower panel) (n = 5/group). *P < 0.05, 1-way ANOVA, Bonferroni post hoc test, 15.0 U group compared with Ctrl group.

In accordance with those findings, histological H&E stainings of infarcted brain tissue sections from vehicle-treated Ctrl mice showed numerous occlusions of vessel lumina. In comparison, the rate of microvascular patency in corresponding brain areas of mice treated with the high-dose of C1-INH (15.0 U) was significantly increased (thrombosis index for occluded vessels: mean 15.8 ± 3.0 [Ctrl] vs. 12.2 ±

2.8 [7.5 U] or 9.8 ± 2.4 [15.0 U], respectively; P < 0.05 [Ctrl vs. 15.0 U]) (**Fig. 24**). This experiment was performed in cooperation with Dr Kerstin Goebel from the neurological university clinic, Münster.

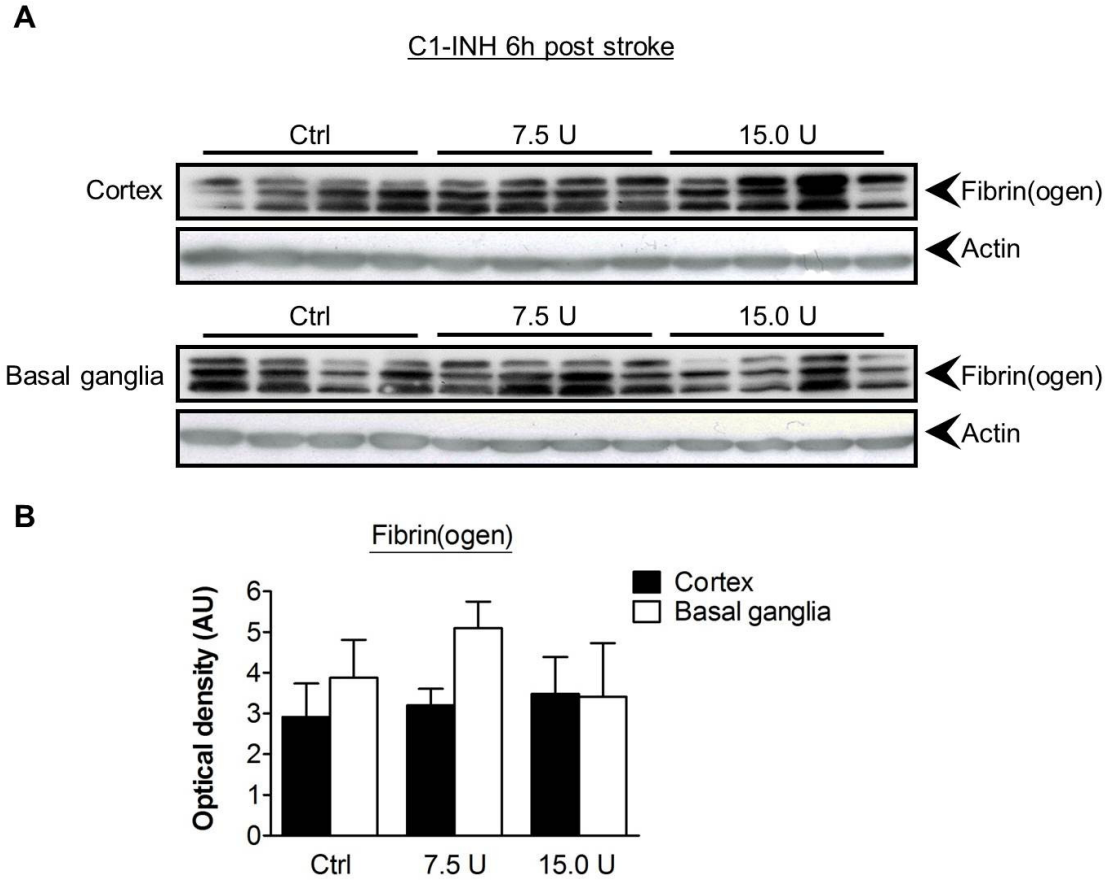

Figure 25: A) Formation of fibrin(ogen) in the ischemic cortices (upper panel) and basal ganglia (lower panel) of control mice (Ctrl) and mice treated with 7.5 U or 15.0 U C1-INH, respectively, 6 hours post stroke as determined by immunoblotting on day 1 after tMCAO. Immunoblots against fibrin(ogen) and actin (loading control) with 4 animals of each group are shown. B) Densitometric quantification of fibrin(ogen) accumulation in the groups and infarcted brain regions indicated (n = 4-5/group). P > 0.05, 1-way ANOVA, Bonferroni post hoc test, C1-INH (7.5 U and 15.0 U)-treated mice compared with Ctrl mice.

Additionally, immunoblot analysis against fibrin(ogen) was performed in mice treated with C1-INH 6 hours post tMCAO and in mice injected with C1-INH 1 hour after the onset of permanent ischemia. As it was already observed for edema formation, C1-INH, when applied in a delayed setting (**Fig. 25**) or in the model of pMCAO (**Fig. 26**), was not able to prevent fibrin accumulation compared with vehicle-treated Ctrl animals (C1-INH 6 hours post stroke: optical density cortex: mean 2.92 ± 0.82 AU [Ctrl] vs. 3.20 ± 0.40 AU [7.5 U] or 3.48 ± 0.90 AU [15.0 U], respectively; P > 0.05;

optical density basal ganglia: mean 3.88 ± 0.94 AU [Ctrl] vs. 5.10 ± 0.66 AU [7.5 U] or 3.41 ± 1.32 AU [15.0 U], respectively; P > 0.05) (pMCAO: optical density cortex: mean 4.07 ± 0.48 AU [Ctrl] vs. 3.85 ± 0.75 AU [7.5 U] or 3.31 ± 0.43 AU [15.0 U], respectively; P > 0.05; optical density basal ganglia: mean 3.55 ± 0.79 AU [Ctrl] vs. 3.33 ± 0.36 AU [7.5 U] or 3.98 ± 0.97 AU [15.0 U], respectively; P > 0.05). These results are indicative for an interference of C1-INH with microvascular thrombosis under conditions of reperfusion and when applied early after ischemic brain injury.

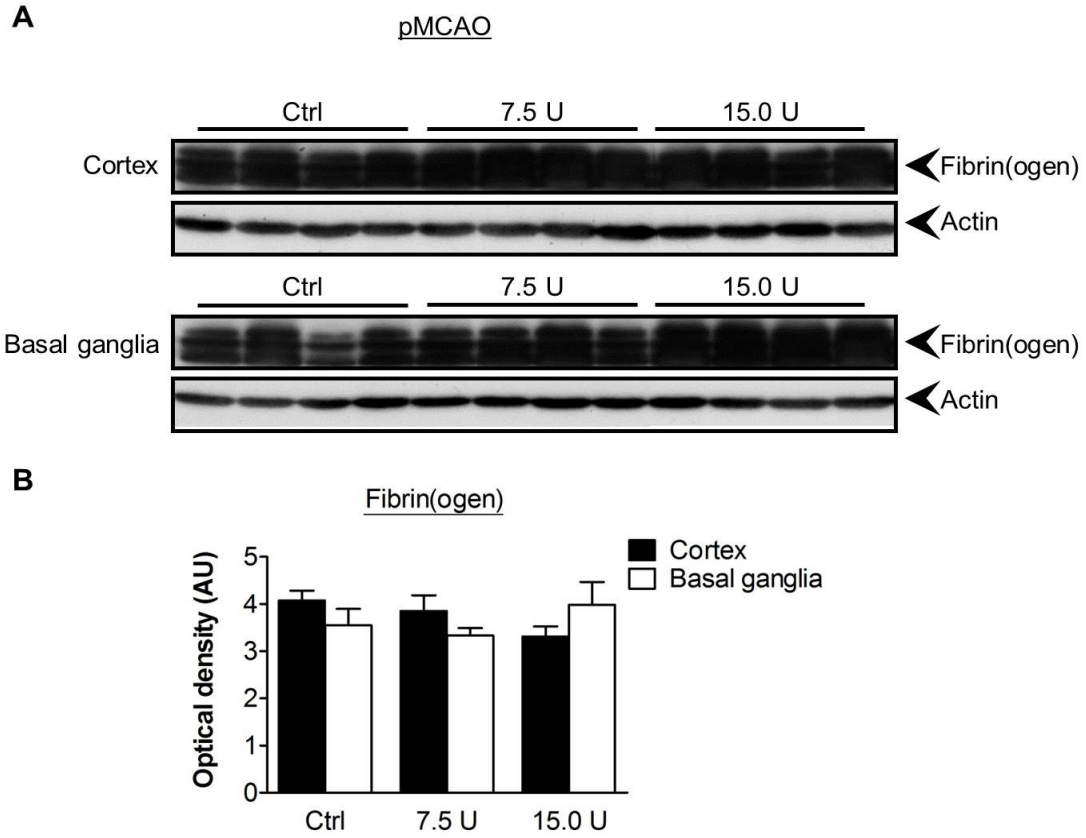

Figure 26: A) Fibrin(ogen) formation in the ischemic cortices (upper panel) and basal ganglia (lower panel) of control mice (Ctrl) and mice treated with 7.5 U or 15.0 U C1-INH 1 hour post stroke as determined by immunoblotting on day 1 after pMCAO. Immunoblots against fibrin(ogen) and actin (loading control) with 4 animals of each group are shown. B) Densitometric quantification of fibrin(ogen) generation in the groups and infarcted brain regions indicated (n = 4-5/group). P > 0.05, 1-way ANOVA, Bonferroni post hoc test, C1-INH-treated mice compared with Ctrl mice.

3.3 The role of macrophage-specific adhesion molecule sialoadhesin in the pathogenesis of cerebral ischemia

Disturbance of the BBB in ischemic stroke is accompanied by microglia activation and secondary recruitment of inflammatory cells into the brain parenchyma (Stoll et al., 1998). The perivascular space is populated by a special cell type of monocyte origin, the perivascular macrophage, characterized by the expression of the ED2 marker in rats (Stoll & Jander, 1999). Perivascular macrophages, moreover, express the adhesion molecule sialoadhesin (Sn) in rodents and are located at the interface between cerebral endothelial cells and the brain parenchyma. Sn is restricted to macrophage-like cells (Crocker et al., 1994) in rodents. This study took advantage of *Sn*$^{-/-}$ mice to address the role of Sn in breakdown of the BBB and lesion development during focal cerebral ischemia.

3.3.1 Sialoadhesin expression after cerebral ischemia in normal mice

In a first step, the expression of Sn was investigated by immunohistochemistry under healthy conditions in 8-12 weeks old sham-operated WT mice (*Sn*$^{+/+}$). Sn was not detectable within normal brain parenchyma, but strongly expressed on cells located around vessels, most likely presenting perivascular macrophages (**Fig. 27**), as reported before (Hartnell et al., 2001). Moreover, Sn expression within ischemic hemispheres was dramatically increased in *Sn*$^{+/+}$ mice in the first 24 hours after tMCAO (mean 970.3 ± 70.8) (**Fig. 27**), where no signal could be detected prior to the insult (compared with sham-operated *Sn*$^{+/+}$ mice).

In order to identify the cellular origin of Sn expression, immunofluorescence double staining against Sn (CD169, specific marker for Sn) and macrophage-like cells (CD11b, specific marker for macrophages/microglia) was performed on brain sections of *Sn*$^{+/+}$ mice. CD11b^{+} microglia showed a strong staining for CD169 in ischemic hemispheres of *Sn*$^{+/+}$ mice 24 hours after tMCAO (**Fig. 27**).

3.3.2 Stroke development in sialoadhesin deficient mice

Since Sn was constitutively expressed on perivascular macrophages in sham-operated *Sn*$^{+/+}$ mice and further induced in microglial cells within 24 hours after tMCAO (**Fig. 27**) the functional role of Sn in stroke development was addressed

using a constitutive full knock-out mouse strain lacking Sn on macrophage-like cells ($Sn^{-/-}$ mice). As expected, immunohistochemistry on day 1 using CD 169 could not detect Sn in coeval $Sn^{-/-}$ littermates following 1 hour of tMCAO, neither in ischemic nor in healthy brain hemispheres (**Fig. 27**).

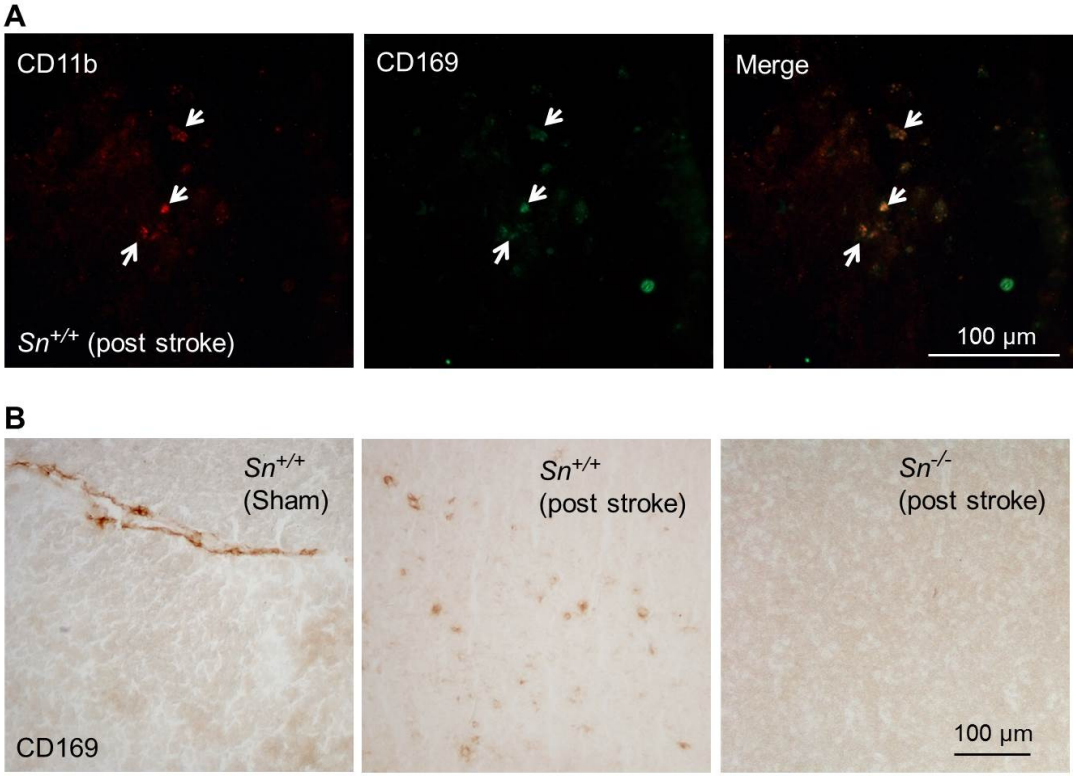

Figure 27: A) Representative immunofluorescence double stainings of microglia/macrophages (CD11b) (red) and sialoadhesin (CD169) (green) in the ischemic hemispheres of sialoadhesin expressing ($Sn^{+/+}$) mice on day 1 after tMCAO. B) Representative immunoperoxidase stainings of sialoadhesin (CD169) in the ipsilateral hemisphere of $Sn^{+/+}$ mice 24 hours after sham-operation (Sham) and in the ipsilateral (ischemic) hemisphere of $Sn^{+/+}$ and $Sn^{-/-}$ (sialoadhesin deficient) mice 24 hours after stroke induction.

Infarct volumes in $Sn^{-/-}$ and $Sn^{+/+}$ mice were assessed by the TTC method for vital tissue staining on day 1 after onset of ischemia. The results revealed only a slight reduction of infarct size in $Sn^{-/-}$ mice compared with WT littermates (mean 102.4 ± 28.1 mm^3 [$Sn^{+/+}$] vs. 84.5 ± 15.6 mm^3 [$Sn^{-/-}$], $P > 0.05$), but did not reach statistical significance (**Fig. 28**). Surprisingly, mice deficient for Sn showed significantly less severe neurological dysfunction (Bederson scores: median 3.0 (3.0, 4.25) [$Sn^{+/+}$] vs. 2.0 (1.0, 3.0) [$Sn^{-/-}$], $P < 0.001$) and less deficits in motor function and coordination (grip test score: median 3.0 (0.0, 4.0) [$Sn^{+/+}$] vs. 4.0 (3.75, 5.0) [$Sn^{-/-}$], $P < 0.05$) despite normal infarct volumes compared with the WT ($Sn^{+/+}$) group (**Fig. 28**).

To assess the consequences of Sn deficiency on subacute stroke development non-invasive serial MRI measurements was performed in living mice. Infarct lesions were already well demarcated on T2*w gradient-echo images on day 1 and the extent of infarction did not change over the next few days in both WT and *Sn*$^{-/-}$ mice (day 1: mean 104.2 ± 38.2 mm^3 [*Sn*$^{+/+}$] vs. 77.7 ± 10.4 mm^3 [*Sn*$^{-/-}$], P > 0.05; day 3: mean 102.5 ± 42.6 mm^3 [*Sn*$^{+/+}$] vs. 67.2 ± 22.8 mm^3 [*Sn*$^{-/-}$], P > 0.05) (**Fig. 29**).

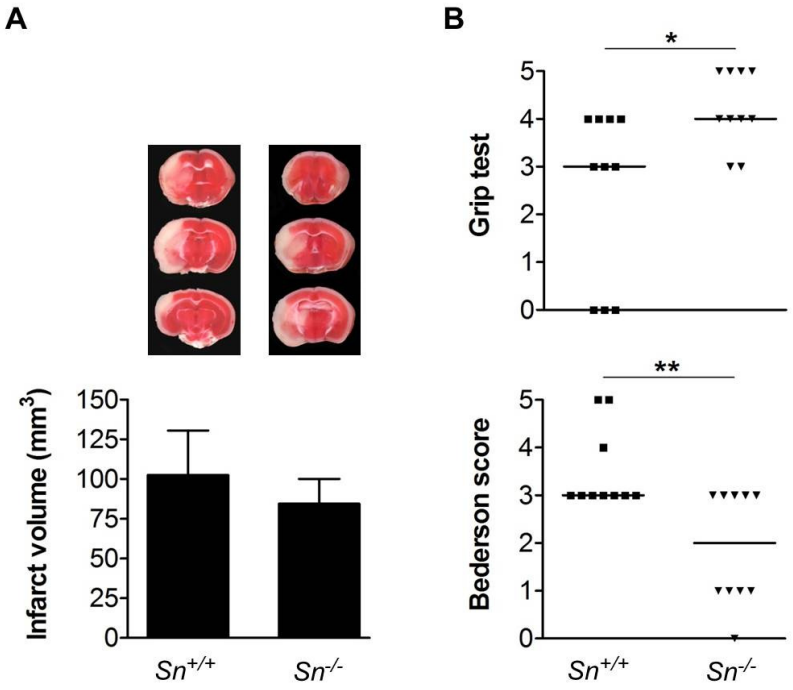

Figure 28: A) Representative 2,3,5-triphenyltetrazolium chloride (TTC) staining of three corresponding coronal brain sections (upper panel) and infarct volumetry from the coronal brain sections of sialoadhesin deficient (*Sn*$^{-/-}$) mice and WT littermates (*Sn*$^{+/+}$) on day 1 after tMCAO (lower panel) (n = 10/group). P > 0.05, unpaired, two-tailed Student´s *t*-test. B) Neurological Bederson score (lower panel) and grip test score (upper panel) of the indicated groups on day 1 after tMCAO (n = 10/group). *P < 0.05, **P < 0.001, two-tailed Mann Whitney-test.

Moreover, MRI on day 1 reaffirmed similar infarct sizes in *Sn*$^{-/-}$ and *Sn*$^{+/+}$ mice, as obtained by the TTC method, with a tendency of smaller infarctions in *Sn*$^{-/-}$ animals. As it was already shown before (**Fig. 28**), *Sn*$^{-/-}$ mice performed significantly better on both days after tMCAO compared with WT littermates (Bederson score: day 1: median 4.0 (3.0, 4.0) [*Sn*$^{+/+}$] vs. 2.0 (1.0, 3.0) [*Sn*$^{-/-}$], P < 0.05; day 3: median 3.0 (2.5, 3.5) [*Sn*$^{+/+}$] vs. 1.5 (1.0, 2.25) [*Sn*$^{-/-}$], P < 0.05; grip test score: day 1: median 3.0 (0.5, 3.5) [*Sn*$^{+/+}$] vs. 4.0 (3.75, 5.0) [*Sn*$^{-/-}$], P < 0.05; day 3: median 3.0 (2.0, 4.0) [*Sn*$^{+/+}$] vs. 5.0 (3.75, 5.0) [*Sn*$^{-/-}$], P < 0.05) (**Fig. 29**).

Given the important role of macrophages in preventing intracerebral bleeding after stroke (Gliem et al., 2012), the bleeding tendency in *Sn*$^{-/-}$ mice after stroke was further assessed using iron-sensitive T2*w MR sequences. Sn deficiency did not induce intracerebral hemorrhage since ischemic lesions always appeared hyperintense (bright) (**Fig. 29**). These findings demonstrate that Sn deficiency in mice is not associated with secondary infarct growth, delayed deterioration of functional outcome, or bleeding complications.

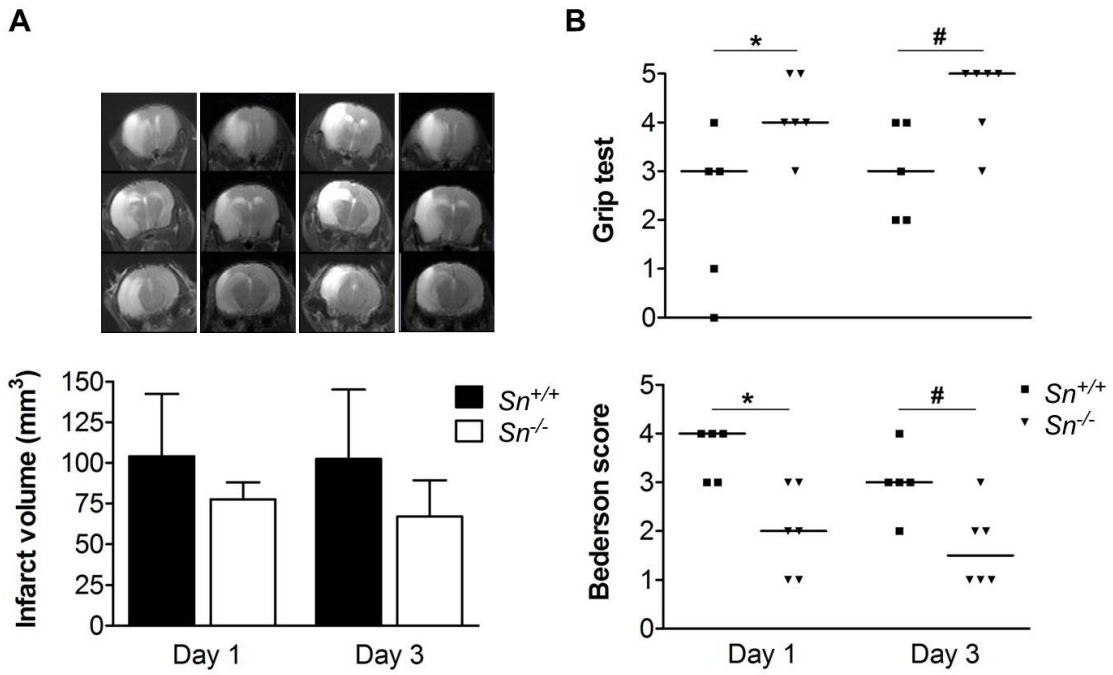

Figure 29: A) Representative panel of magnetic resonance imaging (MRI) from sialoadhesin deficient (*Sn*$^{-/-}$) mice and WT littermates (*Sn*$^{+/+}$ mice) on day 1 and day 3 after tMCAO (upper panel). Ischemic lesions on serial coronal T2*weighted gradient-echo MR sequences are depicted as hypointense (bright) areas. MRI–based infarct volumetry of the groups indicated on day 1 and day 3 after tMCAO (lower panel) (n = 5-6/group). P > 0.05, unpaired, two-tailed Student´s *t*-test, *Sn*$^{+/+}$ compared with *Sn*$^{-/-}$ on day 1 or day 3, respectively. B) Neurological Bederson score (lower panel) and grip test score (upper panel) of the indicated groups on day 1 and day 3 after tMCAO (n = 5-6/group). *P < 0.05, $^{\#}$P < 0.05, two-tailed Mann Whitney-test, *Sn*$^{+/+}$ compared with *Sn*$^{-/-}$ (day 1 (*) or day 3 ($^{\#}$)).

3.4 Functional consequences of sialoadhesin deficiency on blood-brain-barrier integrity and inflammation

To assess the integrity of the BBB following 1 hour of tMCAO in *Sn*$^{-/-}$ mice extravasation of Evans blue into the brain parenchyma was analyzed on day 1.

Therefore, mice were i.v. injected with 100 µl Evans blue immediately after removal of the filament (1 hour after induction of ischemia). Twenty-four hours after stroke $Sn^{+/+}$ mice displayed huge extravasation of the vascular tracer into the brain parenchyma compared with sham-operated WT littermates, indicating lost integrity of the BBB in $Sn^{+/+}$ mice after cerebral ischemia. Importantly, in $Sn^{-/-}$ mice the extravasation of Evans blue into the brain parenchyma did not reach statistical significance compared with sham-operated mice (mean 1.3 ± 0.1 mm^3 [Sham] vs. 93.5 ± 12.5 mm^3 [$Sn^{+/+}$] or 56.7 ± 25.7 mm^3 [$Sn^{-/-}$], respectively; $P < 0.05$ [Sham vs. $Sn^{+/+}$] and $P > 0.05$ [Sham vs. $Sn^{-/-}$]) (**Fig. 30**). This finding provides evidence that Sn deficiency counteracts disruption of the BBB.

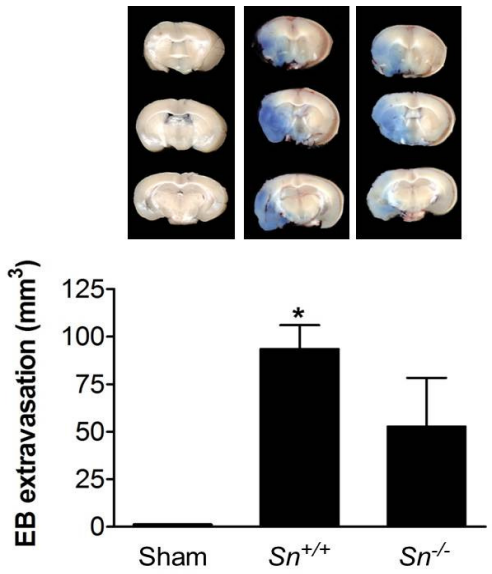

Figure 30: Representative corresponding coronal brain sections of sialoadhesin expressing ($Sn^{+/+}$) sham-operated mice (Sham), $Sn^{+/+}$ mice and $Sn^{-/-}$ mice after injection of Evans blue at 1 hour after stroke onset on day 1 (upper panel). Volume of Evans blue (EB) extravasation as determined by planimetry in the ischemic hemisphere of the indicated groups on day 1 after tMCAO (lower panel) (n = 3/group). *P < 0.05, Kruskal-Wallis test followed by Dunn multiple comparison test, Sham group compared with $Sn^{+/+}$ group.

To elucidate whether the improved functional outcome of $Sn^{-/-}$ mice after tMCAO was due to reduced microglia activation immunoperoxidase staining against CD11b was performed. Under healthy conditions CD11b was not detectable in brain parenchyma of WT mice (data not shown). On day 1 after onset of ischemia the number of $CD11b^+$ cells in ischemic hemispheres of $Sn^{-/-}$ mice was remarkably reduced by more than 50% compared with $Sn^{+/+}$ mice (mean 744.7 ± 129.8 [$Sn^{+/+}$] vs. 299.8 ± 94.5 [$Sn^{-/-}$], $P < 0.0001$) (**Fig. 31**). A similar result was obtained for contralateral hemispheres, with a significant reduction in the number of cells stained positive for CD11b in $Sn^{-/-}$ mice compared with WT littermates (mean 394.5 ± 123.2 [$Sn^{+/+}$] vs. 80.9 ± 40.8 [$Sn^{-/-}$], $P < 0.0001$) (**Fig. 31**). These findings demonstrate that Sn

deficiency is accompanied with a reduced activation of macrophages/microglia ($CD11b^+$) in ischemic lesions.

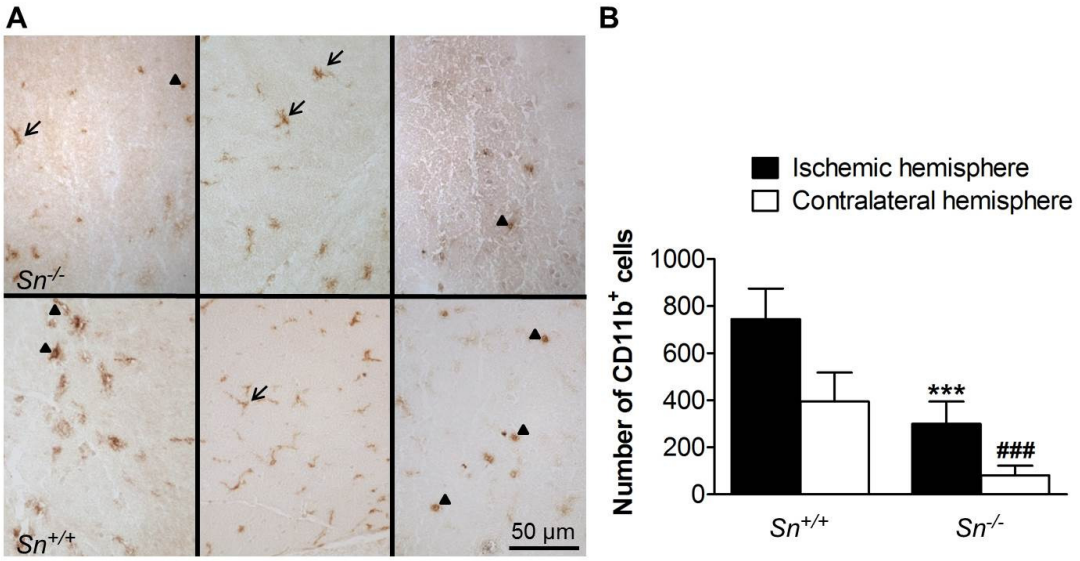

Figure 31: A) Representative immunoperoxidase stainings for activated microglia/macrophages ($CD11b^+$ cells) in ischemic hemispheres of sialoadhesin deficient ($Sn^{-/-}$) mice and WT littermates ($Sn^{-/-}$ mice) on day 1 after tMCAO. Arrowheads indicate cells with a macrophage-like morphology (rounded cell body without branches); arrows indicate cells with a microglia-like morphology (small cell body with several branches). B) Cellular inflammatory response in ischemic and contralateral (healthy) hemispheres of $Sn^{-/-}$ and $Sn^{+/+}$ mice on day 1 after tMCAO. Quantification of immune cell infiltration (microglia/macrophages) in the indicated groups as assessed by immunohistochemistry (n = 4-6/group). ***P < 0.0001, $^{\#\#\#}$P < 0.0001, unpaired, two-tailed Student´s *t*-test, compared with the respective control (ischemic hemisphere (*) or contralateral hemisphere ($^{\#}$)).

As macrophages/microglia are an important source of proinflammatory cytokines, the expression profiles of the proinflammatory cytokines interleukin (IL)-1β and tumor necrosis factor (TNF)-α in the ischemic lesions of $Sn^{+/+}$ and $Sn^{-/-}$ mice were assessed by RT-PCR (**Fig. 32**).

Twenty-four hours after tMCAO IL-1β and TNF-α transcript levels in ischemic cortices of both $Sn^{+/+}$ and $Sn^{-/-}$ mice were significantly increased compared with sham-operated WT littermates (IL-1β: mean 0.8 ± 0.3 [Sham] vs. 88.0 ± 19.4 [$Sn^{+/+}$] or 104.5 ± 57.4 [$Sn^{-/-}$], respectively; P < 0.0001 [Sham vs. $Sn^{+/+}$] and P < 0.0001 [Sham vs. $Sn^{-/-}$]; TNF-α: mean 0.1 ± 0.5 [Sham] vs. 103.3 ± 27.3 [$Sn^{+/+}$] or 93.8 ± 31.2 [$Sn^{-/-}$], respectively; P < 0.0001 [Sham vs. $Sn^{+/+}$] and P < 0.0001 [Sham vs. $Sn^{-/-}$]), whereas there was no significant difference between $Sn^{+/+}$ and $Sn^{-/-}$ mice (P > 0.05) (**Fig. 32**).

In contrast, no significant upregulation was seen in the ischemic basal ganglia (IL-1β: mean 0.1 ± 0.5 [Sham] vs. 16.6 ± 6.0 [$Sn^{+/+}$] or 34.3 ± 16.2 [$Sn^{-/-}$], respectively; P >

0.05; TNF-α: mean 1.2 ± 0.3 [Sham] vs. 15.3 ± 5.8 [$Sn^{+/+}$] or 26.0 ± 16.3 [$Sn^{-/-}$], respectively; P > 0.05) (**Fig. 32**).

These findings demonstrate that absence of Sn from activated microglia/macrophages does not influence cytokine induction in the ischemic brain, although the expression of the microglia/macrophage surface marker CD11b was reduced.

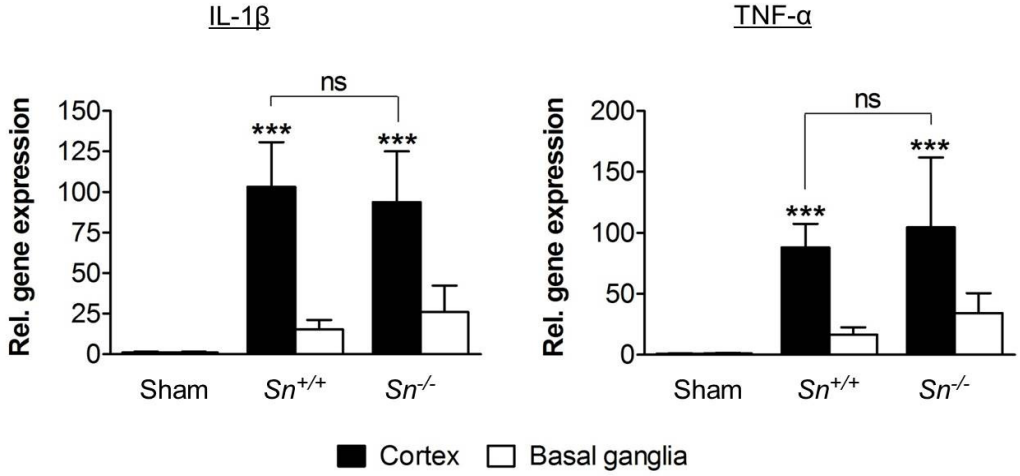

Figure 32: Relative gene expression levels of interleukin (IL)-1β and tumor necrosis factor (TNF)-α in the ischemic cortices and basal ganglia of sialoadhesin expressing ($Sn^{+/+}$) sham-operated mice (Sham) and of sialoadhesin deficient ($Sn^{-/-}$) mice and WT littermates ($Sn^{+/+}$) on day 1 after tMCAO (n = 3-8/group). ***P < 0.0001, 1-way ANOVA, Bonferroni post hoc test, Sham mice compared with $Sn^{+/+}$ or $Sn^{-/-}$ mice, respectively, in respective brain areas; ns: not significant.

3.5 Stroke development in mice defective in macrophage-specific nuclear factor-kappa B activation

To gain further insight into the contribution of macrophages to stroke development tMCAO was induced in conditional knock-out mice (*LysM-Cre*$^{+/-}$/*IKK2*$^{fl/fl}$) displaying a non-functional transcription factor nuclear factor (NF)-ϰB within the myeloid cell lineage, including macrophages and microglia (Kanters et al., 2003). NF-ϰB regulates transcription of proinflammatory signaling molecules such as the proinflammatory cytokines IL-1β and TNF-α, but also chemokines and cell adhesion molecules such as ICAM-1 (Pahl, 1999; Fujihara et al., 2000). Hence, macrophages of *LysM-Cre*$^{+/-}$*/IKK2*$^{fl/fl}$ mice are not able to completely develop their immunological function and thus, represent an ideal target to investigate the hypothesis that macrophages induce tissue damage upon cerebral ischemia.

To address the question whether non-functional NF-κB in macrophages/microglia plays a role in ischemic stroke *LysM-Cre*$^{+/-}$*/IKK2*$^{fl/fl}$ mice underwent 1 hour of tMCAO followed by evaluation 24 hours after stroke.

Similar to *Sn*$^{-/-}$ mice, lesions of *LysM-Cre*$^{+/-}$*/IKK2*$^{fl/fl}$ mice as assessed by the TTC method displayed no significant difference in size compared with the WT littermates (*LysM-Cre*$^{-/-}$*/IKK2*$^{fl/fl}$ mice) (mean 90.6 ± 37.0 [*LysM-Cre*$^{-/-}$*/IKK2*$^{fl/fl}$] vs. 106.3 ± 25.1 [*LysM-Cre*$^{+/-}$*/IKK2*$^{fl/fl}$], P > 0.05) (**Fig. 33**). However, compared with observations made in *Sn*$^{-/-}$ mice, neurological and motor-functional deficits had not improved in the *LysM-Cre*$^{+/-}$*/IKK2*$^{fl/fl}$ mice compared with the WT group (Bederson score: median 3.0 (1.0, 3.0) [*LysM-Cre*$^{-/-}$*/IKK2*$^{fl/fl}$] vs. 3.0 (2.0, 3.0) [*LysM-Cre*$^{+/-}$*/IKK2*$^{fl/fl}$], P > 0.05; grip test score: median 4.0 (3.0, 4.0) [*LysM-Cre*$^{-/-}$*/IKK2*$^{fl/fl}$] vs 3.0 (3.0, 4.0) [*LysM-Cre*$^{+/-}$*/IKK2*$^{fl/fl}$], P > 0.05) (**Fig. 33**). These findings demonstrate that NF-κB activation in macrophages/microglia does not contribute to tissue damage and deteriorated neurological outcome within the first 24 hours after focal cerebral ischemia.

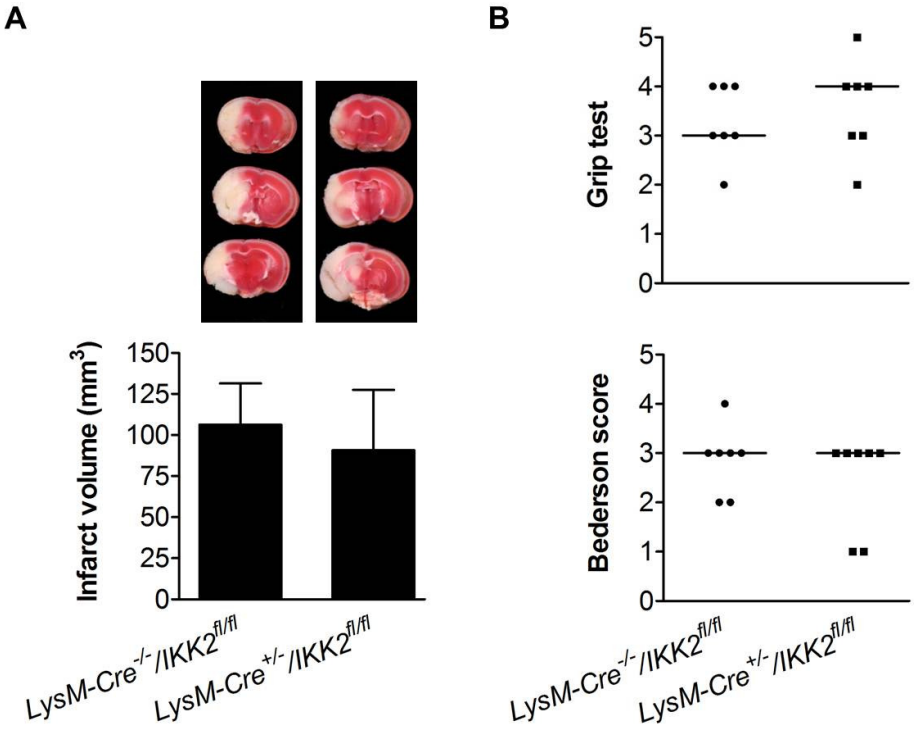

Figure 33: A) Representative 2,3,5-triphenyltetrazolium chloride (TTC) staining of three corresponding coronal brain sections (upper panel) and infarct volumetry from coronal brain sections of *LysM-Cre*$^{-/-}$*/IKK2*$^{fl/fl}$ and *LysM-Cre*$^{+/-}$*/IKK2*$^{fl/fl}$ mice on day 1 after tMCAO (lower panel) (n=7/group). P > 0.05, unpaired, two-tailed Student´s *t*-test. B) Neurological Bederson score (lower panel) and grip test score (upper panel) on day 1 after tMCAO of the indicated groups (n = 7/group). P > 0.05, two-tailed Mann Whitney-test.

4 DISCUSSION

To date, i.v. thrombolysis with rt-PA to resolve vessel occluding clots is the only therapy approved for acute ischemic stroke in humans (NINDS, 1995). However, the effects on clinical outcome are modest and dependent on time. Within 0-90 min one out of 4.5 patients benefit from rt-PA treatment. Between 90-180 min 9 patients require treatment for a favorable outcome in one and at 180-270 min after stroke onset it reaches 14 patients to be treated for one satisfying result. This may partly be due to treatment failure in thrombolysis and reopening of the occluded vessels, but even studies with additional mechanical thrombectomy which revealed higher recanalization rates so far did not improve outcome at a statistically significant level (Chimowitz, 2013). Obviously, reperfusion of ischemic brain tissue is mandatory for clinical recovery after stroke, but does not guarantee a good outcome which is due to a process named ischemia/reperfusion (I/R) injury in the literature. This also applies to other organ systems such as heart or lung (Farb et al., 1993; de Perrot et al., 2003). The mechanisms underlying I/R injury are largely unknown.

The present thesis focused on the role of natural inhibitor C1-inhibitor (C1-INH) Berinert® P in I/R injury in focal cerebral ischemia in young adult mice. The efficacy of C1-INH has been determined using different doses, time points of application and the experimental stroke models of transient (tMCAO) and permanent MCA occlusion (pMCAO). The second part of the thesis addressed the macrophage-specific role in stroke development using two different genetic mouse models deficient for the adhesion molecule sialoadhesin (Sn) and the transcription factor nuclear factor (NF)-κB, respectively.

4.1 Human plasma derived C1-inhibitor protects from ischemic brain damage in clinically relevant scenarios

In the present murine stroke study the efficacy of human plasma derived C1-INH in experimental stroke was addressed. Fundamental, the results revealed that C1-INH acts in a dose-dependent manner and that high dose of 15.0 U C1-INH massively reduced the lesion size and significantly improved neurological and functional outcome in young male mice when C1-INH was applied 1 hour after onset of tMCAO. Of great importance is the finding that high dose of 15.0 U C1-INH was still effective in a delayed setting, i.e. 6 hours after ischemia. C1-INH positively influenced

neurological behavior, although beneficial effects on infarct size could no longer be observed under these conditions. This finding demonstrates that it is possible to improve outcome without affecting infarct size. This discrepancy is probably attributable to the relatively poor correlation between infarct volumes and neurological deficits. Conflicting results have already been demonstrated in animal models of ischemic stroke (Wahl et al., 1992; Kawamata et al., 1996; Kleinschnitz et al., 2007; Kraft et al., 2010b) but also in human stroke patients (Pineiro et al., 2000). Thus, high dose of 15.0 U C1-INH even at a delayed setting of application is promising for the development of new pharmaceuticals for human stroke therapy.

Furthermore, long-term evaluation of ischemic mice early injected with 15.0 U C1-INH on the basis of MRI (day 1, 7) and functional scoring impressively demonstrated sustained neuroprotection from focal cerebral ischemia. This finding confirmed previous observations that revealed a similar effect of C1-INH application (De Simoni et al., 2004).

If the MCA occlusion is permanent as it is the case in the model of pMCAO, the severe perfusion disturbance persists, and infarcts are not reperfused. The present observation that protective effects seen in tMCAO were lost after permanent occlusion of the MCA strikingly indicates that C1-INH targets processes at the neurovascular interface involved in I/R injury. However, permanent ischemia similarly to transient ischemia ultimately leads to brain edema formation. Another explanation for the ineffectiveness of C1-INH in pMCAO might be that C1-INH does not gain sufficient access to the infarct region due to intravascular thrombosis as suggested by De Simoni *et al.* (2003).

Although, 15.0 U C1-INH has been demonstrated to be effective in the murine model of tMCAO, C1-INH doses used here cannot be directly compared with the human situation. This is indicated by the observation that the plasma half-life time of clearance ($t_{1/2}$) of C1-INH in mice and rats is ~9 hours (Dickneite, 1993), whereas in healthy humans the C1-INH plasma $t_{1/2}$ has been reported to range between 28 hours (Caliezi et al., 2000) and 35 hours (de Zwaan et al., 2002). In contrast to the present findings, another plasma derived C1-INH used by De Simoni *et al.* (2004) showed a rather narrow therapeutic time window after focal cerebral ischemia, i.e. 30 min, but was ineffective already after 60 min. To date, the exact reasons for this mismatch are ambiguous but differences in the duration of brain ischemia (30 min vs. 60 min) or the used C1-INH preparations might play a role. The latter is further

underlined by the fact that in the present study 7.5 U C1-INH had only small effects on stroke outcome, whereas the minimal effective dose in mice used by De Simoni *et al.* (2004) was 5.0 U.

Despite discrepancies concerning the doses of C1-INH in different reports, our data obtained from blood-sensitive MRI studies, at least, demonstrate that exogenously applied high dose of 15.0 U C1-INH was not correlated with increased risk of intracerebral bleeding in mice at any time point of data acquisition (day 1, 7). This finding is of critical relevance since C1-INH interferes with the coagulation system via inhibition of FXIIa. This observation corresponds to our previous experience after FXIIa blockade (Kleinschnitz et al., 2006; Hagedorn et al., 2010). In line with this, no effect on hemostasis as assessed by tail bleeding assays was observed after treatment with 15.0 U C1-INH. Hence, normal hemostasis was not affected by excessively applied C1-INH.

Moreover, the present study found that high dose of 15.0 U C1-INH did not interfere with cardiovascular function as assessed by heart rate and mean arterial blood pressure.

Noteworthy, from a translational perspective, the C1-INH used in this study is already approved since 2009 for replacement therapy of C1-INH during acute attacks of hereditary angioedema (HAE) (Craig et al., 2009). To date, there are no major safety concerns (Banerji, 2010; Keating, 2009), although it is obvious that compensation of naturally lacking C1-INH in patients with HAE and rising of C1-INH levels above the normal range in stroke patients reflect different conditions.

As brain ischemia is usually a disease of the elderly (Di Carlo et al., 1999) a potential neuroprotective compound is recommended to be tested not only in young laboratory animals but also in older cohorts (Fisher et al., 2009; Macleod et al., 2009). Other members of our research group, therefore, focused on older animals. The corresponding data were included in a common publication (Heydenreich et al., 2012). Interestingly, the beneficial activity of 15.0 U C1-INH was preserved in male middle-aged mice (6 month) and old mice (12 month) similarly subjected to 1 hour of tMCAO. These animals displayed significantly smaller infarct sizes and ameliorated neurological behaviour following treatment with 15.0 U C1-INH 1 hour post stroke compared with corresponding Ctrl mice. Hence, these findings validated our present results obtained from young laboratory mice.

Not only age can result in differences in stroke development, but also gender influences outcome after brain ischemia (Fisher et al., 2009; Macleod et al., 2009). Importantly, beneficial effects of 15.0 U C1-INH on infarct volumes and neurological performance could also be demonstrated in young female mice injected with C1-INH 1 hour after onset of ischemic stroke (*data included in* Heydenreich et al., 2012).

To confirm our data and to exclude a species-specific effect, collaborating researchers from CSL Behring (Marburg, Germany) investigated the effect of C1-INH on stroke development in young male CD rats (*data included in* Heydenreich et al., 2012). Animals subjected to 1.5 hours tMCAO and injected with 20 U/kg C1-INH 1.5 hours after onset of ischemia displayed reduced infarct sizes and performed significantly better in neurological and motility tests compared with vehicle-treated control rats on day 1 following stroke, confirming our present findings obtained with mice.

In summary, our results revealed that application of 15.0 U C1-INH early after onset of ischemia largely reduced lesion size and neurological deficits, when concomitantly reperfusion was restored. Delayed treatment, at least, improved neurological and motor function of mice, but not infarct size. Moreover, the neuroprotective effect was long-lasting and sustained over an observational period of 7 days in the present study. Importantly, C1-INH did not affect normal hemostasis, accordingly did not induce intracerebral bleeding complications after focal cerebral ischemia and did not interfere with cardiovascular function or other physiological parameters.

4.2 The protective role of C1-inhibitor relies on its combined antiedematous, antiinflammatory and antithrombotic mechanisms

C1-INH represents an interesting compound with a wide spectrum of inhibitory activities that do not exclusively depend on its protease inhibiting function. C1-INH controls the plasma kallikrein-kinin system (KKS) at multiple levels by regulating activation of coagulation factor FXII and plasma kallikrein and the intrinsic coagulation pathway by blocking activity of FXIa. Additionally, C1-INH is the main inhibitor of all three pathways of the innate complement system. On the other hand, ischemic stroke triggers processes that contribute to secondary deterioration such as edema formation and inflammation. The importance of the plasma KKS in stroke development was recently highlighted by studies performed in our group. Following

inhibition of components of the murine plasma KKS, the bradykinin receptor 1 (B1R) (Austinat et al., 2009) and the serine protease kininogen (Langhauser et al., 2012), both acting downstream of FXIIa, genetically modified mice were protected from ischemic stroke. This was due to reduced edema formation and a less pronounced inflammatory response.

Remarkable, in the present study treatment with 15.0 U C1-INH 1 hour post stroke resulted in stabilization of the blood-brain-barrier (BBB) which was indicated by highly reduced Evans blue extravasation into ischemic brain parenchyma and consequently less edema formation as assessed by the wet/dry weight method within ischemic mouse brains following tMCAO. This effect was also seen in areas regularly undergoing infarction, the basal ganglia, in both sham-operated and C1-INH-treated mice following tMCAO (Stoll et al., 2008). Despite a visible ischemic lesion upon TTC staining, the basal ganglia showed no Evans blue extravasation upon 15.0 U C1-INH treatment indicating preservation of the BBB within the infarcts. This finding is of special importance, since small infarcts are always present in basal ganglia despite successful antithrombotic treatments as it was demonstrated by 1 hour tMCAO studies. In contrast, delayed treatment 6 hours after stroke onset could not counteract BBB destabilization. This was indicated by almost identical levels of Evans blue extravasation into the brain parenchyma and edema formation between vehicle and C1-INH-treated groups. Similar negative results were obtained in the model of pMCAO, indicating that C1-INH protects BBB integrity only when reperfusion is achieved within less than 6 hours after stroke induction.

In this study the tight junction protein occludin could be shown to be preserved by C1-INH application 1 hour after tMCAO as assessed by Western blot analysis and immunohistochemistry. According to our findings, loss of occludin has recently been reported to contribute to BBB disruption in models of tMCAO (Yang et al., 2007; Liu et al., 2012). Moreover, the BBB stabilizing effects in mice mediated by C1-INH could also be confirmed in another species, i.e. rats showing less edema formation when 20 U/kg C1-INH was applied 1.5 hours after onset of ischemic stroke (*data included in* Heydenreich et al., 2012). Additionally, rats showed almost no BBB disturbance in ischemic basal ganglia, although infarcts have been regularly present in this region, like in C1-INH-treated mice. This further indicates that the lesser edema formation seen in the C1-INH-treated mice of the present study was a specific phenomenon

secondary to minor damaging effects at the BBB and not simply due to smaller infarct volumes in these animals.

In line with BBB stabilization as seen upon early C1-INH application after onset of tMCAO, almost no induction of Edn-1, a key regulator of BBB functions, could be observed in 15.0 U C1-INH-treated mice. Pharmacological blockade of Edn-1 has already been demonstrated to result in attenuated ischemic brain injury, edema formation and BBB disruption in rats (Dawson et al., 1999; Matsuo et al., 2001).

As stroke development is accompanied by a robust inflammatory response, the finding of the present study that infiltration of leukocytes (macrophages/neutrophils) into ischemic brain parenchyma was limited following application of 15.0 U C1-INH is of interest. In this context, it has previously been shown that C1-INH holds the potential to bind to adhesion molecules (E- and P-selectins) expressed on cell surfaces of e.g. endothelial cells (Cai & Davis III, 2003; Cai et al., 2005). Since selectins are highly important for the regulation of cell migration, those interactions might interfere with cell recruitment to sites of inflammation (De Simoni et al., 2004; Cai et al., 2005; Storini et al., 2005; Gesuete et al., 2009), but also serve to adhere C1-INH on injured brain endothelial walls, thereby controlling local activation of contact-kinin system proteases (Cai & Davis III, 2003). The latter is emphasized by the very recent finding of Marion Hofmeister from the group of Dr Marc Nolte (CSL Behring GmbH, Marburg, Germany), who impressively demonstrated that exogenous applied C1-INH was highly concentrated in the microvasculature of ischemic but not contralateral (healthy) hemispheres following tMCAO. These data have been published in a shared paper (Heydenreich et al., 2012). In line with our findings, Storini *et al.* (2005) reported on the reduction of $CD11b^+$ (specific surface marker for macrophages/microglia) cells after C1-INH treatment, and Gesuete *et al.* (2009) found a reduced number of infiltrated leukocyte-like cells.

Cerebral ischemia also induces release of cytokines, e.g. the proinflammatory cytokines IL-1β and TNF-α, which have been detected 2-6 hours post stroke (Wang et al., 1994). In our study, the induction levels of the proinflammatory cytokines IL-1β and TNF-α in vehicle-treated mice 24 hours after onset of ischemia were extremely elevated, compared with a significantly lower induction in mice treated with 15.0 U C1-INH. This finding is important since actions of these cytokines after brain injury have been proposed to be toxic and to increase tissue damage (Rothwell & Relton, 1993; Scherbel et al., 1999). Similar, the antiinflammatory cytokines IL-10 and

TGFβ-1 after application of 15.0 U C1-INH were less induced 24 hours post stroke. These findings are in accordance with previous data relying on late phase (48 hours) observations (Storini et al., 2005). However, in the same study the induction of IL-10 in the early phase (4 hours) after stroke was significantly elevated after C1-INH treatment compared with sham-operated and saline-treated animals. At later stages IL-10 induction in C1-INH-treated mice dropped and was found to be significantly lower compared with controls 48 hours after stroke. Storinis data point to a C1-INH-mediated shift from the pro- to the antiinflammatory status in the early phase of stroke, which, underlined by our results, is compensated at 24 hours or later phases of ischemia (48 hours). In our study cytokine levels 1 day after stroke were significantly reduced in general by C1-INH action, which argues for a secondary effect due to smaller infarcts, rather than a direct impact mediated by C1-INH at this time.

Additional to the plasma KKS, the intrinsic pathway of blood coagulation with FXIIa representing an interface between both pathways, displays another critical issue in preventing stroke development. For decades, it was assumed that FXII is not relevant for blood clotting and dispensable for normal hemostasis (Mackman, 2004) since human FXII deficiency is not associated with an abnormal bleeding phenotype (Renné et al., 2005). However, this hypothesis was very recently challenged by our group and collaborators demonstrating that FXII deficiency in mice due to genetic disruption (Kleinschnitz et al., 2006) or pharmacological inhibition (Hagedorn et al., 2010) protected from ischemic neurodegeneration by preventing microvascular thrombosis without increasing the risk of intracerebral bleeding.

Remarkably, application of 15.0 U C1-INH 1 hour following tMCAO resulted in massively decreased generation of intracerebral fibrin and higher patency of microvessels within the ischemic brain parenchyma in mice. However, this effect on fibrin(ogen) accumulation was no longer observed when C1-INH was injected in a delayed setting (6 hours) in the reperfusion-dependent model. Because thrombosis or edema formation under delayed treatment conditions were not affected by C1-INH treatment, additional mechanisms apart from those reported here and not yet clarified are responsible for the improved neurological behavior in ischemic mice. Given the profound antithrombotic effect of C1-INH 1 hour after tMCAO, the present observation that C1-INH failed to protect from stroke after pMCAO is coherent because clot formation is unlikely to be influenced in the absence of tissue

reperfusion, i.e. under conditions of persistent occlusion of a large proximal brain vessel like the MCA. Accordingly, C1-INH treatment had no effect on fibrin(ogen) formation after pMCAO. Moreover, the actual finding in the pMCAO model mirrors previous observations of our group in FXII deficient mice (Pham et al., 2010) as well as kininogen deficient mice (Langhauser et al., 2012) and indicates that blocking of the contact-kinin system after stroke is only promising if tissue reperfusion can be achieved in parallel. The present findings obtained by Western blot analysis and immunohistochemistry demonstrate that 15.0 U C1-INH application early after stroke induction interferes with microvascular thrombosis, but only when reperfusion is restored.

Besides its impressive regulatory action on components of the contact-kinin system, C1-INH is also the major inhibitor of all three pathways of the innate complement system, which is activated upon human stroke (Pedersen et al., 2004) as well as in experimental models of cerebral ischemia (Pasinetti et al., 1992; Huang et al., 1999; Schäfer et al., 2000; Van Beek et al., 2000). This study cannot appreciate to what extent suppression of the innate complement system contributed to the profound antiischemic effects of C1-INH (Davis III et al., 2008). De Simoni *et al.* (2004) found that mice deficient for C1q of the classical pathway of the complement system, which displayed a trend towards smaller infarct size following tMCAO, developed significantly smaller infarctions after C1-INH treatment. This finding indicates that C1-INH actions in brain protection are, at least, independent from activation of the classical pathway of the innate complement system.

Summarized, our data demonstrate that treatment with 15.0 U C1-INH post stroke affects different cellular pathways that critically contribute to brain damage involving the plasma KKS and the intrinsic pathway of blood coagulation. C1-INH applied at 1 hour after tMCAO resulted in (1) stabilization of the BBB and reduced brain edema, (2) less inflammation and secretion of inflammatory cytokines and (3) decreased microvascular thrombosis. Hence, C1-INH represents a promising compound for treatment of I/R injury, but not permanent cerebral ischemia.

Whereas the antiinflammatory properties of C1-INH are well established in models of I/R injury of different organ systems (Horstick et al., 1997; Lehmann et al., 2000; Nielsen et al., 2002), including the central nervous system (CNS) (De Simoni et al., 2003; Storini et al., 2005; Gesuete et al,. 2009; Longhi et al., 2009) the present description of C1-INH as powerful antithrombotic and antiedematous compound is

new and further adds to our understanding of this multifaceted molecule. Furthermore, our data underline the existence of an important crosstalk between microvascular thrombosis and inflammation within the scope of brain ischemia. Thus, cerebral ischemia was recently proposed to be a “thromboinflammatory” disorder (Nieswandt et al., 2011; Stoll et al., 2010).

Given the pleotropic actions of C1-INH the contribution of each of these processes (BBB stabilization, inflammation and thrombosis) to the development of ischemic brain lesions is difficult to dissect and would require continuous *in vivo* imaging of cell-cell interactions at the neurovascular unit. However, the fact that C1-INH is able to block different pathways could be of great advantage since therapeutical approaches targeting single pathways so far failed during translation from laboratory animals to stroke patients (O'Collins et al., 2006).

4.3 Functional outcome after ischemic stroke is improved in the absence of macrophage-restricted adhesion molecule sialoadhesin

As ischemic stroke is accompanied by a pronounced inflammatory response (Stoll et al., 1998; Wang et al., 2007), signaling molecules which guide immune cell functions are of special interest for investigations of new therapeutical options to counteract stroke development. Most of those signaling molecules are widely expressed on many types of immune cells. In contrast, expression of Sn, a cell adhesion molecule of yet unknown function, is restricted to macrophage-like cells and upregulated during inflammation. Therefore, Sn might represent a suitable target to analyze macrophage-specific function in focal cerebral ischemia.

The present results revealed that Sn expression is absent on cells within healthy brain parenchyma, confirming previous findings (Perry et al., 1992). However, Sn was found to be expressed on cells located around brain vessels. Ascribed to their position, these Sn^+ cells might be perivascular macrophages (Guillemin & Brew, 2004). These cells represent a very heterogeneous population of bone marrow-derived phagocytes that are found adjacent to brain vessels. Perivascular macrophages have been demonstrated to be activated in different models of CNS inflammation, including stroke, and they are supposed to function as immunmodulatory cells (Williams et al., 2001). In line with the present finding,

Hartnell *et al*. (2001) reported on perivascular macrophages expressing Sn under steady-state (healthy) conditions.

Importantly, the present results confirm findings by Perry *et al.* (1992) that Sn expression can be detected on cells within brain parenchyma after reperfusion-induced breakdown of the BBB. Permeability studies of the present thesis following tMCAO in WT ($Sn^{+/+}$) mice using the vascular tracer Evans blue support the previous hypothesis that expression of Sn can be regulated by different stimuli including serum factors, which might enter the brain parenchyma due to BBB disruption (Perry et al., 1992). However, there is no definite proof, whether Sn is expressed on activated microglia or recruited macrophages or both. The migration of Sn^{+} perivascular macrophages from brain vessels to sites of brain injury might also be conceivable. Challenging, microglia become activated following cerebral ischemia and change their typical ramified morphology to a roundish shape. Thus, they become indistinguishable from infiltrating hematogenous macrophages on morphological grounds (Stoll et al., 1998). Additionally, microglia and macrophages share most cell surface markers such as CD11b (Flaris et al., 1993), which further exacerbate their distinction. Since detailed analyses on the origin of macrophage-like cells were not included in this study, the pool of macrophages within the ischemic parenchyma always contained activated microglia to an uncertain amount.

The present thesis revealed that mice, homozygous deficient for Sn displayed infarcts of similar size as WT mice. However, absence of Sn was associated with significantly improved neurological and motor function and coordination. A discrepancy between infarct size and functional outcome is not unusual in experimental stroke studies (Wahl et al., 1992; Kawamata et al., 1996; Kleinschnitz et al., 2007; Kraft et al., 2010b) and was reported already for the delayed treatment with C1-INH (**4.1**). Importantly, follow-up MRI revealed no secondary infarct growth between day 1 and 3 in $Sn^{-/-}$ mice, demonstrating sustained protection from secondary deterioration. Functional tests additionally performed at more advanced stage of stroke development (day 3) showed less severe neurological and motor deficits in $Sn^{-/-}$ mice compared with WT animals. Similar in the clinical setting, improvement of functional outcome is more important than mere reduction of infarct size.

Interestingly, Gliem *et al.* (2012) impressively demonstrated that depletion of monocytes/macrophages caused bleeding complications at advanced stages of

cerebral ischemia (day 3) in mice. Importantly, in our study blood-sensitive MRI performed in *Sn*$^{-/-}$ mice at day 1 and 3 after tMCAO demonstrated that absence of Sn on macrophages was not associated with an increased risk of intracerebral hemorrhage, indicating that Sn expression itself is not involved in critical steps to maintain the integrity of the BBB following ischemic brain injury.

Summarized, the results presented here revealed that Sn deficiency on macrophages was associated with improved neurological and motor function 24 hours after stroke onset, but did not influence lesion volumes. Moreover, the neuroprotective effect persists, at least, till day 3 of cerebral ischemia. Importantly, absence of Sn was neither accompanied with intracerebral bleeding nor secondary infarct growth even at a more advanced stage of ischemia.

4.4 Sialoadhesin deficiency correlates with reduced inflammatory response and less blood-brain-barrier disruption

Importantly, the present study revealed that the integrity of the BBB 24 hours after tMCAO was less disturbed in absence of Sn compared with WT littermates. One possible explanation might be that Sn is involved in activation of other immune cells via cell-cell interactions, as it was already proposed by other investigators (Crocker et al,. 1990, 1995; van den Berg et al., 1992, 2001; Müerköster et al., 1999; Munday et al., 1999; Hartnell et al., 2001). Without or with less cell-cell interactions due to Sn deletion, less immune cells would be activated followed by a reduced release of immune mediators like metalloproteinases, which have been demonstrated to be involved in damage of the BBB by degradation of BBB proteins (Yang et al., 2007; Liu et al., 2012). In line with this, the number of activated CD11^{+} macrophages/microglia found in ischemic lesions in *Sn*$^{-/-}$ mice on day 1 after tMCAO was significantly reduced. These findings point to a role of Sn in activation or recruitment of, at least, CD11b^{+} immune cells following stroke, and might culminate in reduced damage of the BBB and less neurological and motor deficits. Accordingly, data obtained from other investigators demonstrated improved outcome in a model of hereditary neuropathies due to less macrophage and T cell recruitment in Sn null mice (Kobsar et al., 2006; Ip et al., 2007).

Surprisingly, semiquantitative RT-PCR analysis of relative expression levels of proinflammatory cytokines IL-1β and TNF-α 24 hours after ischemia revealed no

differences between *Sn*$^{-/-}$ mice and WT littermates, although the number of CD11b^{+} cells in *Sn*$^{-/-}$ mice was reduced. This finding indicates that absence of Sn on macrophages does not obviously affect induction of these cytokines at 24 hours and suggest other cells than macrophages (Rothwell & Relton, 1993) as main source of cytokine release, e.g. glia cells or endothelial cells (Barone & Feuerstein, 1999; del Zoppo et al., 2000). So far, we cannot definitely say that Sn deficiency does not affect cytokine expression at later time points, when macrophage/microglia infiltration reaches peak levels (Gliem et al., 2012). However, from this point of view, it seems likely that macrophage-like cells are not harmful by release of proinflammatory cytokines (e.g. IL-1β, TNF-α) 24 hours after onset of ischemia, at least, in the model of tMCAO.

In summary, the present findings provide evidence that deletion of Sn counteracts BBB disruption and demonstrate that Sn deficiency was associated with reduced activation and infiltration of CD11b^{+} macrophages/microglia into ischemic brains. This might be a result of modified interactions between Sn deficient macrophage-like cells and other immune cells and in consequence, might account for less neurological deficits observed in *Sn*$^{-/-}$ mice. Although the expression of macrophages/microglia-specific surface marker CD11b was reduced, no alterations in the expression levels of proinflammatory cytokines 24 hours upon cerebral ischemia could be detected. This indicates that functional effects of Sn deficiency cannot be attributed to reduced cytokine levels.

4.5 Macrophage-specific nuclear factor-kappa B activation does not contribute to stroke development

In a further approach to shed light on the macrophage-specific contribution to stroke development, *LysM-Cre*$^{+/-}$*/IKK2*$^{fl/fl}$ mice lacking NF-ϰB function in macrophages, were included in our study. Since full *IKK2* knockout mice die from TNF-dependent liver apoptosis in the embryonic phase (Tanaka et al., 1999), a conditional mouse model with deletion of IKK2 restricted to the myeloid cell lineage, including macrophages, was used (Kanters et al., 2003). Due to this deletion, NF-ϰB cannot be activated in macrophages of *LysM-Cre*$^{+/-}$*/IKK2*$^{fl/fl}$ mice. Consequently, genes regulated by NF-ϰB will not be activated, e.g. genes that code for proinflammatory cytokines (Pahl, 1999).

Interestingly, in the present thesis lack of NF-κB activity in macrophages did not affect lesion size or neurological outcome in mice 24 hours after onset of ischemia. Findings from other groups regarding the role of NF-κB are highly controversial. Some provide data demonstrating protection from experimental stroke by inhibition of NF-κB activation via a pharmacological approach (Khan et al., 2005) or in a model of constitutive p50 (subunit of NF-κB) knockout (Schneider et al., 1999). In contrast, others report on a detrimental effect of NF-κB inhibition via p50 deficiency in different models of MCAO (Duckworth et al., 2006; Li et al., 2008). However, findings from conventional knockout models like p50 deficiency cannot easily be compared with results obtained from a tissue-specific conditional knockout (i.e. IKK2 deletion) model, since the latter provides cell-specific data contrary to complete deletion of the target gene in all cell types in a full knockout model.

Summarized, mice with a NF-κB activation defect in macrophages did not show neurological improvements or reduced tissue damage after tMCAO, though macrophages are not able to secrete proinflammatory cytokines, e.g. IL-1β or TNF-α underlying the control of NF-κB.

4.6 Concluding remarks and future perspective

This thesis constitutes C1-INH Berinert® P as an attractive and promising pharmacological target in acute cerebral ischemia, since (1) C1-INH treatment protects from stroke in different clinical scenarios, (2) C1-INHs modes of action are multimodal, and (3) C1-INH is already used as pharmacological treatment in humans. Hence, these findings should be taken as a basis for further translational studies in relevant large animal models, which are a crucial requirement to develop safe preclinical protocols in biomedical research.

The second part of this thesis provides novel data about the role of macrophages in the acute phase of stroke using two different approaches of genetically modified mouse models. Our results provide evidence that macrophages are not the main source of proinflammatory cytokines and that macrophage-specific synthesis of proinflammatory cytokines under the regulation of NF-κB does not contribute to neurological deficits and brain damage early after cerebral ischemia. Hence, this thesis suggest a role for macrophages as bystanders of ischemic deterioration, as rather critical effector cells, at least, in the early phase of cerebral ischemia.

5 REFERENCES

Aiyagari V, Diringer MN. Management of large hemispheric strokes in the neurological intensive care unit. *Neurologist*. 2002;8(3):152-62.

Allan SM, Rothwell NJ. Cytokines and acute neurodegeneration. *Nat Rev Neurosci*. 2001;2(10):734-44.

Aronowski J, Strong R, Grotta JC. Reperfusion injury: demonstration of brain damage produced by reperfusion after transient focal ischemia in rats. *J Cereb Blood Flow Metab*. 1997;17(10):1048-56.

Astrup J, Siesjö BK, Symon L. Thresholds in cerebral ischemia - The ischemic penumbra. *Stroke*. 1981;12(6):723-5.

Austinat M, Braeuninger S, Pesquero JB, Brede M, Bader M, Stoll G, Renné T, Kleinschnitz C. Blockade of bradykinin receptor B1 but not bradykinin receptor B2 provides protection from cerebral infarction and brain edema. *Stroke*. 2009;40(1):285-93.

Ayata C, Ropper A. Ischaemic brain oedema. *J Clin Neurosci*. 2002;9(2):113-24.

Banerji A. Current treatment of hereditary angioedema: An update on clinical studies. *Allergy Asthma Proc*. 2010;31(5):398-406.

Baron JC. Mapping the ischaemic penumbra with PET: implications for acute stroke treatment. *Cerebrovasc Dis*. 1999;9(4):193-201.

Barone FC, Feuerstein GZ. Inflammatory mediators and stroke: new opportunities for novel therapeutics. *J Cereb Blood Flow Metab.* 1999;19(8):819-34.

Bederson JB, Pitts LH, Tsuji M, Nishimura MC, Davis RL, Bartkowski H. Rat middle cerebral artery occlusion: evaluation of the model and development of a neurologic examination. *Stroke*. 1986;17(3):472-6. (a)

Bederson JB, Pitts LH, Germano SM, Nishimura MC, Davis RL, Bartkowski HM. Evaluation of 2,3,5-triphenyltetrazolium chloride as a stain for detection and quantification of experimental cerebral infarction in rats. *Stroke*. 1986;17(6):1304-8. (b)

Bednar MM, Gross CE, Russell SR, Short D, Giclas PC. Activation of complement by tissue plasminogen activator, but not acute cerebral ischemia, in a rabbit model of thromboembolic stroke. *J Neurosurg*. 1997;86(1):139-42.

Belayev L, Busto R, Zhao W, Ginsberg MD. Quantitative evaluation of blood-brain barrier permeability following middle cerebral artery occlusion in rats. *Brain Res*. 1996;739(1-2):88-96.

Berrouschot J, Sterker M, Bettin S, Köster J, Schneider D. Mortality of space-occupying ('malignant') middle cerebral artery infarction under conservative intensive care. *Intensive Care Med*. 1998;24(6):620-3.

Bock SC, Skriver K, Nielsen E, Thogersen HC, Wiman B, Donaldson VH, Eddy RL, Marrinan J, Radziejewska E, Huber R, Shows TB, Magnusson S. Human C1 inhibitor: Primary structure, cDNA cloning, and chromosomal localization. *Biochemistry*. 1986;25(15):4292-301.

Bork K, Hardt J, Schicketanz KH, Ressel N. Clinical studies of sudden upper airway obstruction in patients with hereditary angioedema due to C1 esterase inhibitor deficiency. *Arch Intern Med*. 2003;163(10):1229-35.

Braeuninger S, Kleinschnitz C. Rodent models of focal cerebral ischemia: procedural pitfalls and translational problems. *Exp Transl Stroke Med*. 2009;1:8.

Braeuninger S, Kleinschnitz C, Nieswandt B, Stoll G. Focal cerebral ischemia. *Methods Mol Biol*. 2012;788:29-42.

Brede M, Braeuninger S, Langhauser F, Hein L, Roewer N, Stoll G, Kleinschnitz C. α(2)-adrenoceptors do not mediate neuroprotection in acute ischemic stroke in mice. *J Cereb Blood Flow Metab*. 2011;31(10):e1-7.

Cai S, Davis III AE. Complement regulatory protein C1 inhibitor binds to selectins and interferes with endothelial–leukocyte adhesion. *J Immunol*. 2003;171(9):4786-91.

Cai S, Dole VS, Bergmeier W, Scafidi J, Feng H, Wagner DD, Davis AE 3rd. A direct role for C1 inhibitor in regulation of leukocyte adhesion. *J Immunol*. 2005;174(10):6462-6.

Caliezi C, Wuillemin WA, Zeerleder S, Redondo M, Eisele B, Hack CE. C1-Esterase inhibitor: an anti-inflammatory agent and its potential use in the treatment of diseases other than hereditary angioedema. *Pharmacol Rev*. 2000;52(1):91-112.

Carmichael ST. Rodent models of focal stroke: size, mechanism, and purpose. *NeuroRx*. 2005;2(3):396-409.

Carugati A, Pappalardo E, Zingale LC, Cicardi M. C1-inhibitor deficiency and angioedema. *Mol Immunol*. 2001;38(2-3):161-73.

Chiamulera C, Terron A, Reggiani A, Cristofori P. Qualitative and quantitative analysis of the progressive cerebral damage after middle cerebral artery occlusion in mice. *Brain Res*. 1993;606(2):251-8.

Chimowitz MI. Endovascular treatment for acute ischemic stroke--still unproven. *N Engl J Med.* 2013;368(10):952-5.

Cicardi, M. Cicardi M, Zingale LC, Zanichelli A, Deliliers DL, Caccia S. The use of plasma-derived C1 inhibitor in the treatment of hereditary angioedema. *Expert Opin Pharmacother*. 2007;8(18):3173-81.

Clark WM, Lessov NS, Dixon MP, Eckenstein F. Monofilament intraluminal middle cerebral artery occlusion in the mouse. *Neurol Res*. 1997;19(6):641-8.

Clausen BE, Burkhardt C, Reith W, Renkawitz R, Förster I. Conditional gene targeting in macrophages and granulocytes using LysMcre mice. *Transgenic Res*. 1999;8(4):265-77.

Cochrane CG, Griffin JH. The biochemistry and pathophysiology of the contact system of plasma. *Adv Immunol*. 1982;33:241-306

Cochrane CG, Revak SD, Wuepper KD. Activation of Hageman factor in solid and fluid phases. A critical role of kallikrein. *J Exp Med*. 1973;138(6):1564-83.

Connolly ES Jr, Winfree CJ, Stern DM, Solomon RA, Pinsky DJ. Procedural and strain-related variables significantly affect outcome in a murine model of focal cerebral ischemia. *Neurosurgery*. 1996;38(3):523-32.

Craig TJ, Levy RJ, Wasserman RL, Bewtra AK, Hurewitz D, Obtulowicz K, Reshef A, Ritchie B, Moldovan D, Shirov T, Grivcheva-Panovska V, Kiessling PC, Keinecke HO, Bernstein JA. Efficacy of human C1 esterase inhibitor concentrate compared with placebo in acute hereditary angioedema attacks. *J Allergy Clin Immunol.* 2009;124(4):801-8.

Crocker PR, Werb Z, Gordon S, Bainton DF. Ultrastructural localization of a macrophage-restricted sialic acid binding hemagglutinin, SER, in macrophage-hematopoietic cell clusters. *Blood*. 1990;76(6):1131-8.

Crocker PR, Mucklow S, Bouckson V, McWilliam A, Willis AC, Gordon S, Milon G, Kelm S, Bradfield P. Sialoadhesin, a macrophage sialic acid binding receptor for haemopoietic cells with 17 immunoglobulin-like domains. *EMBO J*. 1994;13(19):4490-503.

Crocker PR, Freeman S, Gordon S, Kelm S. Sialoadhesin binds preferentially to cells of the granulocytic lineage. *J Clin Invest*. 1995;95(2):635-43.

Crocker PR, Paulson JC, Varki A. Siglecs and their roles in the immune system. *Nat Rev Immunol.* 2007;7(4):255-66.

Crocker PR, Gordon S. Isolation and characterization of resident stromal macrophages and hematopoietic cell clusters from mouse bone marrow. *J Exp Med*. 1985;162(3):993-1014.

Crocker PR, Gordon S. Properties and distribution of a lectin-like hemagglutinin differentially expressed by murine stromal tissue macrophages. *J Exp Med*. 1986;164(6):1862-75.

Crocker PR, Gordon S. Mouse macrophage hemagglutinin (sheep erythrocyte receptor) with specificity for sialylated glycoconjugates characterized by a monoclonal antibody. *J Exp Med*. 1989;169(4):1333-46.

Davis AE III. C1 inhibitor and hereditary angioneurotic edema. *Annu Rev Immunol*. 1988;6:595-628.

Davis AE III, Mejia P, Lu F. Biological activities of C1 inhibitor. *Mol Immunol*. 2008;45(16):4057-63.

Dawson DA, Sugano H, McCarron RM, Hallenbeck JM, Spatz M. Endothelin receptor antagonist preserves microvascular perfusion and reduces ischemic brain damage following permanent focal ischemia. *Neurochem Res*. 1999;24(12):1499-505.

Décarie A, Raymond P, Gervais N, Couture R, Adam A. Serum interspecies differences in metabolic pathways of bradykinin and [des-Arg9]BK: influence of enalaprilat. *Am J Physiol*. 1996;271(4 Pt 2):H1340-7.

del Zoppo GJ. Microvascular responses to cerebral ischemia/inflammation. *Ann N Y Acad Sci*. 1997;823:132-47.

del Zoppo GJ, Schmid-Schönbein GW, Mori E, Copeland BR, Chang CM. Polymorphonuclear leukocytes occlude capillaries following middle cerebral artery occlusion and reperfusion in baboons. *Stroke*. 1991;22(10):1276-83.

del Zoppo GJ, Poeck K, Pessin MS, Wolpert SM, Furlan AJ, Ferbert A, Alberts MJ, Zivin JA, Wechsler L, Busse O, Greenlee R, Brass L, Mohr JP, Feldmann E, Hacke W, Kase CS, Biller J, Gress D, Otis SM. Recombinant tissue plasminogen activator in acute thrombotic and embolic stroke. *Ann Neurol*. 1992;32(1):78-86.

del Zoppo G, Ginis I, Hallenbeck JM, Iadecola C, Wang X, Feuerstein GZ. Inflammation and stroke: putative role for cytokines, adhesion molecules and iNOS in brain response to ischemia. *Brain Pathol*. 2000;10(1):95-112.

de Perrot M, Liu M, Waddell TK, Keshavjee S. Ischemia-reperfusion-induced lung injury. *Am J Respir Crit Care Med*. 2003;167(4):490-511.

De Simoni MG, Storini C, Barba M, Catapano L, Arabia AM, Rossi E, Bergamaschini L. Neuroprotection by complement (C1) inhibitor in mouse transient brain ischemia. *J Cereb Blood Flow Metab*. 2003;23(2):232-9.

De Simoni MG, Rossi E, Storini C, Pizzimenti S, Echart C, Bergamaschini L. The powerful neuroprotective action of C1-inhibitor on brain ischemia-reperfusion injury does not require C1q. *Am J Pathol*. 2004;164(5):1857-63.

de Zwaan C, Kleine AH, Diris JH, Glatz JF, Wellens HJ, Strengers PF, Tissing M, Hack CE, van Dieijen-Visser MP, Hermens WT. Continuous 48-h C1-inhibitor treatment, following reperfusion therapy, in patients with acute myocardial infarction. *Eur Heart J*. 2002;23(21):1670-7.

Di Carlo A, Lamassa M, Pracucci G, Basile AM, Trefoloni G, Vanni P, Wolfe CD, Tilling K, Ebrahim S, Inzitari D. Stroke in the very old: clinical presentation and determinants of 3-month functional outcome: A European perspective. European BIOMED Study of Stroke Care Group. *Stroke*. 1999;30(11):2313-9.

Dickneite G. Influence of C1-inhibitor on inflammation, edema and shock. *Behring Inst Mitt*. 1993;(93):299-305.

Dirnagl U. Bench to bedside: the quest for quality in experimental stroke research. *J Cereb Blood Flow Metab*. 2006;26(12):1465-78.

Dirnagl U, Kaplan B, Jacewicz M, Pulsinelli W. Continuous measurement of cerebral cortical blood flow by laser-Doppler flowmetry in a rat stroke model. *J Cereb Blood Flow Metab*. 1989;9(5):589-96.

Dirnagl U, Iadecola C, Moskowitz MA. Pathobiology of ischaemic stroke: an integrated view. *Trends Neurosci*. 1999;22(9):391-7.

Duckworth EA, Butler T, Collier L, Collier S, Pennypacker KR. NF-kappaB protects neurons from ischemic injury after middle cerebral artery occlusion in mice. *Brain Res*. 2006;1088(1):167-75.

Durukan A, Tatlisumak T. Acute ischemic stroke: Overview of major experimental rodent models, pathophysiology, and therapy of focal cerebral ischemia. *Pharmacol Biochem Behav*. 2007;87(1):179-97.

Engelhardt S, Hein L, Wiesmann F, Lohse MJ. Progressive hypertrophy and heart failure in beta1-adrenergic receptor transgenic mice. *Proc Natl Acad Sci U S A*. 1999;96(12):7059-64.

Farb A, Kolodgie FD, Jenkins M, Virmani R. Myocardial infarct extension during reperfusion after coronary artery occlusion: pathologic evidence. *J Am Coll Cardiol*. 1993;21(5):1245-53.

Fisher M, Feuerstein G, Howells DW, Hurn PD, Kent TA, Savitz SI, Lo EH. Update of the stroke therapy academic industry roundtable preclinical recommendations. *Stroke*. 2009;40(6):2244-50.

Flaris NA, Densmore TL, Molleston MC, Hickey WF. Characterization of microglia and macrophages in the central nervous system of rats: definition of the differential expression of molecules using standard and novel monoclonal antibodies in normal CNS and in four models of parenchymal reaction. *Glia*. 1993;7(1):34-40.

Fujihara M, Wakamoto S, Ito T, Muroi M, Suzuki T, Ikeda H, Ikebuchi K. Lipopolysaccharide-triggered desensitization of TNF-alpha mRNA expression involves lack of phosphorylation of IkappaBalpha in a murine macrophage-like cell line, P388D1. *J Leukoc Biol*. 2000;68(2):267-76.

Fulgham JR, Ingall TJ, Stead LG, Cloft HJ, Wijdicks EF, Flemming KD. Management of acute ischemic stroke. *Mayo Clin Proc*. 2004;79(11):1459-69.

Furie B, Furie B. Molecular and cellular biology of blood coagulation. *N Engl J Med*. 1992;326(12):800-6.

Garcia JH, Liu KF, Yoshida Y, Lian J, Chen S, del Zoppo GJ. Influx of leukocytes and platelets in an evolving brain infarct (Wistar rat). *Am J Pathol*. 1994;144(1):188- 99.

Gelderblom M, Leypoldt F, Steinbach K, Behrens D, Choe CU, Siler DA, Arumugam TV, Orthey E, Gerloff C, Tolosa E, Magnus T: Temporal and spatial dynamics of cerebral immune cell accumulation in stroke. *Stroke*. 2009;40(5):1849-57.

Gesuete R, Storini C, Fantin A, Stravalaci M, Zanier ER, Orsini F, Vietsch H, Mannesse ML, Ziere B, Gobbi M, De Simoni MG. Recombinant C1 inhibitor in brain ischemic injury. *Ann Neurol*. 2009;66(3):332-42.

Gijbels MJ, van der Cammen M, van der Laan LJ, Emeis JJ, Havekes LM, Hofker MH, Kraal G. Progression and regression of atherosclerosis in APOE3-Leiden transgenic mice: an immunohistochemical study. *Atherosclerosis*. 1999;143(1):15-25.

Ginsberg MD. Adventures in the pathophysiology of brain ischemia: penumbra, gene expression, neuroprotection: the 2002 Thomas Willis Lecture. *Stroke*. 2003;34(1):214-23.

Ginsberg MD, Becker DA, Busto R, Belayev A, Zhang Y, Khoutorova L, Ley JJ, Zhao W, Belayev L. Stilbazulenyl nitrone, a novel antioxidant, is highly neuroprotective in focal ischemia. *Ann Neurol*. 2003;54(3):330-42.

Gliem M, Mausberg AK, Lee JI, Simiantonakis I, van Rooijen N, Hartung HP, Jander S. Macrophages prevent hemorrhagic infarct transformation in murine stroke models. *Ann Neurol*. 2012;71(6):743-52.

Goldlust EJ, Paczynski RP, He YY, Hsu CY, Goldberg MP. Automated measurement of infarct size with scanned images of triphenyltetrazolium chloride-stained rat brains. *Stroke*. 1996;27(9):1657-62.

Green RA, Odergren T, Ashwood T. Animal models of stroke: do they have value for discovering neuroprotective agents? *Trends Pharmacol Sci*. 2003;24(8):402-8.

Griffin JH. Role of surface in surface-dependent activation of Hageman factor (blood coagulation factor XII). *Proc Natl Acad Sci U S A*. 1978;75(4):1998-2002.

Gröger M, Lebesgue D, Pruneau D, Relton J, Kim SW, Nussberger J, Plesnila N. Release of bradykinin and expression of kinin B2 receptors in the brain: role for cell death and brain edema formation after focal cerebral ischemia in mice. *J Cereb Blood Flow Metab*. 2005;25(8):978-89.

Guillemin GJ, Brew BJ. Microglia, macrophages, perivascular macrophages, and pericytes: a review of function and identification. *J Leukoc Biol*. 2004;75(3):388-97.

Hacke W, Schwab S, Horn M, Spranger M, De Georgia M, von Kummer R. 'Malignant' middle cerebral artery territory infarction: clinical course and prognostic signs. *Arch Neurol*. 1996;53(4):309-15.

Hacke W, Kaste M, Bluhmki E, Brozman M, Dávalos A, Guidetti D, Larrue V, Lees KR, Medeghri Z, Machnig T, Schneider D, von Kummer R, Wahlgren N, Toni D; ECASS Investigators. Thrombolysis with alteplase 3 to 4.5 hours after acute ischemic stroke. *N Engl J Med*. 2008;359(13):1317-29.

Hagedorn I, Schmidbauer S, Pleines I, Kleinschnitz C, Kronthaler U, Stoll G, Dickneite G, Nieswandt B. Factor XIIa inhibitor recombinant human albumin Infestin-4 abolishes occlusive arterial thrombus formation without affecting bleeding. *Circulation*. 2010;121(13):1510-7.

Hamer PW, McGeachie JM, Davies MJ, Grounds MD. Evans Blue Dye as an in vivo marker of myofibre damage: optimising parameters for detecting initial myofibre membrane permeability. *J Anat*. 2002;200(Pt 1):69-79.

Hartnell A, Steel J, Turley H, Jones M, Jackson DG, Crocker PR. Characterization of human sialoadhesin, a sialic acid binding receptor expressed by resident and inflammatory macrophage populations. *Blood*. 2001;97(1):288-96.

Hatfield RH, Mendelow AD, Perry RH, Alvarez LM, Modha P. Triphenyltetrazolium chloride (TTC) as a marker for ischaemic changes in rat brain following permanent middle cerebral artery occlusion. *Neuropathol Appl Neurobiol*. 1991;17(1):61-7.

Heydenreich N, Nolte MW, Göb E, Langhauser F, Hofmeister M, Kraft P, Albert-Weissenberger C, Brede M, Varallyay C, Göbel K, Meuth SG, Nieswandt B, Dickneite G, Stoll G, Kleinschnitz C. C1-inhibitor protects from brain ischemia-reperfusion injury by combined antiinflammatory and antithrombotic mechanisms. *Stroke*. 2012;43(9):2457-67.

Holland JA, Pritchard KA, Pappolla MA. Bradykinin induces superoxide anion release from human endothelial cells. *J Cell Physiol*. 1990;143:21-5.

Hong SL. Effect of bradykinin and thrombin on prostacyclin synthesis in endothelial cells from calf and pig aorta and human umbilical cord vein. *Thromb Res*. 1980;18(6):787-95.

Horstick G, Heimann A, Götze O, Hafner G, Berg O, Böhmer P, Becker P, Darius H, Rupprecht HJ, Loos M, Bhakdi S, Meyer J, Kempski O. Intracoronary application of C1 esterase inhibitor improves cardiac function and reduces myocardial necrosis in an experimental model of ischemia and reperfusion. *Circulation*. 1997;95(3):701-8.

Huang J, Kim LJ, Mealey R, Marsh Jr HC, Zhang Y, Tenner AJ, Connolly Jr ES, Pinsky DJ. Neuronal protection in stroke by an sLexglycosylated complement inhibitory protein. *Science*. 1999;285(5427):595-9.

Hudgins WR, Garcia JH. The effect of electrocautery, atmospheric exposure, and surgical retraction on the permeability of the blood-brain-barrier. *Stroke*. 1970;1(5):375-80.

Ignjatovic T, Stanisavljevic S, Brovkovych V, Skidgel RA, Erdös EG. Kinin B1 receptors stimulate nitric oxide production in endothelial cells: signaling pathways activated by angiotensin I-converting enzyme inhibitors and peptide ligands. *Mol Pharmacol*. 2004;66(5):1310-6.

Ip CW, Kroner A, Crocker PR, Nave KA, Martini R. Sialoadhesin deficiency ameliorates myelin degeneration and axonopathic changes in the CNS of PLP overexpressing mice. *Neurobiol Dis*. 2007;25(1):105-11.

Jander S, Kraemer M, Schroeter M, Witte OW, Stoll G. Lymphocytic infiltration and expression of intercellular adhesion molecule-1 in photochemically induced ischemia of the rat cortex. *J Cereb Blood Flow Metab*. 1995;15(1):42-51.

Jiang HR, Lumsden L, Forrester JV. Macrophages and dendritic cells in IRBP-induced experimental autoimmune uveoretinitis in B10RIII mice. *Invest Ophthalmol Visual Sci.* 1999;40(13):3177-85.

Kamiya T, Katayama Y, Kashiwagi F, Terashi A. The role of bradykinin in mediating ischemic brain edema in rats. *Stroke*. 1993;24(4):571-5.

Kanters E, Pasparakis M, Gijbels MJ, Vergouwe MN, Partouns-Hendriks I, Fijneman RJ, Clausen BE, Förster I, Kockx MM, Rajewsky K, Kraal G, Hofker MH, de Winther MP. Inhibition of NF-kappaB activation in macrophages increases atherosclerosis in LDL receptor-deficient mice. *J Clin Invest*. 2003;112(8):1176-85.

Kawamata T, Alexis NE, Dietrich WD, Finklestein SP. Intracisternal basic fibroblast growth factor (bFGF) enhances behavioral recovery following focal cerebral infarction in the rat. *J Cereb Blood Flow Metab*. 1996;16(4):542-7.

Keating GM. Human C1-esterase inhibitor concentrate (Berinert). *BioDrugs*. 2009;23(6):399-406.

Khan M, Sekhon B, Giri S, Jatana M, Gilg AG, Ayasolla K, Elango C, Singh AK, Singh I. S-Nitrosoglutathione reduces inflammation and protects brain against focal cerebral ischemia in a rat model of experimental stroke. *J Cereb Blood Flow Metab*. 2005;25(2):177-92.

Kleinschnitz C, Brinkhoff J, Zelenka M, Sommer C, Stoll G. The extent of cytokine induction in peripheral nerve lesions depends on the mode of injury and NMDA receptor signaling. *J Neuroimmunol*. 2004;149(1-2):77-83.

Kleinschnitz C, Stoll G, Bendszus M, Schuh K, Pauer HU, Burfeind P, Renné C, Gailani D, Nieswandt B, Renné T. Targeting coagulation factor XII provides protection from pathological thrombosis in cerebral ischemia without interfering with hemostasis. *J Exp Med*. 2006;203(3):513-8.

Kleinschnitz C, Pozgajova M, Pham M, Bendszus M, Nieswandt B, Stoll G. Targeting platelets in acute experimental stroke: impact of glycoprotein Ib, VI, and IIb/IIIa blockade on infarct size, functional outcome, and intracranial bleeding. *Circulation*. 2007;115(17):2323-30.

Kleinschnitz C, Schwab N, Kraft P, Hagedorn I, Dreykluft A, Schwarz T, Austinat M, Nieswandt B, Wiendl H, Stoll G. Early detrimental T-cell effects in experimental cerebral ischemia are neither related to adaptive immunity nor thrombus formation. *Blood*. 2010;115(18):3835-42. (a)

Kleinschnitz C, Grund H, Wingler K, Armitage ME, Jones E, Mittal M, Barit D, Schwarz T, Geis C, Kraft P, Barthel K, Schuhmann MK, Herrmann AM, Meuth SG, Stoll G, Meurer S, et al. Post-stroke inhibition of induced NADPH oxidase type 4 prevents oxidative stress and neurodegeneration. *PLoS Biol*. 2010;8(9). (b)

Kleinschnitz C, Blecharz K, Kahles T, Schwarz T, Kraft P, Göbel K, Meuth SG, Burek M, Thum T, Stoll G, Förster C. Glucocorticoid insensitivity at the hypoxic blood-brain barrier can be reversed by inhibition of the proteasome. *Stroke*. 2011;42(4):1081-9.

Kobsar I, Oetke C, Kroner A, Wessig C, Crocker P, Martini R. Attenuated demyelination in the absence of the macrophage-restricted adhesion molecule sialoadhesin (Siglec-1) in mice heterozygously deficient in P0. *Mol Cell Neurosci*. 2006;31(4):685-91.

Koizumi J, Yoshida Y, Nakazawa T, Ooneda G. Experimental studies of ischemic brain edema: 1. A new experimental model of cerebral embolism in rats in which recirculation can be introduced in the ischemic area. *Jpn J Stroke*. 1986;8(1):1-8.

Kraft P, Schwarz T, Meijers JC, Stoll G, Kleinschnitz C. Thrombin-activatable fibrinolysis inhibitor (TAFI) deficient mice are susceptible to intracerebral thrombosis and ischemic stroke. *PLoS One*. 2010;5(7):e11658. (a)

Kraft P, Benz PM, Austinat M, Brede ME, Schuh K, Walter U, Stoll G, Kleinschnitz C. Deficiency of vasodilator-stimulated phosphoprotein (VASP) increases blood-brain-barrier damage and edema formation after ischemic stroke in mice. *PLoS One*. 2010;5(12):e15106. (b)

Laemmli UK. Cleavage of structural proteins during the assembly of the head of bacteriophage T4. *Nature*. 1970;227(5259):680-5.

Langhauser F, Göb E, Kraft P, Geis C, Schmitt J, Brede M, Göbel K, Helluy X, Pham M, Bendszus M, Jakob P, Stoll G, Meuth SG, Nieswandt B, McCrae KR, Kleinschnitz C. Kininogen deficiency protects from ischemic neurodegeneration in mice by reducing thrombosis, blood-brain barrier damage, and inflammation. *Blood*. 2012;120(19):4082-92.

Larrue V, von Kummer R, del Zoppo G, Bluhmki E. Hemorrhagic transformation in acute ischemic stroke. Potential contributing factors in the European Cooperative Acute Stroke Study. *Stroke*. 1997;28(5):957-60.

Lehmann TG, Heger M, Münch S, Kirschfink M, Klar E. In vivo microscopy reveals that complement inhibition by C1-esterase inhibitor reduces ischemia/reperfusion injury in the liver. *Transpl Int*. 2000;13 Suppl 1:S547-50.

Li J, Lu Z, Li WL, Yu SP, Wei L. Cell death and proliferation in NF-kappaB p50 knockout mouse after cerebral ischemia. *Brain Res*. 2008;1230:281-9.

Liu J, Jin X, Liu KJ, Liu W. Matrix metalloproteinase-2-mediated occludin degradation and caveolin-1-mediated claudin-5 redistribution contribute to blood-brain barrier damage in early ischemic stroke stage. *J Neurosci*. 2012;32(9):3044-57.

Livak KJ, Schmittgen TD. Analysis of relative gene expression data using real-time quantitative PCR and the 2(-Delta Delta C(T)) Method. *Methods*. 2001;25(4):402-8.

Lo AC, Chen AY, Hung VK, Yaw LP, Fung MK, Ho MC, Tsang MC, Chung SS, Chung SK. Endothelin-1 overexpression leads to further water accumulation and brain edema after middle cerebral artery occlusion via aquaporin 4 expression in astrocytic end-feet. *J Cereb Blood Flow Metab*. 2005;25(8):998-1011.

Longhi L, Perego C, Ortolano F, Zanier ER, Bianchi P, Stocchetti N, McIntosh TK, De Simoni MG. C1-inhibitor attenuates neurobehavioral deficits and reduces contusion volume after controlled cortical impact brain injury in mice. *Crit Care Med*. 2009;37(2):659-65.

Mackman N. Role of tissue factor in hemostasis, thrombosis, and vascular development. *Arterioscler Thromb Vasc Biol*. 2004;24(6):1015-22.

Macleod MR, Fisher M, O'Collins V, Sena ES, Dirnagl U, Bath PM, Buchan A, van der Worp HB, Traystman R, Minematsu K, Donnan GA, Howells DW. Good laboratory practice: preventing introduction of bias at the bench. *Stroke*. 2009;40(3):e50-2.

Mandle R Jr, Kaplan AP. Hageman factor substrates. Human plasma prekallikrein: mechanism of activation by Hageman factor and participation in hageman factor-dependent fibrinolysis. *J Biol Chem*. 1977;252(17):6097-104.

Marchal G, Beaudouin V, Rioux P, de la Sayette V, Le Doze F, Viader F, Derlon JM, Baron JC. Prolonged persistance of substantial volumes of potentially viable brain tissue after stroke: a correlative PET-CT study with voxel-based data analysis. *Stroke*. 1996;27(4):599-606.

Matsuo Y, Mihara Si, Ninomiya M, Fujimoto M. Protective effect of endothelin type A receptor antagonist on brain edema and injury after transient middle cerebral artery occlusion in rats. *Stroke*. 2001;32(9):2143-8.

Moran PM, Higgins LS, Cordell B, Moser PC. Age-related learning deficits in transgenic mice expressing the 751-amino acid isoform of human beta-amyloid precursor protein. *Proc Natl Acad Sci U S A*. 1995;92(12):5341-5.

Mouse Genome Sequencing Consortium, Waterston RH, Lindblad-Toh K, Birney E, Rogers J, Abril JF, Agarwal P, Agarwala R, Ainscough R, Alexandersson M, An P, Antonarakis SE, Attwood J, Baertsch R, Bailey J, Barlow K, Beck S, et al. Initial sequencing and comparative analysis of the mouse genome. *Nature*. 2002;420(6915):520-62.

Müerköster S, Rocha M, Crocker PR, Schirrmacher V, Umansky V. Sialoadhesin-positive host macrophages play an essential role in graft-versus-leukemia reactivity in mice. *Blood*. 1999;93(12):4375-86.

Munday J, Floyd H, Crocker PR. Sialic acid binding receptors (siglecs) expressed by macrophages. *J Leukoc Biol*. 1999;66(5):705-11.

Murray CJ, Lopez AD. Global mortality, disability, and the contribution of risk factors: Global Burden of Disease Study. *Lancet*. 1997;349(9063):1436-42.

Nath D, Hartnell A, Happerfield L, Miles DW, Burchell J, Taylor-Papadimitriou J, Crocker PR. Macrophage-tumour cell interactions: identification of MUC1 on breast cancer cells as a potential counter-receptor for the macrophage-restricted receptor, sialoadhesin. *Immunology*. 1999;98(2):213-9.

Ng LK, Nimmannitya J. Massive cerebral infarction with severe brain swelling: a clinicopathological study. *Stroke*. 1970;1(3):158-63.

Nielsen EW, Mollnes TE, Harlan JM, Winn RK. C1-inhibitor reduces the ischaemia-reperfusion injury of skeletal muscles in mice after aortic cross-clamping. *Scand J Immunol.* 2002;56(6):588-92.

Nieswandt B, Kleinschnitz C, Stoll G. Ischaemic stroke: a thrombo-inflammatory disease? *J Physiol*. 2011;589(Pt 17):4115-23.

NINDS (The National Institute of Neurological Disorders and Stroke) rt-PA Stroke Study Group. Tissue plasminogen activator for acute ischemic stroke. *N Engl J Med*. 1995;333(24):1581-7.

O'Collins VE, Macleod MR, Donnan GA, Horky LL, van der Worp BH, Howells DW. 1,026 experimental treatments in acute stroke. *Ann Neurol*. 2006;59(3):467-77.

Oetke C, Vinson MC, Jones C, Crocker PR. Sialoadhesin-deficient mice exhibit subtle changes in B- and T-cell populations and reduced immunoglobulin M levels. *Mol Cell Biol*. 2006;26(4):1549-57.

Pahl HL. Activators and target genes of Rel/NF-kappaB transcription factors. *Oncogene*. 1999;18(49):6853-66.

Pham M, Kleinschnitz C, Helluy X, Bartsch AJ, Austinat M, Behr VC, Renné T, Nieswandt B, Stoll G, Bendszus M. Enhanced cortical reperfusion protects coagulation factor XII-deficient mice from ischemic stroke as revealed by high-field MRI. *Neuroimage*. 2010;49(4):2907-14.

Pham M, Stoll G, Nieswandt B, Bendszus M, Kleinschnitz C. Blood coagulation factor XII--a neglected player in stroke pathophysiology. *J Mol Med (Berl).* 2012;90(2):119-26.

Pasinetti GM, Johnson SA, Rozovsky I, Lampert-Etchells M, Morgan DG, Gordon MN, Morgan TE, Willoughby D, Fnch CE. Complement C1qB and C4 mRNAs responses to lesioning in rat brain. *Exp Neurol.* 1992;118(2):117-25.

Pasparakis M, Courtois G, Hafner M, Schmidt-Supprian M, Nenci A, Toksoy A, Krampert M, Goebeler M, Gillitzer R, Israel A, Krieg T, Rajewsky K, Haase I. TNF-mediated inflammatory skin disease in mice with epidermis-specific deletion of IKK2. *Nature*. 2002;417(6891):861-6.

Pedersen ED, Waje-Andreassen U, Vedeler CA, Aamodt G, Mollnes TE. Systemic complement activation following human acute ischaemic stroke. *Clin Exp Immunol*. 2004;137(1):117-22.

Perry VH, Gordon S. Macrophages and the nervous system. *Int Rev Cytol*. 1991;125:203-44.

Perry VH, Crocker PR, Gordon S. The blood-brain barrier regulates the expression of a macrophage sialic acid-binding receptor on microglia. *J Cell Sci*. 1992;101(Pt 1):201-7.

Perry VH, Andersson PB, Gordon S. Macrophages and inflammation in the central nervous system. *Trends Neurosci*. 1993;16(7):268-73.

Pineiro R, Pendlebury ST, Smith S, Flitney D, Blamire AM, Styles P, Matthews PM. Relating MRI changes to motor deficit after ischemic stroke by segmentation of functional motor pathways. *Stroke*. 2000;31(3):672-9.

Pixley RA, Schapira M, Colman RW. The regulation of human factor XIIa by plasma proteinase inhibitors. *J Biol Chem*. 1985;260(3):1723-9.

Pope JG, Vanderlugt CL, Rahbe SM, Lipton HL, Miller SD. Characterization of and functional antigen presentation by central nervous system mononuclear cells from mice infected with Theiler's murine encephalomyelitis virus. *J Virol.* 1998;72(10):7762-71.

Qureshi AI, Suarez JI, Yahia AM, Mohammad Y, Uzun G, Suri MF, Zaidat OO, Ayata C, Ali Z, Wityk RJ. Timing of neurologic deterioration in massive middle cerebral artery infarction: A multicenter review. *Crit Care Med*. 2003;31(1):272-7.

Relton JK, Beckey VE, Hanson WL, and Whalley ET. CP-0597, a selective bradykinin B2 receptor antagonist, inhibits brain injury in a rat model of reversible middle cerebral artery occlusion. *Stroke*. 1997;28(7):1430-6.

Renné T, Pozgajová M, Grüner S, Schuh K, Pauer HU, Burfeind P, Gailani D, Nieswandt B. Defective thrombus formation in mice lacking coagulation factor XII. *J Exp Med*. 2005;202(2):271-81.

Revak SD, Cochrane CG, Bouma BN, Griffin JH. Surface and fluid phase activities of two forms of activated Hageman factor produced during contact activation of plasma. *J Exp Med*. 1978;147(3):719-29.

Rodi D, Couture R, Ongali B, Simonato M. Targeting kinin receptors for the treatment of neurological diseases. *Curr Pharm Des*. 2005;11(10):1313-26.

Roger VL, Go AS, Lloyd-Jones DM, Adams RJ, Berry JD, Brown TM, Carnethon MR, Dai S, de Simone G, Ford ES, Fox CS, Fullerton HJ, Gillespie C, Greenlund KJ, Hailpern SM, Heit JA, et al. Heart disease and stroke statistics - 2011 update: a report from the American Heart Association. *Circulation*. 2011;123(4):e18-e209.

Rosenberg GA, Yang Y. Vasogenic edema due to tight junction disruption by matrix metalloproteinases in cerebral ischemia. *Neurosurg Focus*. 2007;22(5):E4.

Rothwell NJ, Relton JK. Involvement of cytokines in acute neurodegeneration in the CNS. *Neurosci Biobehav Rev.* 1993;17(2):217-27.

Sarker MH, Hu DE, Fraser PA. Acute effects of bradykinin on cerebral microvascular permeability in the anaesthetized rat. *J Physiol*. 2000;528 Pt 1:177-87.

Schäfer MK, Schwaeble WJ, Post C, Salvati P, Calabresi M, Sim RB, Petry F, Loos M, Weihe E. Complement C1q is dramatically up-regulated in brain microglia in response to transient global cerebral ischemia. *J Immunol.* 2000;164(10):5446-52.

Schapira M, Scott CF, Colman RW. Contribution of plasma protease inhibitors to the inactivation of kallikrein in plasma. *J Clin Invest*. 1982;69(2):462-8.

Scherbel U, Raghupathi R, Nakamura M, Saatman KE, Trojanowski JQ, Neugebauer E, Marino MW, McIntosh TK. Differential acute and chronic responses of tumor necrosis factor-deficient mice to experimental brain injury. *Proc Natl Acad Sci U S A.* 1999;96(15):8721-6.

Schilling M, Besselmann M, Leonhard C, Mueller M, Ringelstein EB, Kiefer R. Microglial activation precedes and predominates over macrophage infiltration in transient focal cerebral ischemia: a study in green fluorescent protein transgenic bone marrow chimeric mice. *Exp neurol*. 2003;183(1):25–33.

Schmaier AH. The elusive physiologic role of Factor XII. *J Clin Invest*. 2008;118(9):3006-9.

Schneider A, Martin-Villalba A, Weih F, Vogel J, Wirth T, Schwaninger M. NF-kappaB is activated and promotes cell death in focal cerebral ischemia. *Nat Med*. 1999;5(5):554-9.

Schroeter M, Jander S, Witte OW, Stoll G. Local immune responses in the rat cerebral cortex after middle cerebral artery occlusion. *J Neuroimmun*. 1994;55(2):195-203.

Schroeter M, Jander S, Huitinga I, Witte OW, Stoll G. Phagocytic response in photochemically induced infarction of rat cerebral cortex. The role of resident microglia. *Stroke*. 1997;28(2).382-6.

Shaw CM, Alvord EC Jr, Berry RG. Swelling of the brain following ischemic infarction with arterial occlusion. *Arch Neurol*. 1959;1:161-77.

Stoll G, Jander S, Schroeter M. Inflammation and glial responses in ischemic brain lesions. *Prog Neurobiol*. 1998;56(2):149-71.

Stoll G, Jander S. The role of microglia and macrophages in the pathophysiology of the CNS. *Prog Neurobiol*. 1999;58(3):233-47.

Stoll G, Bendszus M. Inflammation and atherosclerosis: novel insights into plaque formation and destabilization. *Stroke*. 2006;37(7):1923-32.

Stoll G, Kleinschnitz C, Nieswandt B. Molecular mechanisms of thrombus formation in ischemic stroke: novel insights and targets for treatment. *Blood*. 2008; 112(9):3555-62.

Stoll G, Kleinschnitz C, Nieswandt B. Combating innate inflammation: a new paradigm for acute treatment of stroke? *Ann N Y Acad Sci*. 2010;1207:149-54.

Storini C, Rossi E, Marrella V, Distaso M, Veerhuis R, Vergani C, Bergamaschini L, De Simoni MG. C1-inhibitor protects against brain ischemia-reperfusion injury via inhibition of cell recruitment and inflammation. *Neurobiol Dis*. 2005;19(1-2):10-7.

Tanaka M, Fuentes ME, Yamaguchi K, Durnin MH, Dalrymple SA, Hardy KL, Goeddel DV. Embryonic lethality, liver degeneration, and impaired NF-kappa B activation in IKK-beta-deficient mice. *Immunity*. 1999;10(4):421-9.

Tong D, Reeves MJ, Hernandez AF, Zhao X, Olson DM, Fonarow GC, Schwamm LH, Smith EE. Times From Symptom Onset to Hospital Arrival in the Get With The Guidelines-Stroke Program 2002 to 2009: Temporal Trends and Implications. *Stroke*. 2012;43(7):1912-7.

Van Beek J, Bernaudin M, Petit E, Gasque P, Nouvelot A, MacKenzie ET, Fontaine M. Expression of receptors for complement anaphylatoxins C3a and C5a following permanent focal cerebral ischemia in the mouse. *Exp Neurol*. 2000;161(1):373-82.

van den Berg TK, Brevé JJ, Damoiseaux JG, Döpp EA, Kelm S, Crocker PR, Dijkstra CD, Kraal G. Sialoadhesin on macrophages: its identification as a lymphocyte adhesion molecule. *J Exp Med*. 1992;176(3):647-55.

van den Berg TK, Nath D, Ziltener HJ, Vestweber D, Fukuda M, van Die I, Crocker PR. Cutting edge: CD43 functions as a T cell counterreceptor for the macrophage adhesion receptor sialoadhesin (Siglec-1). *J Immunol*. 2001;166(6):3637-40.

van den Berg JSP, de Jong G. Why ischemic stroke patients do not receive thrombolytic treatment: results from a general hospital. *Acta Neurol Scand*. 2009;120(3):157-160.

Vinson M, van der Merwe PA, Kelm S, May A, Jones EY, Crocker PR. Characterization of the sialic acid-binding site in sialoadhesin by site-directed mutagenesis. *J Biol Chem*. 1996;271(16):9267-72.

Wagner S, Kalb P, Lukosava M, Hilgenfeldt U, and Schwaninger M. Activation of the tissue kallikrein-kinin system in stroke. *J Neurol Sci*. 2002;202(1-2):75-6.

Wagner DC, Deten A, Härtig W, Boltze J, Kranz A. Changes in T2 relaxation time after stroke reflect clearing processes. *Neuroimage*. 2012;61(4):780-5

Wahl F, Allix M, Plotkine M, Boulu RG. Neurological and behavioral outcomes of focal cerebral ischemia in rats. *Stroke*. 1992;23(2):267-72.

Wang X, Yue T-L, Barone FC, White RF, Gagnon RC, Feuerstein GZ. Concommitant cortical expression of TNF-a and IL-1b mRNA following transient focal ischemia. *Mol Chem Neuropathol*. 1994;23(2-3):103-14.

Wang Q, Tang XN, Yenari MA. The inflammatory response in stroke. *J Neuroimmunol*. 2007;184(1-2):53-68.

Waytes AT, Rosen FS, Frank MM. Treatment of hereditary angioedema with a vapor-heated C1 inhibitor concentrate. *N Engl J Med.* 1996;334(25):1630-4.

WHO (World Health Organization). The top 10 causes of death. Fact sheet number 310. 2008; Geneva: World Health Organization. Update 2011. Available at http://who.int/mediacentre/factsheets/fs310/en/

Wiggins RC. Kinin release from high molecular weight kininogen by the action of Hageman factor in the absence of kallikrein. *J Biol Chem*. 1983;258(14):8963-70.

Williams K, Alvarez X, Lackner AA. Central nervous system perivascular cells are immunoregulatory cells that connect the CNS with the peripheral immune system. *Glia*. 2001;36(2):156-64.

Winer J. Jung CK, Shackel I, Williams PM. Development and validation of real-time quantitative reverse transcriptase-polymerase chain reaction for monitoring gene expression in cardiac myocytes in vitro. *Anal Biochem*. 1999;270(1):41-9.

Wuillemin WA, Minnema M, Meijers JC, Roem D, Eerenberg AJM, Nuijens JH, ten Cate H and Hack CE. Inactivation of factor XIa in human plasma assessed by measuring factor XIa-protease inhibitor complexes: Major role of C1-inhibitor. *Blood*. 1995;85(6):1517-26.

Xia CF, Yin H, Borlongan CV, Chao L, and Chao J. Kallikrein gene transfer protects against ischemic stroke by promoting glial cell migration and inhibiting apoptosis. *Hypertension*. 2004;43(2):452-9.

Yang GY, Betz AL. Reperfusion-induced injury to the blood-brain barrier after middle cerebral artery occlusion in rats. *Stroke*. 1994;25(8):1658-65.

Yang Y, Estrada EY, Thompson JF, Liu W, Rosenberg GA. Matrix metalloproteinase-mediated disruption of tight junction proteins in cerebral vessels is reversed by synthetic matrix metalloproteinase inhibitor in focal ischemia in rat. *J Cereb Blood Flow Metab*. 2007;27(4):697-709.

Zuidema MY, Zhang C. Ischemia/reperfusion injury: The role of immune cells. *World J Cardiol*. 2010;2(10):325-32.

6 APPENDIX

Abbreviations

Ab	antibody
ANOVA	analysis of variance
APS	ammonium peroxide disulfate
ATPase	adenosintriphosphatase
AU	arbitrary units
BBB	blood-brain-barrier
BCA	bicinchoninic acid
BK	bradykinin
B1R/B2R	bradykinin receptor 1/2
bp	base pairs
BSA	bovine serum albumin
Ca^{2+}	calcium
CBF	cerebral blood flow
CCA	common carotid artery
cDNA	copy DNA
CD11b	cluster of differentiation 11b
C1-INH	C1-inhibitor
CISS	constructed interference in steady state
Cl^-	chloride
CNS	central nervous system
CP	carboxypeptidases
CT	computed tomography
Ctrl	control
Cy3	indocarbocyanin
DAB	3,3`- diaminobenzidin
ddH_2O	double distilled water
DEPC	diethyldicarbonat
des-Arg^9-BK	des-$arginine^9$-bradykinin
DNA	deoxyribonucleic acid
dATP	deoxyadenosine triphosphate
dCTP	deoxycytidine triphosphate

dGTP	deoxyguanosine triphosphate
dTTP	deoxythymidine triphosphate
dNTP	deoxyribonucleotide triphosphates
ECA	external carotid artery
ECL	enhanced chemiluminescence
ECM	endothelial cell membrane
Edn-1	endothelin-1
EDTA	ethylenediaminetetraacetic acid
EtBr	ethidium bromide
EtOH	ethanol
FDA	Food and Drug Administration
FIX, FX, FXI, FXII	coagulation factor IX, X, XI, XII
(FIX/FX/FXI/FXII)a	activated form of FIX/FX/FXI/FXII
fl	floxed
GAPDH	glyceraldehyde 3-phosphate dehydrogenase
GPCR	G-protein coupled receptor
HAE	hereditary angioedema
H&E	hematoxylin/eosin
HMWK	high molecular weight kininogen
H_2O_2	hydrogen peroxide
HRP	horseradish peroxidase
ICA	internal carotid artery
ICAM-1	intercellular adhesion molecule-1
Ig	immunoglobulin
IgG	immunoglobulin G
IgM	immunoglobulin M
IL-1β	interleukin-1beta
IκB	inhibitor of NF-κB
IKK2	IκB kinase 2
i.p.	intraperitoneal
I/R	ischemia/reperfusion
i.v.	intravenous
K^+	potassium
KCl	potassium chloride

kDa	kilo Dalton
kg	kilogram
KKS	kallikrein-kinin system
mAB	monoclonal antibody
MCA	middle cerebral artery
MCAO	MCA occlusion
MeOH	methanol
$MgCl_2$	magnesium chloride
min	minute(s)
mM	milli molar
MRI	magnetic resonance imaging
mRNA	messenger ribonucleic acid
Na^+	sodium
NaCl	sodium chloride
Na_2HPO_4	disodium hydrogen phosphate
NaH_2PO_4	sodium dihydrogen phosphate
NaOH	sodium hydroxide
NF-κB	nuclear factor-kappa B
NO	nitric oxid
NP-40	Nonidet^{TM}P40
pAB	polyclonal antibody
PAGE	polyacrylamide gel electrophoresis
PBS	phosphate buffered saline
PBST	PBS Tween
PCR	polymerase chain reaction
PFA	paraformaldehyde
PK	prekallikrein
pMCAO	permanent MCAO
POD	peroxidase
polyP	polyphosphate(s)
PVDF	polyvinylidene fluoride
RT-PCR	real time PCR
rCBF	regional CBF
RIPA	radio-immunoprecipitation assay

RNase	ribonuclease
ROS	reactive oxygen species
rpm	revolution per minute
rt-PA	recombinant tissue plasminogen activator
sec	second(s)
SER	sheep erythrocyte binding receptor
Serpin	serine protease inhibitor
SD	standard deviation
SDS	sodium dodecyl sulfate
Siglec	sialic acid immunoglobulin-like lectins
Sn	sialoadhesin
$Sn^{-/-}$	sialoadhesin deficient
$Sn^{+/+}$	sialoadhesin expressing
$T_{1/2}$	half-life time of clearance
T2*w	T2*weighted
TAE	TRIS base-acetic acid-EDTA
Taq	thermophilus acquaticus
TBS	TRIS buffered saline
TBST	TBS Tween
TEMED	tetramethylethylenediamine
TG	transgenic
TGFβ-1	transforming growth factor beta-1
tMCAO	transient MCAO
TNF-α	tumor necrosis factor-alpha
TRIS	tris(hydroxymethyl)-aminomethan
TTC	2,3,5-triphenyltetrazolium chloride
Tween	polyoxyethylenesorbitan monolaurate
U	units
WT	wildtype
vs.	versus

Acknowledgements

The work presented here was accomplished at the department of Neurology, university clinics of Würzburg, in the group of Professor Dr Guido Stoll. During the period of my PhD project (December 2008 - December 2012), many people helped and supported me. Therefore, I would like to thank:

My first supervisor Professor Guido Stoll, for giving me the opportunity to work in his laboratory and for his fruitful supervision and support. Especially, I would like to thank him for allowing me to present my work at various international conferences, which enabled me to gain important experience for my future career, and for giving me the opportunity to actively participate in different programs offered by the Graduate School of Life Sciences, University of Würzburg.

Professor Christoph Kleinschnitz, for collaboration and fruitful supervision during my PhD, for very helpful discussions and for giving me the opportunity to work in his laboratory.

Professor Bernhard Nieswandt, for allowing me to participate in his groups´ weekly seminar at the Chair of Vascular Medicine and the Rudolf Virchow Center, DFG Research Center for Experimental Biomedicine, University of Würzburg, and the retreat in Ernst, Germany and for fruitful discussions and reviewing my thesis.

Professor Thomas Dandekar, for helpful discussions and for reviewing my thesis.

My colleagues and friends Daniela Urlaub, Kathrin Waßmuth, Melanie Glaser, Marion Hofmeister, Stine Mencl, Virgil Michels and Andrea Sauer, for a great working atmosphere, their support of my PhD project and their kind technical assistance.

Christiane Albert-Weißenberger, Eva Göb and Stine Mencl, for helpful discussions and carefully reading my thesis.

My mentor Katrin Heinze, for her great and helpful supervision regarding my future career.

Andreas Weisshaupt, for his support during my PhD program and helpful discussions regarding my future career.

All other members of the Laboratory of Professor Stoll and Professor Kleinschnitz, and all collaboration partners, who have not been mentioned by name, for their support and the helpful discussions.

Publications

Articles

Heydenreich N, Nolte MW, Göb E, Langhauser F, Hofmeister M, Kraft P, Albert-Weissenberger C, Brede M, Varallyay C, Göbel K, Meuth SG, Nieswandt B, Dickneite G, Stoll G, Kleinschnitz C. C1-Inhibitor Protects from Brain Ischemia-Reperfusion Injury by Combined Antiinflammatory and Antithrombotic Mechanisms. ***Stroke***. 2012 Sep;43(9):2457-67.

Kraft P, Schwarz T, Göb E, **Heydenreich N**, Brede M, Meuth SG, Kleinschnitz C. The Phosphodiesterase-4 Inhibitor Rolipram Protects from Ischemic Stroke in Mice by Reducing Blood-Brain-Barrier Damage, Inflammation and Thrombosis. ***Exp Neurol***. 2013 Sep:247:80-90.

Oral presentations

21st meeting of the European Neurological Society (ENS), Lisbon (Portugal), May 28-31, 2011: 'The functional role of sialoadhesin, a macrophage-restricted adhesion molecule, in experimental stroke'

22nd meeting of the ENS, Prague (Czech Republic), June 9-12, 2012: 'C1-inihibitor protects from ischemic stroke in rodents by combined anti-inflammatory and anti-thrombotic mechanisms'

85th Congress of the German Society of Neurology (DGN), Hamburg (Germany), September 26-29, 2012: 'Human C1-inhibitor protects from cerebral ischemia in rodents through reduced local thrombosis and inflammation'

Posters

6th International Doctoral Students Symposium of the Graduate School of Life Sciences (GSLS), Wuerzburg (Germany), October 19-20, 2011: 'The functional role of sialoadhesin, a macrophage-restricted adhesion molecule, in experimental stroke'

16th Congress of the European Federation of Neurological Societies (EFNS), Stockholm (Sweden), September 8-11, 2012: 'The anti-thrombotic and anti-inflammatory actions of C1-inhibitor protect from focal cerebral ischemia in rodents'

7th International Doctoral Students Symposium of the Graduate School of Life Sciences, Wuerzburg (Germany), October 16-17, 2012: 'C1-Inhibitor protects from brain ischemia-reperfusion injury by combined anti-inflammatory and anti-thrombotic mechanisms'

Affidavit

I hereby confirm that my thesis entitled **'Studies on the Contact-Kinin System and Macrophage Activation in Experimental Focal Cerebral Ischemia'** is the result of my own work. I did not receive any help or support from commercial consultants. All sources and/or materials applied are listed and specified in the thesis.

Furthermore, I confirm that this thesis has not yet been submitted as part of another examination process neither in identical nor in similar form.

…….. ……..

Place, Date Signature

Eidesstattliche Erklärung

Hiermit erkläre ich an Eides statt, die Dissertation **'Untersuchungen zum Kontakt-Kinin-System und zur Makrophagen-Aktivierung beim Experimentellen Schlaganfall'** eigenständig, d. h. insbesondere selbstständig und ohne Hilfe eines kommerziellen Promotionsberaters, angefertigt und keine anderen als die von mir angegebene Quellen und Hilfsmittel verwendet zu haben.

Ich erkläre außerdem, dass die Dissertation weder in gleicher noch in ähnlicher Form bereits in einem anderen Prüfungsverfahren vorgelegen hat.

…… ……..

Ort, Datum Unterschrift